TU Delft

Performance of nonlinear time series models to simulate synthetic groundwater table time series from an unsaturated zone model

Martin Vonk
MSc Thesis
09 October 2021

Delft University of Technology
Faculty of Civil Engineering & Geosciences
Water Management - Hydrology

Performance of nonlinear time series models to simulate synthetic groundwater table time series from an unsaturated zone model

Martin Vonk
4481348

to obtain the degree of Master of Science
at the Delft University of Technology

Thesis Committee:
Prof.dr.ir. Mark Bakker - Delft University of Technology
Frans Schaars - Artesia B.V.
Raoul Collenteur - University of Graz
Prof.dr.ir. Remko Uijlenhoet - Delft University of Technology
Dr.ir. Edo Abraham - Delft University of Technology

Faculty of Civil Engineering & Geosciences
Water Management - Hydrology
Netherlands

Aerial Photograph Swifterbant Flevopolder - Netherlands

Summary

Transfer function noise (TFN) modelling is a form of time series analysis which regularly uses the recharge as a stress to explain the groundwater table fluctuations. Often the recharge flux is estimated as a linear combination of the precipitation and the (potential) evaporation. However, this is a simplification of the actual hydrological processes in the unsaturated zone. This is tried to be overcome by implementing a nonlinear recharge model in TFN time series models. Additionally, TFN models can use different impulse response functions, where some of them account for dispersion and retardation due to the unsaturated zone.

In this report the performance of a linear and nonlinear recharge model, inside the TFN model, are tested against synthetic time series of the groundwater table. These time series for the groundwater table are created with the unsaturated/saturated zone model HYDRUS-1D. With HYDRUS-1D, thirty-five synthetic time series are created for five different soil types and seven different unsaturated zone thicknesses (up to 5 m). The three most commonly used response functions, exponential, gamma and four-parameters are also tested for these thirty-five time series.

The results show that TFN models using the nonlinear recharge model are almost always better in estimating the groundwater table time series than the linear recharge model. This is confirmed in both the calibration and validation period. The common disadvantage of the linear recharge model, undershooting the groundwater table in (dry) summers, is not observed for the nonlinear recharge model. This can improve the forecasting abilities of TFN models during droughts.

Additionally, the nonlinear recharge model gives a more realistic representation of the fluxes in the root zone. This is confirmed goodness-of-fit parameters when comparing of the recharge flux and evaporation reduction calculated by HYDRUS-1D and the nonlinear recharge model. Especially when using the exponential response function, the recharge flux can be estimated quite well by the nonlinear recharge model. However, the nonlinear recharge model is currently not able to estimate groundwater uptake (upwards recharge) while it is observed in the HYDRUS-1D simulations.

The linear model does perform decently for shallow groundwater tables down to a depth of 150 cm since that is where large groundwater fluctuations and more days with groundwater uptake (upward recharge) are observed. The use of the gamma and four-parameter response functions significantly improves the performance of the linear recharge model. This can be explained by the compensation of these response functions for dispersion and retardation in the root zone. Nevertheless, when performing groundwater table time series analysis on synthetic time series created with HYDRUS-1D, the nonlinear recharge model is preferred to simulate the groundwater table.

Contents

List of Figures

List of Tables

Nomenclature

Abbreviations

1D	One-Dimensional
2D	Two-Dimensional
EVP	Explained Variance Percentage
FLEX	Flux Exchange - Hydrological Nonlinear Recharge Model
KNMI	Royal Netherlands Meteorological Institute
R^2	Coefficient of Determination
RMSE	Root Mean Squared Error
TFN	Transfer Function Noise

Symbols

α	Van Genuchten Shape Parameter or TFN Noise Decay Parameter
$\alpha(\psi)$	Root Water Uptake Stress Response Function
$\Gamma(n)$	Gamma Function $= (n-1)!$
γ	FLEX Parameter that Determines how Nonlinear the Recharge is with Respect to the Saturation of the Root Zone
$\mathcal{P}$	Pore Water Pressure
ω	Reservoir Coefficient (originally j)
ψ	Pressure Head
ψ_{50}	Pressure Head at which the Water Extraction Rate by Roots is Reduced by 50%
ρ_w	Water Density
σ	Variance
Θ	Step Response Function
θ	Water Content
θ_r	Residual Water Content
θ_s	Saturated Water Content
ϑ	Impulse Response Function
ϑ_b	Block Response Function
A	Gain of the Step Response Function
a	Interception (Evaporation) Constant
$b(z)$	Normalized Water Uptake Distribution (Related to Root Distribution)

c	Drainage Resistance
D	Dispersion Coefficient
d	Drainage LevelBase or Surface Water Level
E_i	Interception (Evaporation)
E_p	Potential (Penman-Monteith) Evaporation
E_s	Soil Evaporation
E_t	Transpiration (Evaporation)
$E_{t,p}$	Potential Soil Evaporation
$E_{t,p}$	Transpiration (Evaporation)
f	Linear Recharge Model Parameter for the Crop/Evaporation Factor
g	Gravitational Constant
H	Saturated Thickness
h	Head
K	Hydraulic Conductivity
k	Constant for Radiation Extinction by Canopy
K_s	Relative Hydraulic Conductivity
K_s	Saturated Hydraulic Conductivity
k_v	FLEX Parameter for the Vegetation Coefficient for the Maximum Evaporation
K_z	Vertical Hydraulic Conductivity
L	Length (of the domain between surface waters)
l	Pore Connectivity Parameter
l_p	FLEX Parameter that Determines at what Fraction of $S_{r,max}$ the Evaporation Flux is Limited by the Availability of Soil Water
L_{AI}	Leaf Area Index
m	Van Genuchten Parameter $= 1 - \frac{1}{n}$
N	Precipitation Surplus
n	Van Genuchten Parameter
P	Precipitation
p	Shape Parameter for the Root Water Uptake Stress Response Function $\alpha(\psi)$ (commonly equal to 3)
P_e	Effective Precipitation
q	Discharge
$Q(\psi)$	Sink Term (for Root Water Uptake)
R	Recharge
r	Residuals of a TFN model
R_o	Runoff
S	Storativity or Specific Yield
S_e	Effective Saturation
S_p	Potential Root Water Uptake

S_u	Storage in the Unsaturated Zone
S_{CF}	Soil Cover Fraction
$S_{i,max}$	FLEX Parameter for the Maximum Storage Capacity of the Interception Zone Reservoir
$S_{r,max}$	FLEX Parameter for the Maximum Storage Capacity of the Root Zone Reservoir
T	Transmissivity (sometimes reffered to as KD)
t	Time
u	Effective Propagation Velocity of a Pressure Wave
v	Innovations of the noise model
x	Position
z	Elevation

1 Introduction

Describing groundwater table fluctuations is a challenging task in hydrology that is often done with groundwater models. There are different types of models to do this. White box models describe the physical processes using deterministic equations. These kind of models often need detailed knowledge of both the subsurface and the physical boundary conditions. Additionaly, they need extensive parameterisation and are time consuming to develop (Bakker & Schaars, 2019).

In contrast to white box models there are black box models which are entirely data-driven. Black box models try to determine a relation between input and output series without any physical understanding of the system (Bakker & Schaars, 2019). In the current age of big data these black box models are becoming increasingly popular. However it can be argued that black box models "neglect centuries of scientific understanding of physical processes to empirically look for relationships among data that underlie all natural phenomena" - Siegel & Hinchey (2019).

In between these white and black box models is a wide range (shades) of grey box models. In hydrology, time series analysis is becoming a popular grey box model to analyse groundwater table measurements in an observation well. The Python package Pastas (Collenteur et al., 2019) applies time series analysis with transfer function noise (TFN) modelling using predefined impulse response functions (von Asmuth; et al., 2002). The models are still data driven but they are often much simpler and faster using a relatively low amount of parameters. To make a good TFN model, the response function of each stress has to be estimated, including the uncertainty (Bakker & Schaars, 2019).

The most commonly used stress in TFN models to explain groundwater table fluctuations is the recharge flux. The recharge flux can be approximated by a linear combination of precipitation and (potential) evaporation. With this simple linear recharge model, often remarkably good fits are obtained (Collenteur et al., 2019). However, the linear recharge model is a simplification given that soil water flow can be highly nonlinear, since the hydraulic conductivity and the pressure head depend on the soil water content (Feddes et al., 1988).

The lack of incorporation of these nonlinear processes is often observed with linear TFN models, resulting in bad fits and predictions, especially for deeper groundwater systems (Zaadnoordijk et al., 2019). Also for climate forecasting it is a big disadvantage that (multiyear) droughts are not able to be simulated well with the linear recharge model due to undershooting of the groundwater table (Peterson & Western, 2014).

Research has been done to implement nonlinear recharge models in time series models. For instance, the model of Berendrecht et al. (2006) introduced nonlinearity by modelling the degree of water saturation of the root zone. Peterson & Western (2014) added a flexible vertically integrated soil moisture module to account for nonlinear processes. Recently, Collenteur; et al. (2021) tested a nonlinear recharge model loosely based on the FLEX conceptual modelling framework (Fenicia et al., 2006)

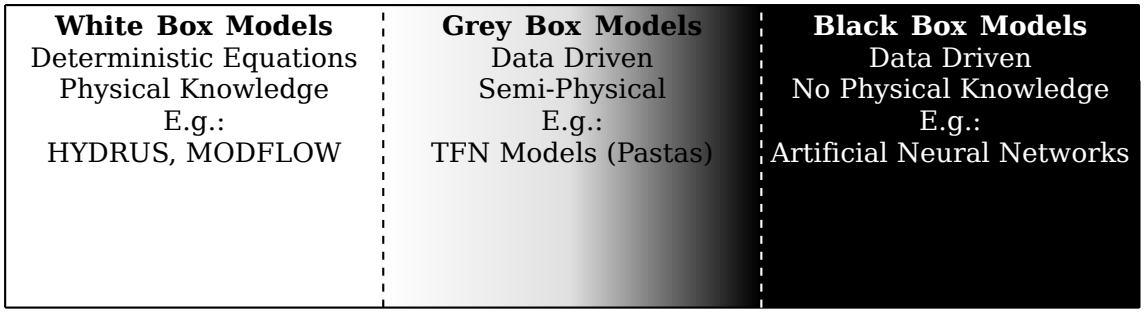

Figure 1.1: Grey Scale of Model Types

and compared the estimated recharge flux to independent lysimeter seepage data. The estimate of the recharge from the nonlinear recharge model was in reasonably good agreement with the lysimeter data.

According to the authors of these three publications, all these nonlinear TFN models showed a better performance compared to the linear model. This theory here is that using some physical knowledge of the system, as advocated by Siegel & Hinchey (2019), can lead to a better understanding model of the system.

However, Peterson & Western (2014) invite others to develop and test nonlinear transfer function noise models. Collenteur; et al. (2021) call for additional research using larger groundwater table data sets to investigate the general applicability of nonlinear root zone models in time series analysis under different hydrogeological settings.

1.1 Research Questions

The aim of this study identify how the nonlinear recharge model proposed by Collenteur; et al. (2021) performs in the TFN modelling. The performance of the nonlinear recharge model is compared to the linear recharge model and tested with synthetic time series for the groundwater table. The synthetic time series are created created with a one-dimensional unsaturated zone model under different hydrogeological settings.

HYDRUS-1D is used as the unsaturated zone model, because it is a physically based, white box model that numerically solves the deterministic equations which describe the unsaturated zone processes. The idea is that by using this physical model, we can create relatively realistic time series for the groundwater table and can say something about the physical conditions under which the grey box TFN model works. To do this we have the following research questions for this study:

R.Q. 1 What lower boundary condition can be used for a one-dimensional model to generate realistic synthetic time series of the groundwater table?

R.Q. 2 How does the unsaturated zone affect the nonlinear behaviour of the groundwater table?

R.Q. 3 How does the TFN model, using the linear or nonlinear recharge model, perform in modelling synthetic groundwater table time series created with an unsaturated zone model?

R.Q. 4 When is it recommended to use the linear or nonlinear recharge model when doing groundwater table time series analysis using TFN modelling?

1.2 Methodology and Outline

To answer the research questions we split the thesis into three main chapters which all contain some results and answer the research questions.

Chapter 2 discusses the basics of time series analysis using transfer function noise modelling. Here the concepts of input stresses and response functions are explained which are needed later when incorporating the unsaturated zone in time series analysis. Chapter 2 also discusses the responses of some elementary groundwater systems. We create some synthetic time series without an unsaturated zone and see that the performance of the TFN model is very good in these situations. From the comparison between the elementary groundwater systems, we learn what boundary condition to use for the one-dimensional unsaturated zone model. This way we do not limit the answers on the research questions only to one-dimensional domains or systems that are not realistic.

In chapter 3 we discuss the equations that describe the unsaturated zone which are also used by the unsaturated zone model HYDRUS-1D. In this chapter we run some simulations with HYDRUS-1D to demonstrate the nonlinear effects that the unsaturated zone has on the groundwater table to answer research question 2.

Chapter 4 first discusses how the TFN model Pastas tends to deal with the unsaturated zone effects with the use of response functions and recharge models. Next up we follow the procedure in Figure 1.2. We test the methods of the TFN model to incorporate the unsaturated zone when modelling synthetic time series from HYDRUS-1D. In total thirty-five synthetic time series for the groundwater table and recharge are made with five different soil types and seven unsaturated zone thicknesses. All profiles are homogeneous and the soil types range in permeability from 83.2 cm/d down to 0.9 cm/d. The thickness of the unsaturated zone ranges from 100cm up to 500cm. With the results of the TFN model we want to answer research question 3. For the nonlinear recharge model an extra comparison for the evaporation reduction is done.

In chapter 5, the conclusions and discussion, we go over on the answers on research question 1 to 3. Then we answer the last research question 4, when to use the linear or nonlinear recharge model and how the different response functions affect the choices.

Chapter 6 discusses the limitations of this research and offers some recommendations for future research.

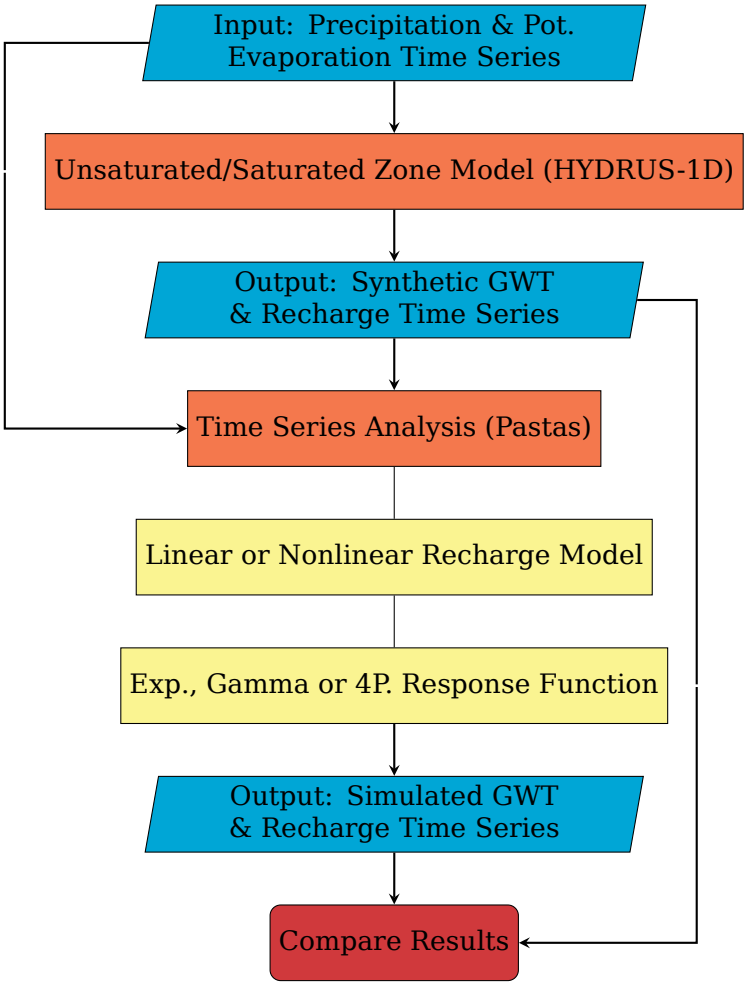

Figure 1.2: Methodology Flowchart for Chapter 3. Blue cells indicate time series. Orange cells indicate models. Yellow cells indicate model options.

2 Time Series Analysis with Transfer Function Noise Modelling

This chapter gives an introduction on time series analysis using transfer function noise modelling in Section 2.1. Section 2.2 discusses TFN modelling on elementary groundwater systems without an unsaturated zone. In the last subsection 2.3 the impulse response functions of the elementary groundwater systems are compared. This way we want to determine if we can use a one-dimensional model to simulate the groundwater table (research question 1) and what boundary conditions to use if so.

2.1 Transfer Function Noise Modelling with Pastas

A time series is a set of chronologically arranged observations, mainly of a dynamic system. The order of occurrence is a crucial part of the observations containing much information (Hipel & McLeod, 1994). Time series analysis is a form of data-analysis to find a relation between input and output time series.

Transfer function noise (TFN) modelling is a form of time series analysis that estimate an output series using one or multiple input time series. TFN models can be called grey box models since they are semi-physical (Bakker & Schaars, 2019), having both a deterministic and stochastic process (Hipel & McLeod, 1994). The Python package Pastas implements transfer function noise models to simulate a time series of observed heads using predefined, physically realistic response functions (Collenteur et al., 2019). The basic model structure can be written as:

$$h(t) = \sum_{m=1}^{M} h_m(t) + d + r(t) \tag{2.1}$$

where $h(t)$ are the observed heads [L], $h_m(t)$ is the contribution of stress m to the head [L], d is the base elevation (or drainage level) of the model [L] and $r(t)$ are the residuals [L]. M is the number of stresses that contribute to the head variation such as precipitation, evaporation, river levels and pumping wells. The contribution of a stress m to the head is calculated through convolution:

$$h_m(t) = \int_{-\infty}^{t} S_m(\tau)\vartheta_m(t-\tau)d\tau \tag{2.2}$$

where S_m is a time series of stress m , and ϑ_m is the impulse response function for stress m (von Asmuth; et al., 2002).

A stress S_m can be a combination of multiple stresses, for instance the precipitation surplus N [L/T]. In this case the potential evaporation E_p [L/T] is multiplied by a

factor f [-] and then subtracted from the precipitation P [L/T] such that $N = P - fE_p$. The combined stress is then added as S_m in Equation 2.2 to obtain the effect on the head.

2.1.1 Response Function

A simple impulse response function is the exponential impulse response function (von Asmuth et al., 2021):

$$\vartheta_m(t) = \frac{A}{a} e^{\frac{-t}{a}} \tag{2.3}$$

where only two parameters A and a have to be estimated by fitting Equation 2.1 to the measured heads.

The step response $\Theta(t)$ is the change in head due to a constant unit of stress starting at $t = 0$. The step response can be derived from integrating the impulse over time (Collenteur et al., 2019):

$$\Theta(t) = \int_0^t \vartheta(\tau) d\tau \tag{2.4}$$

For the exponential response function, the step response becomes:

$$\Theta(t) = A(1 - e^{\frac{-t}{a}}) \tag{2.5}$$

If $t \to \infty$, the head reaches a steady state which is called the gain of the response function (Bakker & Schaars, 2019). For the exponential response function the gain is equal to A.

In the discrete time domain, where a uniform stress is only present for one time interval Δt, we use the block response, which is obtained by superposition of two unit step responses (Bakker & Post, 2021):

$$\theta_b(t) = \begin{cases} \Theta(t) & 0 \leq t < \Delta t \\ \Theta(t) - \Theta(t - \Delta t) & t \geq \Delta t \end{cases} \tag{2.6}$$

Pastas computes the contribution of a stress (equation convolution with the block response.

2.1.2 Residuals

The residuals $r(t)$ in Equation 2.1 of the TFN model often show strong autocorrelation. A noise model with exponential decay of the residuals is used of the following form (von Asmuth & Bierkens, 2005):

$$r(t_i) = v(t_i) + r(t_{i-1}) e^{-\Delta t_i / a} \tag{2.7}$$

where a [T^{-1}] is the decay parameter, Δt_i is the timestep between observations at t_i and t_{i-1} and $v(t_i)$ is the (hopefully) white noise resulting from a random process.

2.1.3 Metrics

To quantify the performance of a TFN model, goodness-of-fit metrics are used. These metrics help to compare and quantify the different outcomes. Since all metrics have their strengths and weaknesses, two metrics are used which both evaluate the model performance differently. The metrics that are used are the root mean squared error (RMSE) and the explained variance percentage (EVP). Both indicate a goodness-of-fit for simulation of the time series mode as compared to the original time series.

Root Mean Squared Error

The root mean squared error [L] is (Jackson et al., 2019):

$$RMSE = \sqrt{\frac{1}{N}\sum_{i=1}^{N} r_i^2} \tag{2.8}$$

where r_i are the model residuals calculated from equation 2.1 and N is the number of residuals. The range is $0 \leq RMSE < \infty$ with the smaller the RMSE, the better the fit. The RMSE cannot indicate model bias and highlights larger errors.

Explained Variance Percentage

The explained variance [-] is (von Asmuth;, 2012):

$$\text{EV} = \frac{\sigma_h^2 - \sigma_r^2}{\sigma_h^2} = 1 - \frac{\sigma_r^2}{\sigma_h^2} = 1 - \frac{\frac{1}{N}\sum_{i=1}^{N}\left(r_i - \bar{r}\right)^2}{\frac{1}{N}\sum_{i=1}^{N}\left(h_i - \bar{h}\right)^2} = 1 - \frac{\sum_{i=1}^{N}\left(r_i - \bar{r}\right)^2}{\sum_{i=1}^{N}\left(h_i - \bar{h}\right)^2} \tag{2.9}$$

where σ_h^2 is the variance of the observations h_i and σ_r^2 is the variance of the residuals r_i. The variance indicates the squared average distance of the values from the mean. In this case the mean is $\bar{r}$ and $\bar{h}$ for the residuals and observations respectively. The EVP is fairly similar to the coefficient of determination R^2 [-] which is calculated from the residual and total sum of squares (Field, 2017):

$$\text{R}^2 = 1 - \frac{\sum_{i=1}^{N} r_i^2}{\sum_{i=1}^{N}\left(h_i - \bar{h}\right)^2} \tag{2.10}$$

Note that if the mean of the residuals $\bar{r}$ is equal to zero, the EV is equal to the R^2. Both the EVP and R^2 give an indication of the goodness of fit of the model compared to using the mean to predict the outcome variable (Field, 2017). If the value of the EVP is large, the model is very different from using the mean to predict the outcome variable, in this case the groundwater table. If the explained variance is small then using the model is little better than using the mean of the observations. This usually indicates that the model is missing one or more predicting variables. (von Asmuth;, 2012). Since the EVP is more commonly used in time series analysis in the Netherlands, we do not use the R^2 in this thesis. The range is $-\infty \leq EVP < 100\%$ with the closer to 100%, the better the fit. In Pastas the minimal value for the EVP is set to 0%.

2.2 TFN Modelling on Synthetic Time Series without an Unsaturated Zone

In this section first the behaviour of a linear reservoir groundwater system is discussed in subsection 2.2.1. In the next subsection 2.2.2 a TFN model is tested on a head time series from this linear reservoir system. In subsection 2.2.3 the Kraijenhoff van de Leur groundwater system is described and in the last subsection 2.3 the behaviour is compared to the linear reservoir system including a TFN model.

2.2.1 Response of a Linear Reservoir System Groundwater System

A one-dimensional soil column can be modelled as a simple linear reservoir system (Knotters & Bierkens, 2000) as seen in Figure 2.1. The water balance of this simple linear reservoir system can be written as:

$$S\frac{dh}{dt} = R - q \tag{2.11}$$

where q is the discharge [L/T], h is the head [L] with respect to a vertical axis z, S is the storativity [-] and R is the recharge [L/T]. The storativity defines the rise in head due to a unit N of recharge. A unit of N recharge results in an instantaneous head rise of SN (von Asmuth;, 2012). The relationship between the discharge and the head for this system is:

$$q = \frac{h - d}{c} \tag{2.12}$$

where c is the drainage resistance [T] and d is the drainage level [L] (outside of the one-dimensional soil column). This equation can be substituted in for q in Eq. 2.11 such that:

$$S\frac{dh}{dt} = R - \frac{h - d}{c} \tag{2.13}$$

When this differential equation is solved for a unit $N(= 1)$ impulse of recharge, the impulse response function $\vartheta(t)$ can be written as (von Asmuth;, 2012):

$$\vartheta(t) = h(t) - d = \frac{N}{S} e^{\frac{-t}{cS}} = \frac{1}{S} e^{\frac{-t}{cS}} \tag{2.14}$$

The impulse response function is an exponential function dependent on the storativity and the drainage resistance. Note that this is basically the same response function as the exponential response function (Eq. 2.3) present in the TFN model only with a different way of writing the parameters as A and a. This response function completely ignores the effect of an unsaturated zone and assumes that the recharge reaches the saturated zone instantly. In other words the impulse response function only represents the response of the groundwater table. The step response function of this system, for $N = 1$, is written as:

$$\Theta(t) = \int_0^t \frac{1}{S} e^{\frac{-\tau}{cS}} d\tau = c(1 - e^{\frac{-t}{cS}}) \tag{2.15}$$

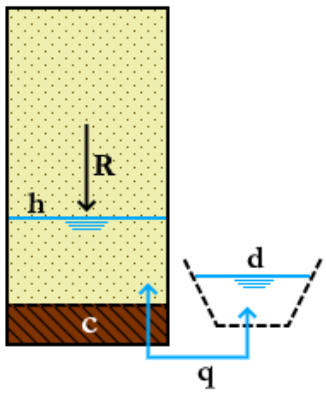

Figure 2.1: Linear Reservoir System according to Knotters & Bierkens (2000) and von Asmuth; (2012)

2.2.2 TFN Modelling of a Linear Reservoir Groundwater System

A head time series is simulated with the response function for a linear reservoir system (Eq. 2.14) and a time series of a stress. We obtain a time series for the stress by calculating the precipitation surplus from the precipitation and potential evaporation data from KNMI weather station De Bilt in The Netherlands. The parameters used for the response function are $S = 0.04$, $c = 46.82$ d and a base elevation d of 1 m is added to the head time series. After convolution (Eq. 2.2) of the precipitation surplus and the response function, the resulting head time series can be seen in Figure 2.2.

A TFN model is built with Pastas to test the performance on this head series. The results are shown in Figure 2.3. The obtained fit is perfect with an explained variance percentage (EVP) of 100% and a root mean square error of 0 m. The residuals of this system are negligible at an order of magnitude 10^{-15} m. The TFN model also returns three optimal parameter values for A, a and d where we find $A = 46.82$, $a = 1.8728$ and $d = 1.00$ m respectively. The parameters can be used to calculate S and c for which $c = A = 46.82$ d and $S = \frac{a}{A} = 0.04$. These values are exactly the same values as the ones used for the original input variables of the impulse response function of the linear reservoir system (Eq. 2.14).

From this analysis we can conclude that if we have a linear reservoir system, the original system parameters can be found using TFN modelling. Provided that the original input recharge time series is known exactly and there are no unsaturated zone effects or noise.

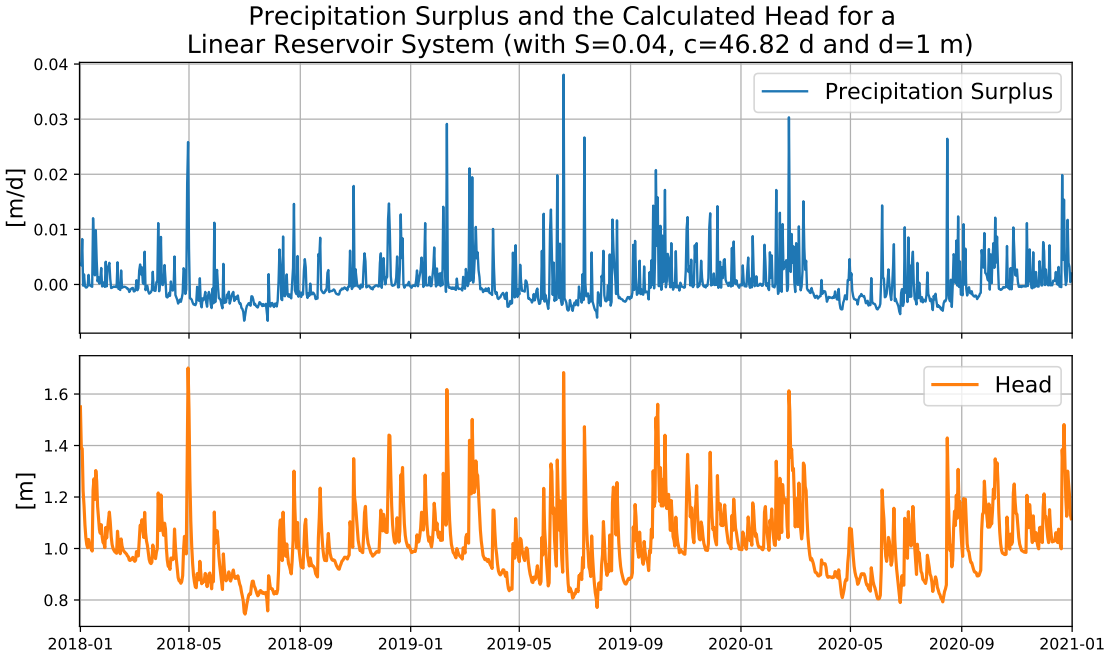

Figure 2.2: The precipitation surplus from De Bilt and the obtained head after convolution for a linear reservoir system. The time series for the precipitation surplus is originally from 1981 till 2020 but here only the last three years are shown.

2.2.3 Response of a Kraijenhoff van de Leur Groundwater System

Now we know that the behaviour of a linear reservoir system (without an unsaturated zone) can be described with a TFN model, we want to do the same for the Kraijenhoff van de Leur domain. We obtain the system from Kraijenhoff van de Leur (1958) for an idealised two dimensional situation as shown in Figure 2.4. Since the flow in this system is dependent on only one spatial coordinate (x), it is actually a one-dimensional system. However there are many domains in the Netherlands for which the equations of this system hold.

In a groundwater system with a horizontal head gradient the water balance Equation can be written as a partial differential Equation (von Asmuth;, 2012):

$$S\frac{\partial h}{\partial t} = R + \frac{\partial q_x}{\partial x} \tag{2.16}$$

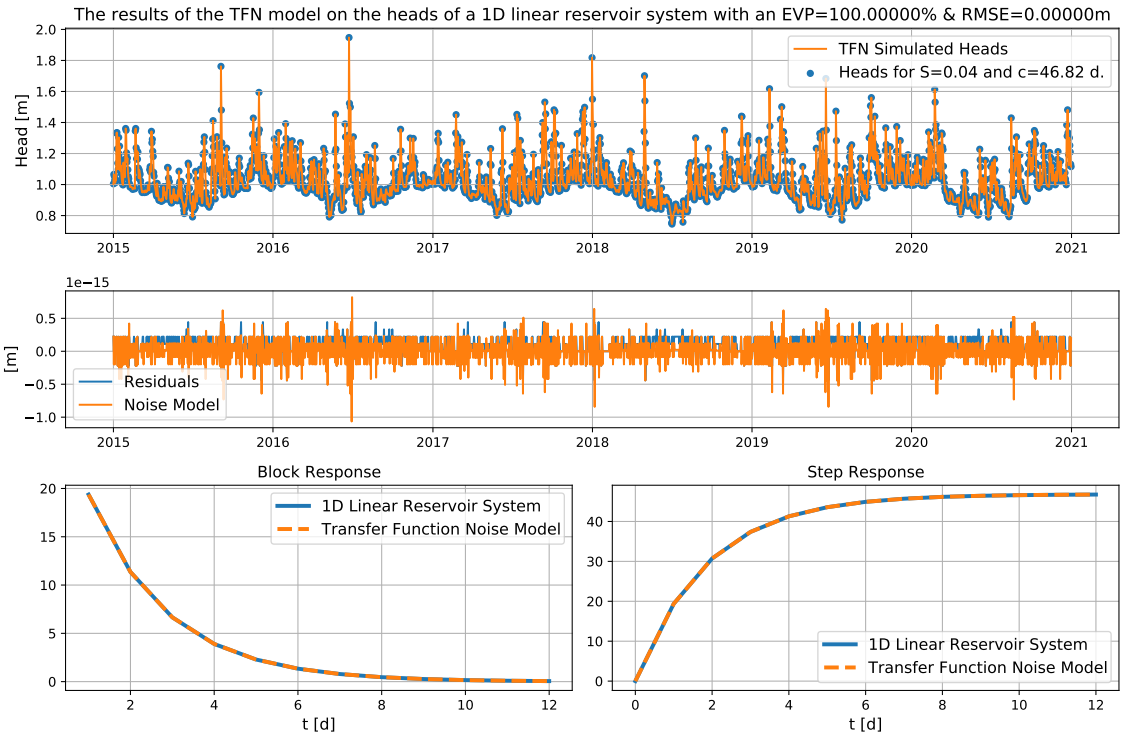

Figure 2.3: Transfer Function Noise Model for the linear Reservoir System

where q_x can be written with Darcy's law as:

$$q_x = -KH\frac{dh}{dx} \tag{2.17}$$

where K is the hydraulic conductivity [L/T] and H is the saturated thickness [L]. H is approximated as constant such that we have a constant transmissivity $KH(=T)$ [L^2/T]. The term q_x can be substituted in Equation 2.16:

$$S\frac{dh}{dt} = R + KH\frac{\partial^2 h}{\partial x^2} \tag{2.18}$$

This equation can be solved analytically for a unit $N = 1$ impulse of recharge (Kraijenhoff van de Leur, 1958):

$$\vartheta(t) = h(t) - d = \frac{4}{\pi S}\sum_{n=1,3,5\ldots}^{\infty}\left(\frac{1}{n}\exp\left(\frac{-n^2\pi^2 KHt}{SL^2}\right)\sin\left(\frac{n\pi x}{L}\right)\right) \tag{2.19}$$

where L is the length of the domain between surface waters [L]. This expression is simplified with a reservoir coefficient ω [T]:

$$\omega = \frac{SL^2}{\pi^2 KH} \tag{2.20}$$

such that Equation 2.21 becomes:

$$\vartheta(t) = \frac{4}{\pi S}\sum_{n=1,3,5\ldots}^{\infty}\frac{1}{n}e^{-n^2\frac{t}{\omega}}\sin\left(\frac{n\pi x}{L}\right) \tag{2.21}$$

The step response for this system can be described by:

$$\Theta(t) = \frac{4}{\pi S}\sum_{n=1,3,5\ldots}^{\infty}\frac{1}{n^3}\left(\omega - \omega e^{-n^2\frac{t}{\omega}}\right)\sin\left(\frac{n\pi x}{L}\right) \tag{2.22}$$

This equation is based on four main approximations namely (Kraijenhoff van de Leur, 1958; von Asmuth;, 2012):

- The storativity S and the hydraulic conductivity K of the aquifer are constant;
- The resistance to vertical flow is neglected (Dupuit approximation);
- The change in head $h(t)$ is small with regards to the saturated thickness of the aquifer such that H can be approximated as constant;
- The water level of the surface water is constant (d), and fully penetrates the aquifer at the boundaries ($x = 0$ & $x = L$).

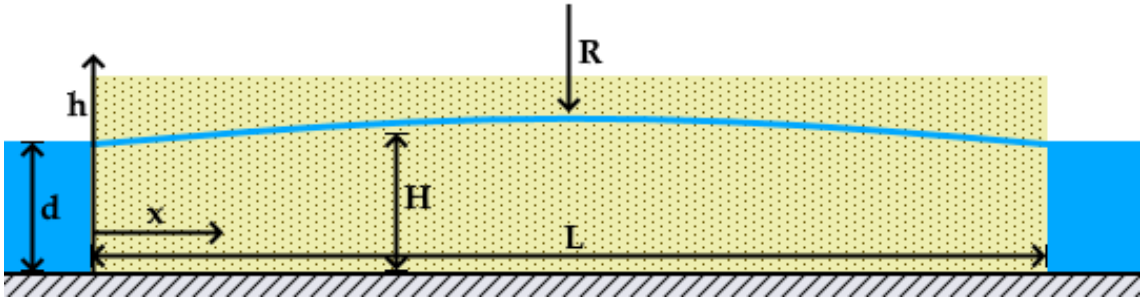

Figure 2.4: Homogeneous Kraijenhoff van de Leur Domain With a Horizontal Head Gradient (Kraijenhoff van de Leur, 1958)

2.2.4 TFN Modelling of a Kraijenhoff van de Leur Groundwater System

We perform the same exercise as in Section 2.2.2 where a synthetic time series for the head was obtained. This is done for a Kraijenhoff van de Leur system with parameters from a Dutch polder (J25) near Swifterbant in the province of Flevoland. The parameters are obtained from Ven (1979) with $\omega = 1.92$ days, $S = 0.04$ and we take $x = \frac{L}{2}$ such that we are in the middle between the surface water.

For this (relatively) fast responding system we see in Figure 2.5 that the TFN model gives a good fit on this system. The EVP is 99.97% and the RMSE is 0.00294 m. We see larger residuals, up to a few centimetres, but all of the residuals can be explained by the noise model. Figure 2.5 also shows the block and step response from Kraijenhoff van de Leur and the TFN model. Contrary to the linear reservoir system the response functions (Fig. 2.3) do not overlap perfectly anymore.

This shows that we can use the exponential response function (which is related to a the linear reservoir system) to create a very accurate TFN model on a synthetic time series of a Kraijenhoff van de Leur system. However the model is not exact anymore and compared to the linear reservoir system the residuals are a bit larger and the EVP & RMSE are slightly worse.

2.3 Relating the Impulse Responses of the Elementary Groundwater Systems

From the previous subsection we saw that a Kraijenhoff van de Leur system can be analysed by the TFN model using the exponential response function. However this was only at one location in the middle of the domain. The question rises how the two impulse responses for the linear reservoir system and the Kraijenhoff van de Leur domain compare in all the places within the domain domain. If we are able to obtain

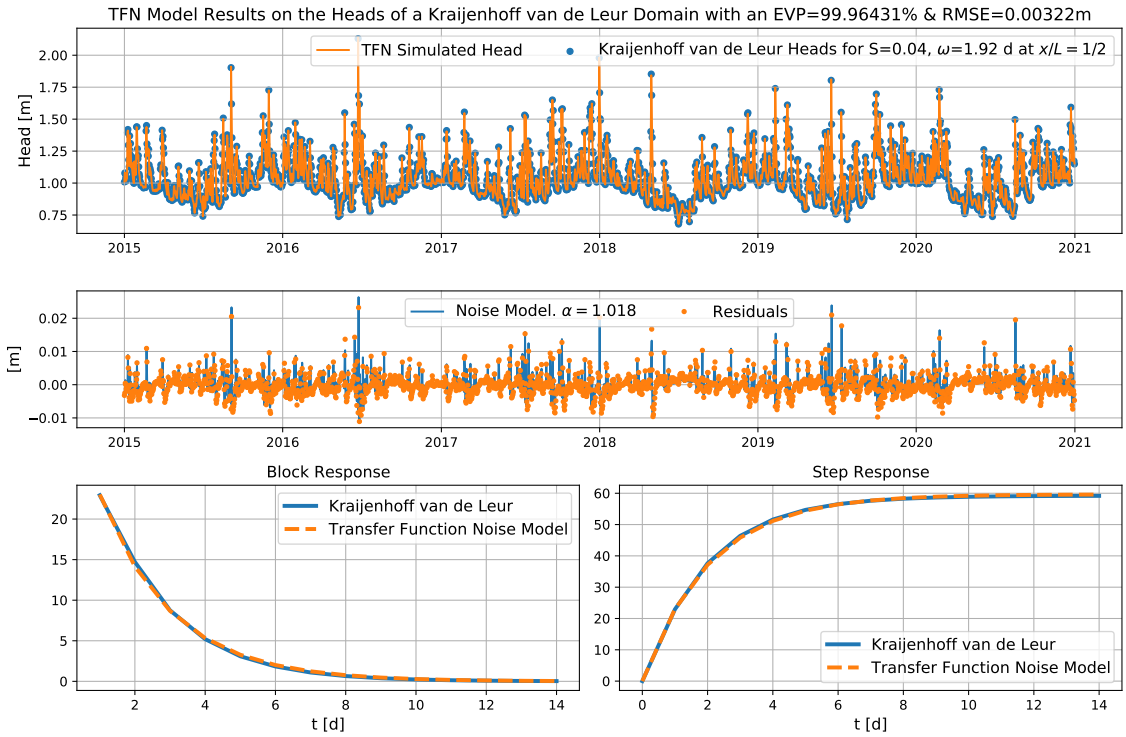

Figure 2.5: Transfer Function Noise Model for the domain from Kraijenhoff van de Leur (1958) with a horizontal head gradient at $x = \frac{L}{2}$.

a value for the drainage resistance c, we might be able to relate that to an actual Kraijenhoff van de Leur system. This way we can obtain an answer to our first research question what bottom boundary condition to use in the one-dimensional unsaturated zone model to create synthetic time series.

Our goal is then to compare the impulse responses of the two groundwater systems and to see at which locations, $\frac{x}{L}$, the impulse responses are most similar. Both the Kraijenhoff van de Leur and the linear reservoir system make use of the storativity S, so that parameter is the same for both systems. For the Kraijenhoff van de Leur system we have the reservoir coefficient ω and the length L of the domain. We can then run through x along the length of the domain L and calculate the impulse response with Equation 2.21. This Kraijenhoff van de Leur impulse response can then be compared with the linear reservoir systems impulse response to find the parameter for the drainage resistance c in Eq. 2.14, which gives the best fit of the two response functions.

To make sure that we do not draw a conclusion which is only applicable to one domain we use two Kraijenhoff van de Leur parameter sets. Kraijenhoff van de Leur (1958) gives information on a drainage area between small rivers in the Netherlands. The distance between the two small rivers is 3000 m and the soil is a coarse grained soil. The second domain is the same Dutch polder as used previously. The Kraijenhoff van de Leur parameters for these two systems are given in Table 2.1.

The best value of the drainage resistance c is found using least squares on both the impulse responses. The total time on which the impulse responses are fitted is five times the reservoir coefficient ω, because after that duration, the impulse has almost dissipated. The optimal values found for the drainage resistance c can be seen in Figure 2.6 for the Kraijenhoff van de Leur river system and in Figure 2.7 for the Dutch polder.

Table 2.1: Kraijenhoff van de Leur parameters for two drainage areas in the Netherlands.

Kraijenhoff van de Leur Parameters	Diluvial Soil between Rivers (Kraijenhoff van de Leur, 1958)	Flevoland Polder J25 (Ven, 1979)
L [m]	3000	300
T [m^2/d]	500	190 (calculated)
S [-]	0.2	0.04
ω [d]	365 (calculated)	1.92

Figure 2.7 and 2.6 shows the drainage resistance c versus the location x along the domain length. In the same Figure the root mean square error is shown for the response functions. The RMSE shows that we always make an error when comparing the linear reservoir system and kraijenhoff van de leur impulse response. There are however locations within both the domains where the root mean square error is relatively small (when $\frac{x}{L} = \frac{11}{40}$ or $\frac{29}{40}$). This can also be seen in from the impulse response at $\frac{x}{L} = \frac{11}{40}$ where the Kraijenhoff van de Leur impulse response shows the same exponential decay as the linear reservoir impulse response. Near the outflow channels (at $\frac{x}{L} = \frac{5}{1000}$ or $\frac{995}{100}$) the responses of the two systems are also similar but so fast that the drainage resistance is very low.

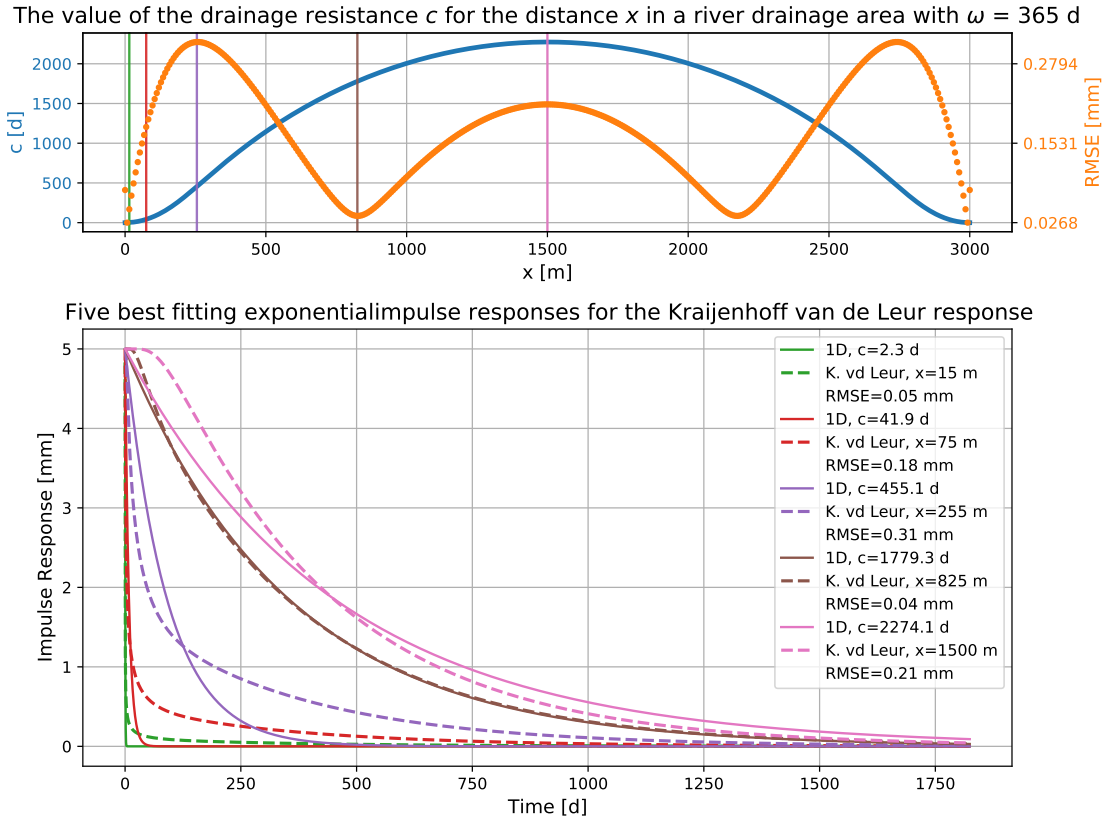

Figure 2.6: The best fit based on the impulse response of the drainage resistance c for a location x in a river drainage area with a diluvial soil (blue line) and the corresponding root mean square error (orange dots)

As expected with the Kraijenhoff van de Leur response the response at the centre of the domain shows some delay at first because the initial head gradient is zero. At the boundaries of the domain the water level drains quickly at first but stabilises due to the water coming through from the centre. The linear reservoir systems re-

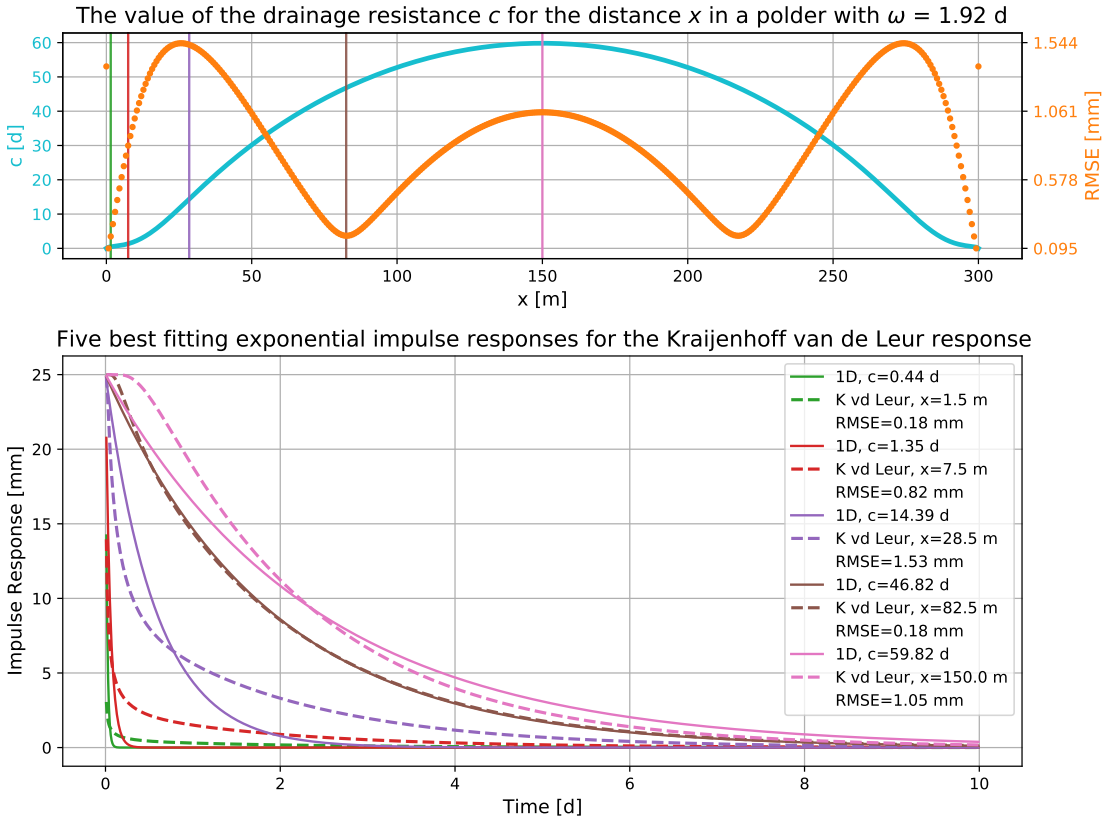

Figure 2.7: The best fit based on the impulse response of the drainage resistance c for a location x in a polder in Flevoland (cyan line) and the corresponding root mean square error (orange dots)

sponse is not able to capture these processes with the exponential response function.

We go back to the TFN model for the Dutch polder with the Kraijenhoff van de Leur equations. If we now use the location where $\frac{x}{L} = \frac{11}{40}$ the TFN model should improve since the responses are most similar at this location. The model results can be seen in Figure 2.8. The model has a high EVP of 99.993% and a RMSE of 0.0011 m which is better than the model at $\frac{x}{L} = \frac{1}{2}$.

Since Figure 2.7 shows that the location $\frac{x}{L} = \frac{11}{40}$ for the polder corresponds to a drainage resistance c of 46.82 days and storativity S of 0.04, these parameters should also be obtained from the TFN model. However a value of 47.07 d is found for A which relates to a value of $c = 47.07$ d. The value of the parameter $a = 1.8676$ d, which can is related to $S = \frac{a}{A} = 0.0397$ in a linear reservoir system. These values come close to the original values found in Figure 2.7 but are not exactly the same. This is due to the difference in the response functions used.

2.4 Findings of Chapter 2

Two things are shown in this chapter. First that the TFN model, using an exponential response function, can be used for a Kraijenhoff van de Leur groundwater systems at the cost of a slightly higher error. Second it can be reasoned the other way around that a system with certain drainage resistance c can be related to a realistic Kraijenhoff van de Leur system with certain properties at location $\frac{x}{L} = \frac{11}{40}$. For this case

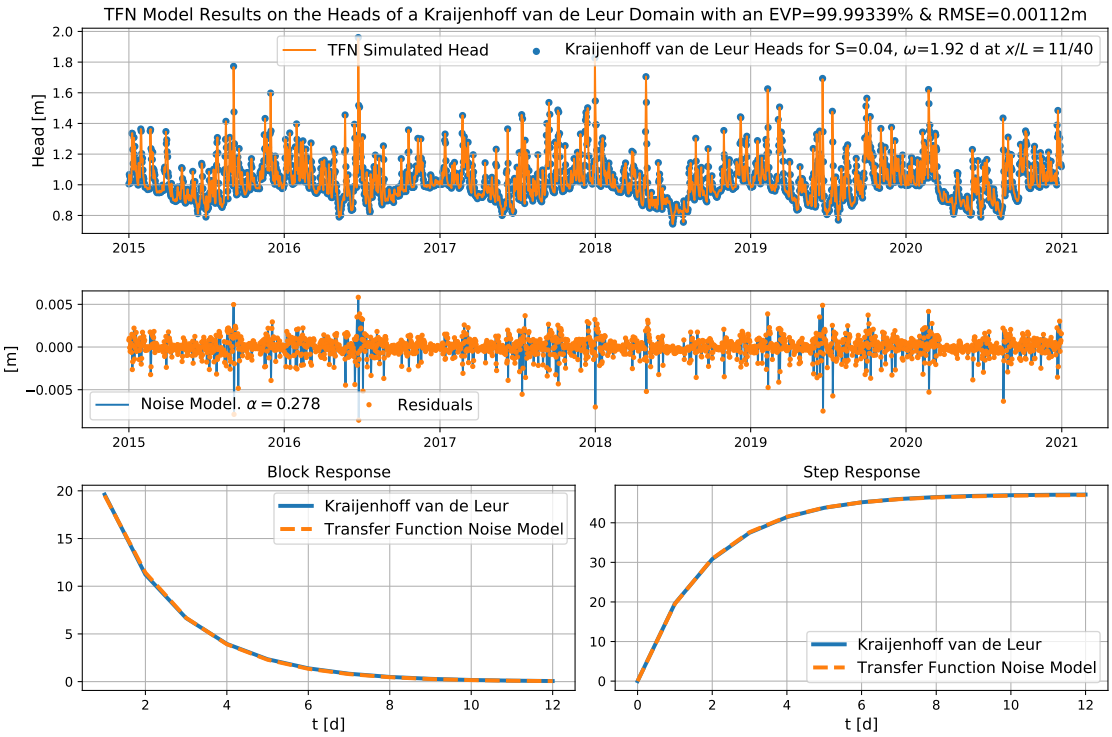

Figure 2.8: Transfer Function Noise Model for the domain from Kraijenhoff van de Leur (1958) with a horizontal head gradient at $\frac{x}{L} = \frac{11}{40}$.

specifically that would mean that a drainage resistance of 46.82 days can be related to the J25 polder in Flevoland at $x = 82.5$ m. This all comes at the cost of very small error which is made in using the exponential response for system that behaves with a Kraijenhoff van de Leur response.

This answers research question 1 such that we can now use a drainage resistance of 46.82 days as a bottom boundary condition for our one-dimensional unsaturated zone model. This way our time series will be as realistic as possible and the conclusions can be related to the polder Kraijenhoff van de Leur domain.

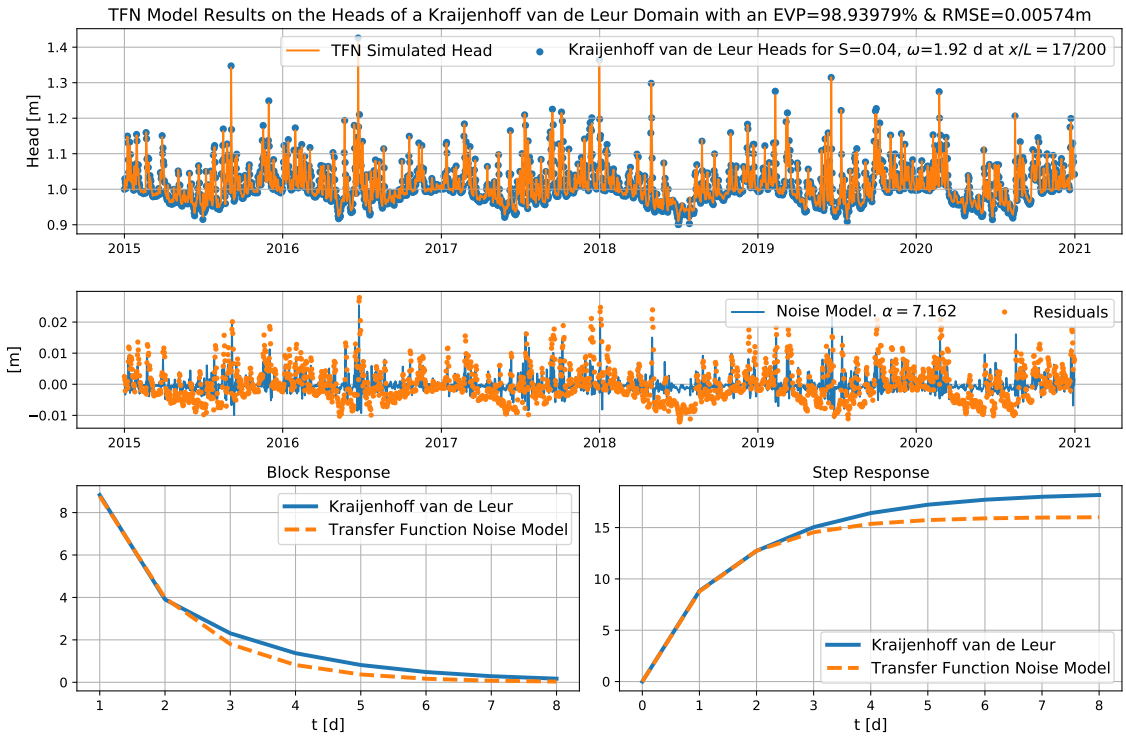

Figure 2.9: Transfer Function Noise Model for the domain from Kraijenhoff van de Leur (1958) with a horizontal head gradient at $\frac{x}{L} = \frac{17}{200}$.

3 | Unsaturated Zone

The unsaturated zone, also referred to as the vadose zone, is the portion of the subsurface above the groundwater table. The soil and rock in this zone contains air as well as water in its pores. The unsaturated zone is the main factor controlling water movement from the land surface to the groundwater.

This chapter looks at the processes concerning water in the unsaturated zone. First by looking at (the flow of) water in the unsaturated zone, second by how water movement is modeled in the unsaturated zone with a one-dimensional model (HYDRUS-1D). The third section describes some nonlinear processes in the unsaturated zone modelled with HYDRUS-1D to answer research question 2.

3.1 Water in the Unsaturated Zone

In the unsaturated zone the pore water pressure $\mathcal{P}$ [F/A] is less than the atmospheric pressure. The pressures in the unsaturated zone are always taken with respect to the atmospheric pressure. Forces such as the attraction between water and the soil matrix play a significant role here. The water content θ [-] in the unsaturated zone is defined as the volume of water over the total volume. The lower the water content, the lower the pore water pressure. As θ decreases, flowing water must navigate through a smaller, more tortuous network of water passageways in the soil. As a result, the hydraulic conductivity K [L/T] decreases as θ decreases (Fitts, 2013).

Since the pore water pressure above the water table is negative, the pressure head $\frac{\mathcal{P}}{\rho_w g}$ [L] is also negative negative, where ρ_w is the density of water [M/L^3] and g is the gravitational constant [L/T^2]. There is a capillary fringe above the water table where the soil is saturated ($\theta \simeq$ porosity $= \theta_s$) and the pressure is less than atmospheric ($\mathcal{P} < 0$). The saturation of the soil θ as a function of the pressure head is often approximated by the van Genuchten equation (van Genuchten, 1980):

$$\theta(\psi) = \theta_r + \frac{\theta_s - \theta_r}{[1 + (\alpha|\psi|)^n]^m} \tag{3.1}$$

where $\psi = \frac{\mathcal{P}}{\rho_w g}$ [L], θ_r is the residual saturation (field capcity), α is a shape parameter [L^{-1}] related to the inverse of the air suction, n is a dimensionless measure of the pore size distribution and $m = 1 - \frac{1}{n}$. All these parameters are dependent on the soil type and properties. For each soil type's specific parameters, the pressure head against the water content can then be plotted. The resulting curve is called the water retention curve which can be seen in Figure 3.1 for five different soil types.

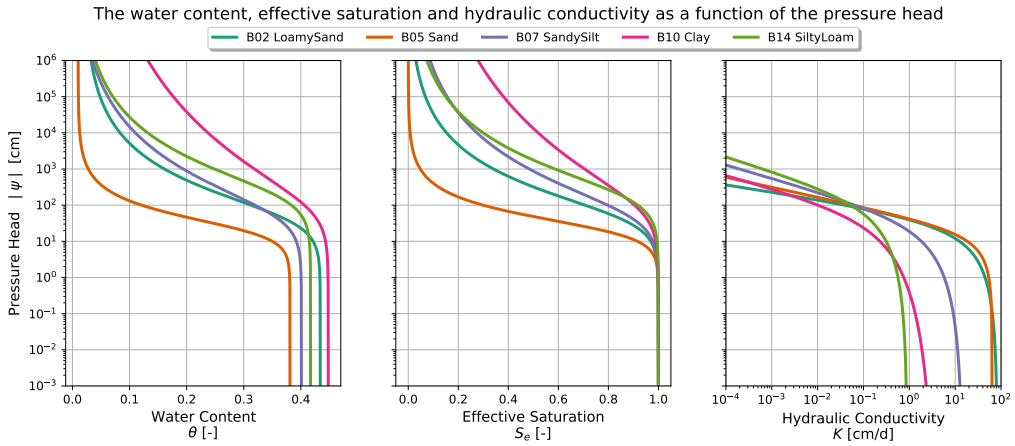

Figure 3.1: The soil water retention curve (left) based on the van Genuchten equation 3.1 for different soil types. On the right the hydraulic conductivity for the same soil types.

3.1.1 Vertical Flow

Vertical discharge q_z [L/T] can be described with Darcy's law as (Fitts, 2013):

$$q_z = -K_z \left(\frac{\partial \psi}{\partial z} + 1 \right) \tag{3.2}$$

where K_z [L/T] is the vertical hydraulic conductivity. In the unsaturated zone the vertical hydraulic conductivity can be described as a function of the relative K_r and saturated K_s hydraulic conductivity [L/T]. The relative hydraulic conductivity is then a function of the water content such that the vertical hydraulic conductivity becomes (van Dam & Feddes, 2000):

$$K_z(\theta(\psi)) = K_s K_r(\theta(\psi)) = K_s \left(\frac{\theta(\psi) - \theta_r}{\theta_s - \theta_r} \right)^l \left[1 - \left[1 - \left(\frac{\theta(\psi) - \theta_r}{\theta_s - \theta_r} \right)^{\frac{1}{m}} \right]^m \right]^2 \tag{3.3}$$

where l is the pore connectivity parameter [-]. $\frac{\theta(\psi)-\theta_r}{\theta_s-\theta_r}$ is the same as S_e [-], the effective saturation:

$$S_e = \frac{\theta(\psi) - \theta_r}{\theta_s - \theta_r} \tag{3.4}$$

Combination of Darcy's law (Eq. 3.2) and the principle of mass conservation results in the Richards equation for vertical flow (as soil moisture) in the unsaturated zone (Simunek et al., 2009):

$$\frac{\partial \theta}{\partial t} = \frac{\partial}{\partial z} \left(K_z(\theta(\psi)) \left(\frac{\partial \psi}{\partial z} + 1 \right) \right) - Q(\psi) \tag{3.5}$$

where $Q(\psi)$ [T^{-1}] is the sink term, for example root water extraction.

The water content θ in the unsaturated zone is time-dependent. A precipitation event, and the infiltration thereafter, increases $\theta, \mathcal{P}, \psi$, and K in the soil, increases pore water pressures and results in downward flow. The water from a precipitation event migrates downward vertically as a pulse of higher water content. This pulse sinks through the unsaturated zone, ultimately adding to the saturated zone and raising the groundwater level (Fitts, 2013). Evaporation decreases the water content in the soil, the near surface soil develops lower $\theta, \mathcal{P}, h$ and K and upward flow may result. The soil moisture content of the unsaturated zone has both influence on the amount of infiltration after a precipitation event and the amount of the evaporation (Mays, 2010).

3.1.2 Groundwater Table or Head

The groundwater table is the location where the pressure head ψ is equal to zero. At this point the water content θ is equal to the saturated water content θ_s (=porosity). Full saturation can occur above the groundwater table. This zone is called the capillary fringe. The pressure at the top of the capillary fringe is called the air entry pressure.

The head is the pressure head plus the elevation at which the pressure head is measured.

3.2 Saturated / Unsaturated Zone Model

For the purpose of this research, synthetic time series for the groundwater table are generated. HYDRUS-1D is used to simulate a profile with physically realistic processes in the unsaturated zone. HYDRUS-1D computes the infiltration, recharge, actual soil evaporation, actual transpiration fluxes as well as the saturation (and pressure head) for a one-dimensional soil profile. The computation is done by solving the Richards Equation (3.5) (Simunek et al., 2009). HYDRUS-1D is run using pHydrus which is a Python package to create, run, optimise and visualise HYDRUS-1D models (Collenteur et al., 2020).

The 1D model of HYDRUS-1D is based on a number of approximations. Most important of which is that the Richards Equation (3.5) is valid. This implies that the air phase and thermal gradients play an insignificant role in the process of water flow (Simunek et al., 2009). Changes in the volume of water in the soil profile caused by water flow are matched immediately by changes in gas volume. This can result in unrealistic simulations especially when the soil is very dry. For the models of this research the profiles are always relatively wet so this is not an issue.

HYDRUS-1D has been extensively used for the simulation of one-dimensional vertical flow. Less frequent is the simulation of the groundwater table with the use of HYDRUS-1D (Wang & Pozdniakov, 2014; Neto et al., 2016). This is due to the model limitation that the groundwater is only dependent on vertical flow. This is an approximation because in reality flow in the unsaturated and saturated zones is three-dimensional.

3.2.1 HYDRUS-1D Model Description

A one-dimensional vertical saturated-unsaturated profile was modeled in HYDRUS-1D. The profile has two layers with the lower layer always as a 2 cm thick, low permeable clay soil ($K_s = 0.0427$ cm/d, $\theta_r = 0.07$, $\theta_s = 0.36$, $\alpha = 0.005$ cm$^{-}1$, $n = 1.09$, $\lambda = 0.5$). This way the drainage resistance c is 46.82 days from which it is known that it can be related to a 2D polder domain as explained in section 2.3. The upper layer is homogeneous and no hysteresis is present in the system. Each model starts at hydrostatic conditions with the groundwater table within the domain of the model. The groundwater table is taken at the elevation where the pressure head ψ is equal to zero.

Boundary Conditions

The lower boundary is located below the low permeable clay layer. The lower boundary condition is a Dirichlet-type boundary condition with a constant pressure head. The constant pressure head is set to 20 cm such that the drainage level is always cm above the lowest cell.

The upper boundary of the profile is the soil surface. The upper boundary condition is set to an atmospheric boundary condition with a surface layer with no runoff. At the surface layer the precipitation and soil evaporation flux is applied. The flux across the top boundary is controlled by the externally applied fluxes but is dependent on the prevailing soil moisture conditions near the surface. The soil surface boundary condition may change from a prescribed flux to a prescribed head type condition (and vice-versa). Water that ponds on the surface will infiltrate according to the hydraulic conductivity and pressure head gradient (Simunek et al., 2009).

Soil Hydraulic Properties

For the soil hydraulic model, the van Genuchten model with air-entry pressure of -2cm is used. The model has six soil hydraulic parameters which are taken from the Staring series. The most recent version (2018) of this database is used, which contains the soil physical properties for common top- and subsoils in the Netherlands (Heinen et al., 2020). A topsoil can be distinguished from a subsoil due to a difference in physical characteristics and texture. A topsoil usually contains more organic material and has a larger saturated conductivity. A topsoil always lies on top of a subsoil. From this database five different topsoils are chosen with a wide range in saturated conductivity K_s. The soil hydraulic parameters of these soil types can be found in Table 3.1.

Table 3.1: Staring Series Soil Hydraulic Parameters

Soil Sample	θ_r [−]	θ_s [−]	α [cm^{-1}]	n [−]	K_s [$\frac{\text{cm}}{\text{d}}$]	l [−]	Description
B02	0.02	0.434	0.0216	1.349	83.24	7.202	Loamy Sand
B05	0.01	0.381	0.0428	1.808	63.65	0.024	Sand
B07	0.00	0.401	0.0183	1.248	14.58	0.952	Sandy Silt
B10	0.01	0.448	0.0128	1.135	3.83	4.581	Clay
B14	0.01	0.417	0.0054	1.302	0.90	-0.335	Silty Loam

Temporal and Spatial Discretization

The time discretization associatied with the implementation of boundary conditions, model output and t boundary conditions is with a daily time step. The internal time discretization associated with the numerical solution of HYDRUS-1D is done according to the notes on discretization (Simunek, 2009).

For the spatial discretization an finite element mesh is constructed by dividing the soil profile into elements whose sizes are defined by the z-coordinates of the nodes that form the element corners (Simunek, 2009). The nodes in the root zone (upper cells) are relatively much smaller since there the hydraulic gradients are expected to be largest. The hydraulic gradients at the bottom of the soil profile are expected to be smaller and thus the size of the elements is larger.

With coarse-textured soils, having relatively high n and a van Genuchten parameters, the discretization needs to be finer than finer-textured soils. That is because soil hydraulic functions are more nonlinear and thus the numerical solution may be less stable.

In practice all the simulations used a 0.5 cm mesh size for the root zone. Below the root zone the mesh size increased up to 2 cm, but so that the ratio of the sizes of two neighbouring elements would not exceed 1.5. If the simulations did not converge, the mesh size below the root zone would increase up to 1 cm.

Atmosphere

The meteorologic data is preprocessed according to the HYDRUS-1D manual (Simunek et al., 2009) and Sutanto et al. (2012). This means that, based on the vegetation properties, interception takes place and potential evaporation is split into potential soil evaporation and potential transpiration. In the research of Sutanto et al. (2012) this way of partitioning of potential evaporation was tested against isotope measurements. Approximately the same values of this research, which looked at the vegetation properties of grass, were also used for this research.

Interception in HYDRUS-1D is modeled with a daily threshold. The threshold E_i [L/T] is a function of the amount of precipitation P [L/T], the leaf area index L_{AI} [-], the soil cover fraction S_{CF} [-] and a constant a [L]:

$$E_i = aL_{AI}\left(1 - \frac{1}{1 + \frac{S_{CF}P}{aL_{AI}}}\right) \tag{3.6}$$

where the $L_{AI} = 0.24 \cdot h_{grass}$ (h_{grass} = crop height = 15 cm), $S_{CF} = 1 - e^{-k \cdot L_{AI}}$ and a = 0.4 mm. The constant k corrects for the radiation extinction by the canopy and is equal to 0.463. The net precipitation reaching the top cell of the model is $max(P - E_i, 0)$.

The potential transpiration ($E_{t,p}$ [L/T]) and potential soil evaporation ($E_{s,p}$ [L/T]) are partitioned according to Beer's law (Simunek et al., 2009) using the soil cover fraction:

$$E_{t,p} = \max\left(E_p - E_i, 0\right) \cdot S_{CF} \tag{3.7}$$

$$E_{s,p} = \max\left(E_p - E_i, 0\right) \cdot (1 - S_{CF}) \tag{3.8}$$

when E_p [L/T] is the Penman Monteith potential evaporation calculated with the equation from Allen et al. (1998). We use Penman Monteith instead of Makkink evaporation since the Penman Monteith equation takes into account both the radiation and aerodynamic aspects of evaporation. The Makkink evaporation does not incorporate the aerodynamic aspects which results in a lower estimate for the potential evaporation, especially in winter (Schuurmans & Droogers, 2010).

Based on the available water in the profile, HYDRUS-1D calculates the actual fluxes of transpiration E_t and soil evaporation E_s. The potential transpiration flux is used for the root water uptake in the root zone, the potential soil evaporation is extracted from the top node of the profile if there is enough water available.

The data for calculating the meteorological fluxes are used from the Royal Netherlands Meteorological Institute (KNMI) weather station in De Bilt. This station is chosen since it has the longest time series in the Netherlands with evaporation data reaching back to 1957 and precipitation data up to 1906. The four years preceding 2021 are visualised in Figure 3.2.

Root Water Uptake

The sink term $Q(\psi)$ [T$^-$1] in the Richards equation (Eq. 3.5) is taken as the root water uptake in the HYDRUS-1D model. The root water uptake is described by:

$$Q(\psi) = a(\psi)S_p \tag{3.9}$$

and is taken as a function of the pressure head instead of the soil water content. S_p is the potential water uptake rate [T^{-1}] and $a(\psi)$ is the dimensionless root-water uptake stress response function with $0 \leq a \leq 1$. This function is described by an S-shaped formula proposed by van Genuchten (1987):

$$a(\psi) = \frac{1}{1 + \left(\frac{\psi}{\psi_{50}}\right)^p} \tag{3.10}$$

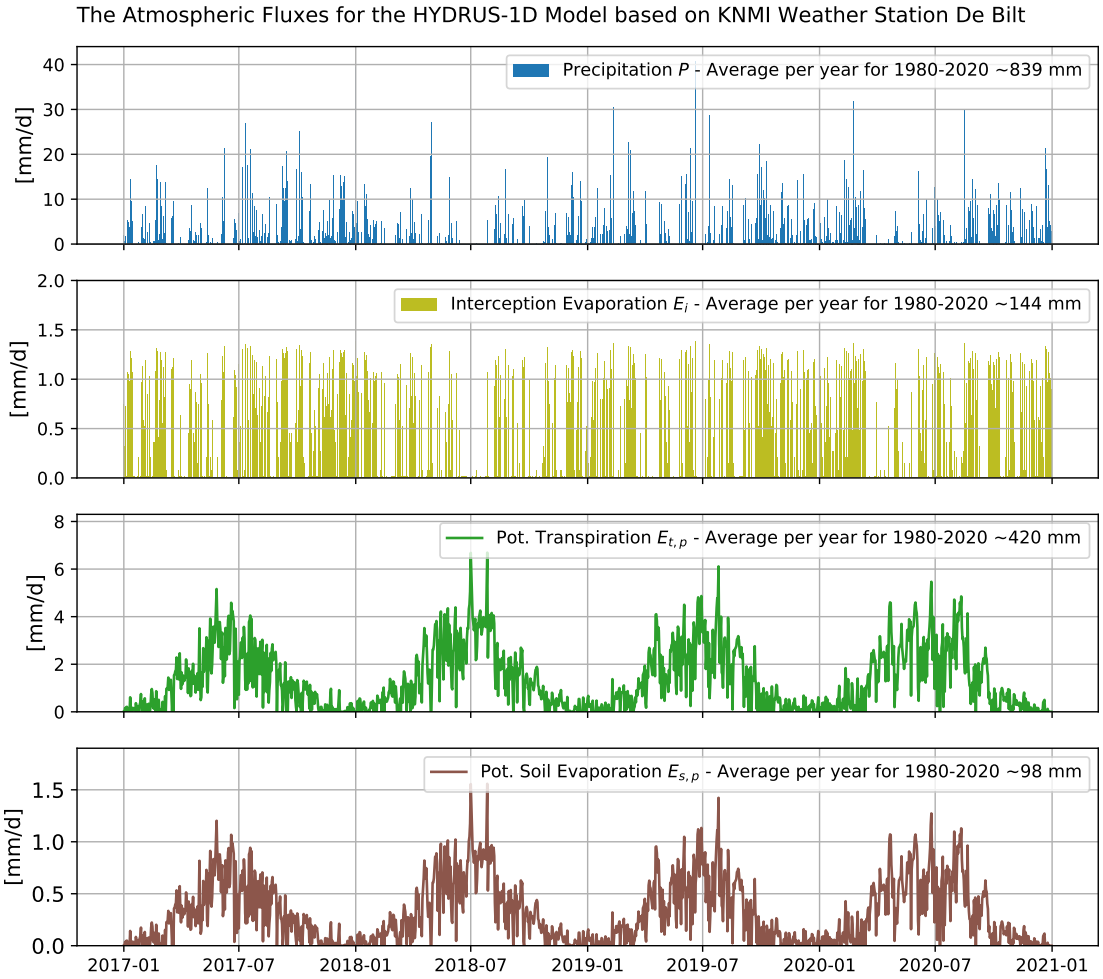

Figure 3.2: The atmospheric fluxes for the HYDRUS-1D model. Note that that the actual time series are longer. The average flux per year is calculated for the years 1980-2020.

where p is the shape parameter and ψ_{50} [L] is the pressure head at which the extraction rate is reduced by 50%. This method has significant numerical advantages over the Feddes root uptake model due to its shape and characterisation by only two parameters (van Genuchten, 1987). It does however not consider near-saturation transpiration reduction but that is justified when near-saturation conditions only occur for short periods of time. The determination of ψ_{50} is a bit ambiguous and depends on the soil type. However from Grinevskii (2011) we can see that for grassy vegetation on different soil types, a value of -4000 cm for ψ_{50} is acceptable for the purpose of this research.

The potential water uptake S_p can be distributed over the root zone with a function $b(z)$ [L^{-1}] which is the normalized water uptake distribution. The function $b(z)$ describes the spatial variation over the root zone and is related to the root distribution. The potential water uptake is a function of $b(z)$ and the potential transpiration rate $E_{t,p}$:

$$S_p = b(z)E_{t,p} \tag{3.11}$$

The root distribution for the HYDRUS-1D model is described by the function (Simunek et al., 2009):

$$b(z) = \begin{cases} \frac{5/3}{L_r} & z > -0.2L_r \\ \frac{25/12}{L_r}\left(1 + \frac{z}{L_r}\right) & -L_r \leq z \leq -0.2L_r \\ 0 & z < -L_r \end{cases} \tag{3.12}$$

where L_r is the maximum root depth [L], z [L] is the elevation with the soil surface always at the zero-datum.

3.3 Nonlinear Groundwater Behaviour due to the Unsaturated Zone

Before we look at nonlinear behaviour is, we first define what linear behaviour of the groundwater table is. With linear behaviour, one expects that if twice the amount of water precipitates (and fully infiltrates), the response of the groundwater table is twice as large (e.g. Peterson & Western, 2014).

Many nonlinear processes are present in the unsaturated zone. For instance the nonlinear relation between degree of saturation and the hydraulic conductivity. As a result the percolation to the water table in the root zone is highly nonlinear (Feddes et al., 1988). Another source of nonlinearity is the actual evaporation since the degree of saturation influences the water uptake by roots (Berendrecht et al., 2006).

In this section some aspects of the nonlinearity due to the unsaturated zone are described. The first section describes the groundwater response with changing precipitation amounts. The second section looks at the how the initial groundwater table and saturation changes the effect for the same precipitation event. In the third section the impact of a precipitation event under normal weather conditions is assessed.

3.3.1 Groundwater Response to Different Precipitation Events

In Figure 3.3 the effect of an infiltration event of 10 mm of precipitation in one day is shown. The drainage level is located at -100 cm. No evaporation or transpiration is simulated during this simulation. Each model starts from hydrostatic conditions. The only real difference between the soils is that the wetting front is smoother. Dependent on the soil type the system has a fast or slow response, where the silty loam has the fastest response. The sand and loamy sand soils have the slowest response. This may sound counter intuitive but the saturation under hydrostatic conditions for a sandy soil is relatively low, resulting in a low hydraulic conductivity.

The precipitation amount is changed for each model and the results are shown in Figure 3.4. In this figure there are five different precipitation amounts modelled; 1, 3, 5, 10, 15 and 20 mm of precipitation in one day. For each precipitation amount and soil type the modelled response of the groundwater table is shown.

Two clear trends are observed in the responses. The first trend is that the response of the groundwater table becomes more than twice as large if the precipitation amount doubles. This is a clear sign of non-linearity. The second trend is that not only does the size increase, also the peak of the response shifts to an earlier moment if the precipitation amount increases. Note however that the model has a daily time-step.

Figure 3.5 shows the same modelled responses as Fig. 3.4, but then focused on the B10 clay soil type. In this Figure the linear response is shown for the system. The linear response is based on multiplication of the the response of 1mm precipitation in one day. Here the big discrepancy is observed between the modelled and linear

response, especially for the larger precipitation amounts. The response of 1mm precipitation in one day is also what Pastas uses as the block response for convolution.

It is concluded that both the shape and the magnitude of the response of the groundwater table can significantly differ when the precipitation amount is doubled. The fact that the maximum response of the groundwater table is not doubled after doubling in the precipitation amount demonstrates that the unsaturated zone behaves non-linearly for this model setup.

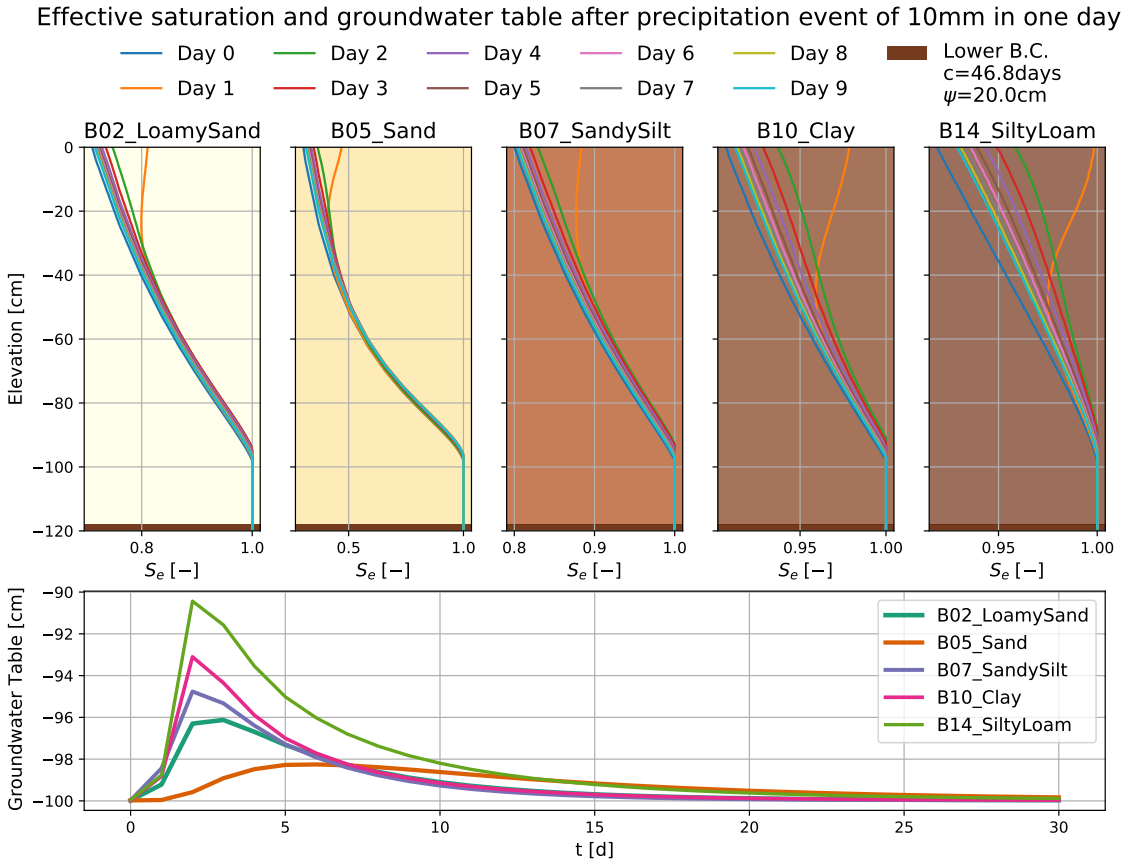

Figure 3.3: Infiltration of a 10 mm precipitation amount over time and the corresponding groundwater table for a groundwater depth of 100 cm.

3.3.2 Groundwater Response to Wetter Conditions

For this subsection the state of the unsaturated zone is changed by applying different amounts of precipitation until the profile reaches an equilibrium state. The higher the amount of this 'base' precipitation, the higher the groundwater table and water content of the unsaturated zone. On top of this constant precipitation, every 300 days 10 mm of extra precipitation is applied. The drainage level is located at -100cm. No evaporation or transpiration occurs during this simulation.

The results of this simulation are shown in Figure 3.6. The response of the groundwater table to the 10mm extra precipitation can be seen more closely in Figure 3.7. This figure also shows the saturation profile and initial water table before the precipitation infiltrates. As the profile becomes more saturated and the groundwater level rises, the response of the groundwater table becomes higher and quicker. This demonstrates that not just the amount of precipitation, but also the state of the unsat-

urated zone affects the response of the groundwater table. Note that this simulation again does not incorporate evaporation and transpiration.

3.3.3 Groundwater Response under Normal Conditions

To take into account the groundwater response under normal conditions two simulations are run for a model with precipitation, soil evaporation, and transpiration (Fig. 3.8). For this simulation every 180 days 10 mm precipitation is added in one day on top of the normal precipitation series (so once in summer and once in winter). The two groundwater table time series simulated are subtracted from one another to asses the impact of the extra precipitation.

Figure 3.9 shows the change in the groundwater response after the 10 mm of extra precipitation in one day. It is observed that when the soil is dry and a lot of evaporation and transpiration occurs (in summer) the response of the groundwater is very small. Almost all the water that enters the soil profile evaporates and does not flow as recharge towards the groundwater table. In winter, when the profile is wet and transpiration rates are low, the response is larger and more similar to what was observed for a single precipitation event in the previous experiment (Fig. 3.6 & 3.7. Do note that the shape of the response can have two peaks. This means that more water, from a later precipitation event, flows towards the water table than in the first simulation.

For soil types with relatively fast responses there is a smaller impact of precipitation events that occur later. However for silty loam, where ponding can occur due to the low permeability, large changes are observed in the groundwater table response. In this specific case even a negative response is observed due to the groundwater level dropping sooner after full saturation and ponding occurs. This can be seen in Figure A.1.

3.4 Findings of Chapter 3

To conclude this chapter we answer research question 2: How does the unsaturated zone affect the nonlinear behaviour of the groundwater table? It is seen from section 3.3 that the unsaturated zone causes for highly nonlinear behaviour. When the amount of precipitation doubles, the response does not become twice as large. Also the state of the unsaturated zone is of a large influence. When the unsaturated zone is more wet, the response is larger. In the last simulation it is seen that there can even be no response at all to 10mm of precipitation if the conditions are dry.

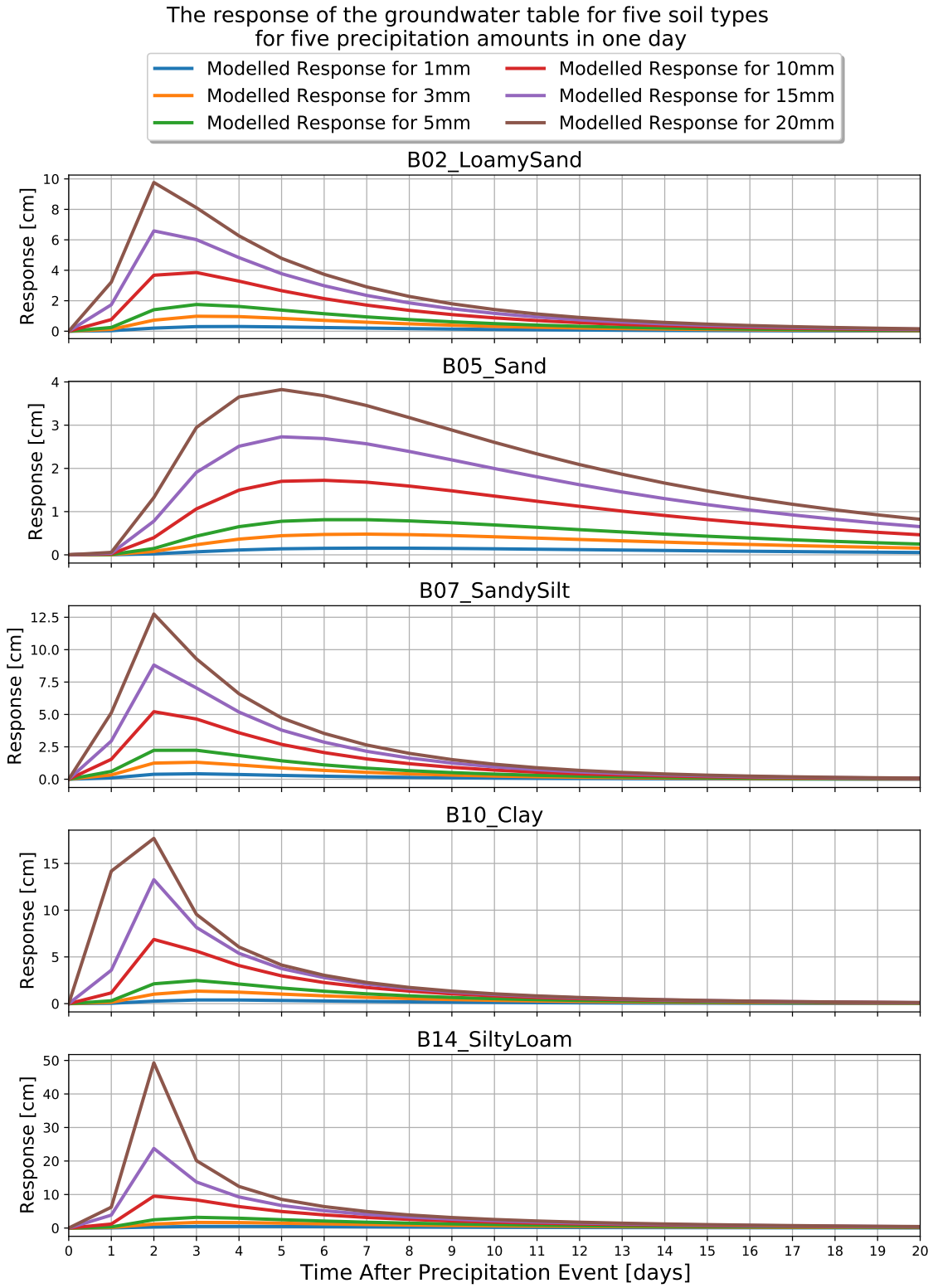

Figure 3.4: The modelled groundwater response of five soil types for different precipitation amounts in one day.

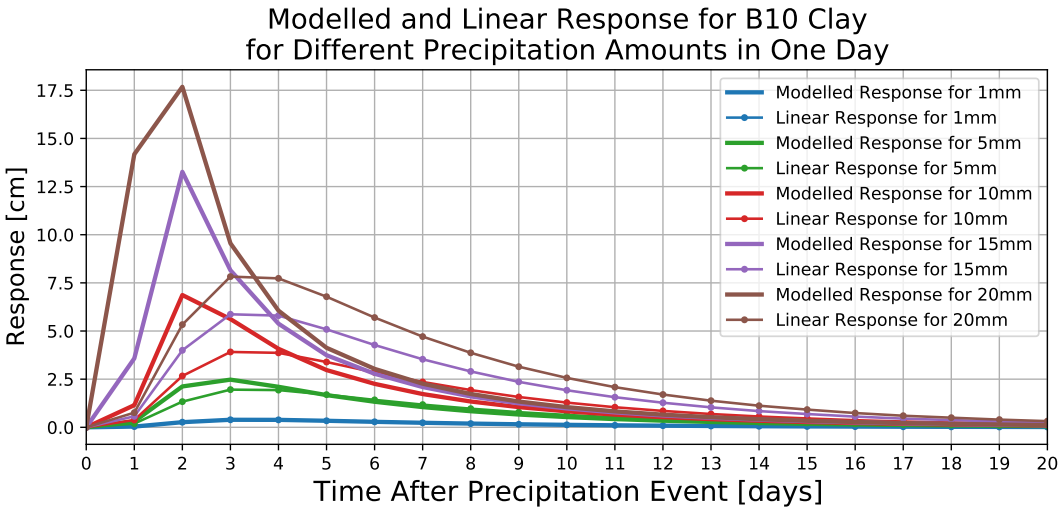

Figure 3.5: The modelled and linear response for B10 clay. The linear response is based on multiplication of the block response of a 1 mm precipitation event.

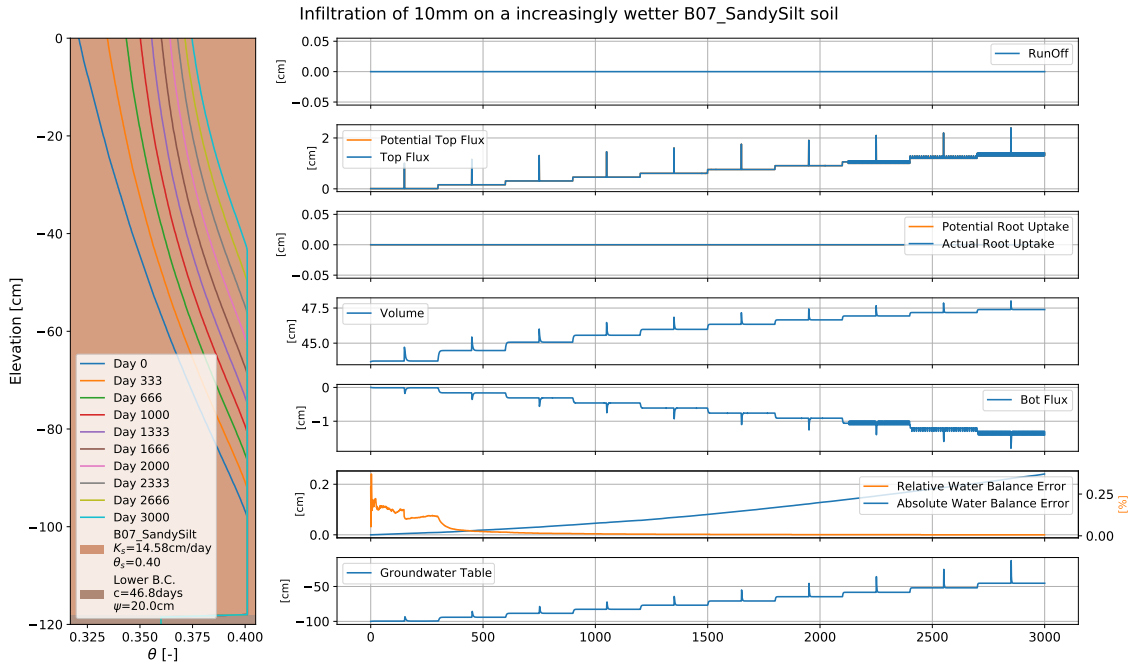

Figure 3.6: Overview of the HYDRUS-1D model with sandy silt (B07). The amount of precipitation increases with steps of 1.5 mm to bring the profile to a wetter equilibrium. A precipitation event of 10 mm in one day occurs every 300 days. Some numerical wiggles are seen near the end of the simulation but this does not effect the result.

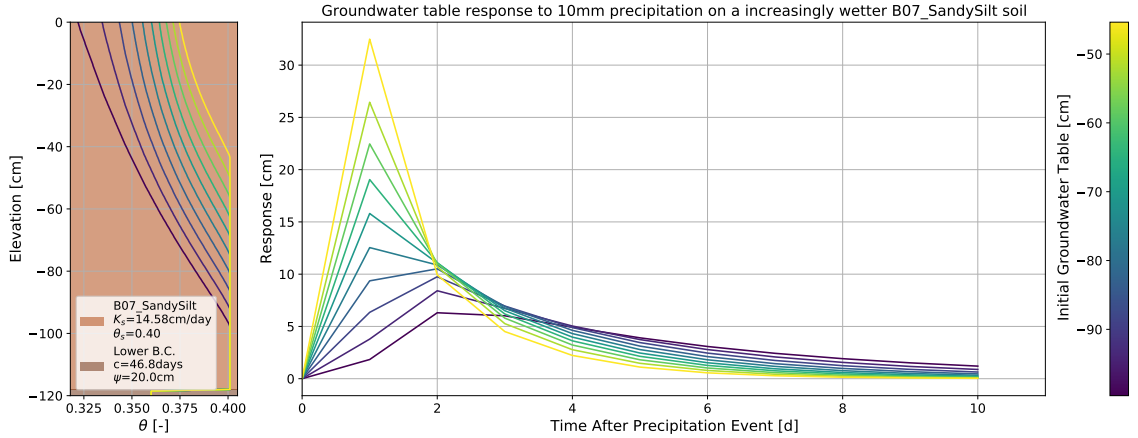

Figure 3.7: The response of the groundwater table

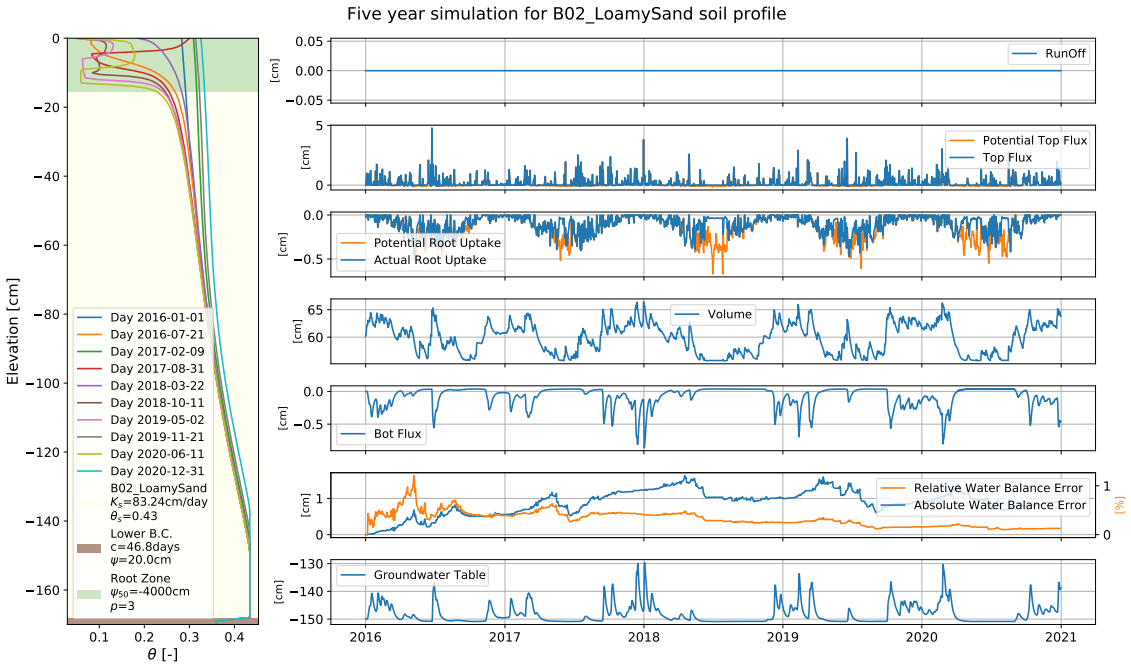

Figure 3.8: Overview of the HYDRUS-1D base model with loamy sand (B02). This simulation has the measured precipitation time series.

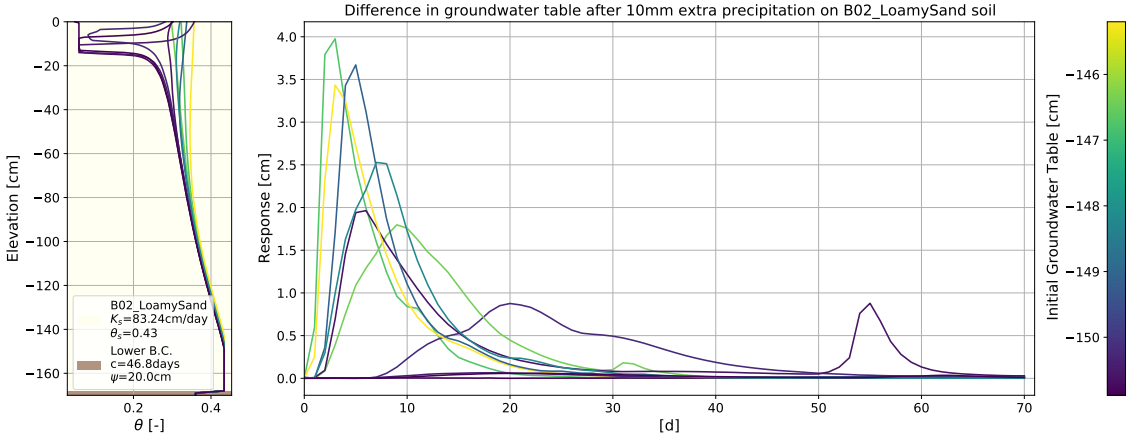

Figure 3.9: Change in groundwater table after 10mm of extra precipitation on top of normal weather conditions.

4 Unsaturated Zone in Time Series Analysis

In chapter 2 the unsaturated zone was completely ignored in the time series analysis. However in the previous chapter, as an answer to research question 2, it was shown that the unsaturated zone has a large effect on the groundwater table. The saturation degree of the unsaturated zone has a large effect on the evaporation and recharge fluxes in the system. Especially the root zone is a large cause of this non-linear behaviour.

To get an answer to research question 3 this chapter focuses on the ways time series models try to tackle this problem of non-linearity. TFN models have two methods to account for the unsaturated zone. The first is changing the impulse response function $\vartheta(t)$ (of the recharge flux) which is discussed in section 4.1. The second method uses the recharge as the main stress. In this case the time series model is coupled with an unsaturated zone model to estimate the recharge which is discussed in 4.2. The third section answers research question 3 and compares the performance of the linear and nonlinear recharge models for synthetic time series created with the HYDRUS-1D unsaturated zone model.

4.1 Response Functions and the Unsaturated Zone

If the unsaturated zone's main effect is retardation and dispersion of infiltration, then the convection-dispersion equation can be used to describe the 'average' effect of the unsaturated zone. A solution for the impulse response from the convection-dispersion equation can be derived from linearization of the Richards' equation (Eq. 3.5) around some constant water content using Taylor expansion (von Asmuth;, 2012):

$$\vartheta(z,t) = \frac{z}{4\sqrt{\pi D t^3}} \exp\left(\frac{-(z-ut)^2}{4Dt}\right) \tag{4.1}$$

D is the dispersion coefficient [L^2/T] and z is the elevation [L] (with the top of the unsaturated zone at z=0). u is the effective propagation velocity [L/T] of the pressure wave (pulse). This effective velocity of the water is much smaller. We can use this estimate for the unsaturated zone impulse response function to estimate the combined response function $\vartheta_c(t)$. This is done by convolution of the two separate responses of the saturated zone ϑ_{sz} and the saturated zone:

$$\vartheta_c = \int_{-\infty}^{t} \vartheta_{sz}(t-\tau)\vartheta_{uz}(\tau)d\tau \tag{4.2}$$

This process of combining the responses is shown visually in Figure 4.1. The resulting combined response has the shape of a skewed distribution function. That is why in Pastas there is a response function that uses the scaled gamma distribution (which is also a skewed distribution). This function is a continuous function and is described

as (Collenteur et al., 2019):

$$\vartheta(t) = A\frac{t^{n-1}}{a^n\Gamma(n)}e^{\frac{-t}{a}}, \quad t \geq 0 \tag{4.3}$$

where A is the scaling factor, a and n are shape parameters and $\Gamma(n)$ is the Gamma function. Note that the last response function is similar to the exponential response function (Eq. 2.3) but with one extra parameter n, where if $n = 1$ the exponential response function is obtained.

Another response function that is available in Pastas is the four-parameters function:

$$\vartheta(t) = A\frac{t^{n-1}}{a^n\Gamma(n)}e^{-\frac{t}{a}-\frac{ab}{t}}, \quad t \geq 0 \tag{4.4}$$

where there is an extra shape parameter b (Bakker et al., 2008). This parameter delays the response and if its equal to zero, the gamma response function is obtained.

The three response functions; exponential, gamma and four-parameters are shown in Figure 4.2. In this Figure both the gamma and four-parameters function have a peak of the response that is delayed. Both functions, but especially the four-parameters function show approximately the same shape as the combined response found in Figure 4.1. So by using the four-parameters or gamma response function we incorporate an effect of the unsaturated zone in the TFN model, assuming that the effect is linear.

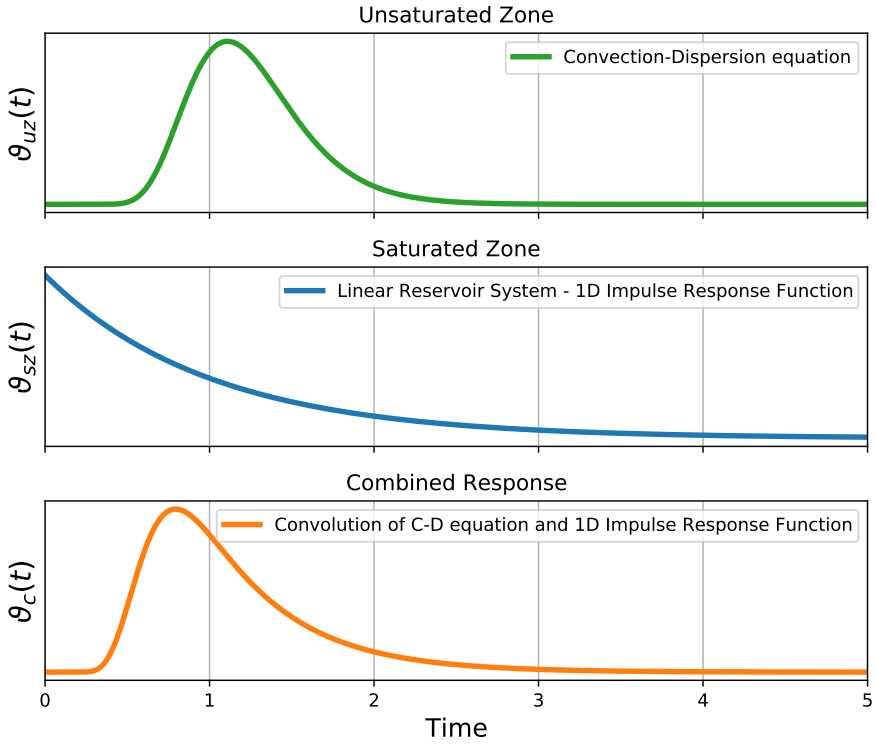

Figure 4.1: The combined impulse response computed by convolution as a function of the unsaturated zone response (Eq. 4.1) and the saturated zone (1D) response (Eq. 2.14).

4.2 Recharge Models

A TFN model can have multiple stresses as input to create an output for the head. In theory, if the actual recharge is used as a input stress for the TFN-model and the

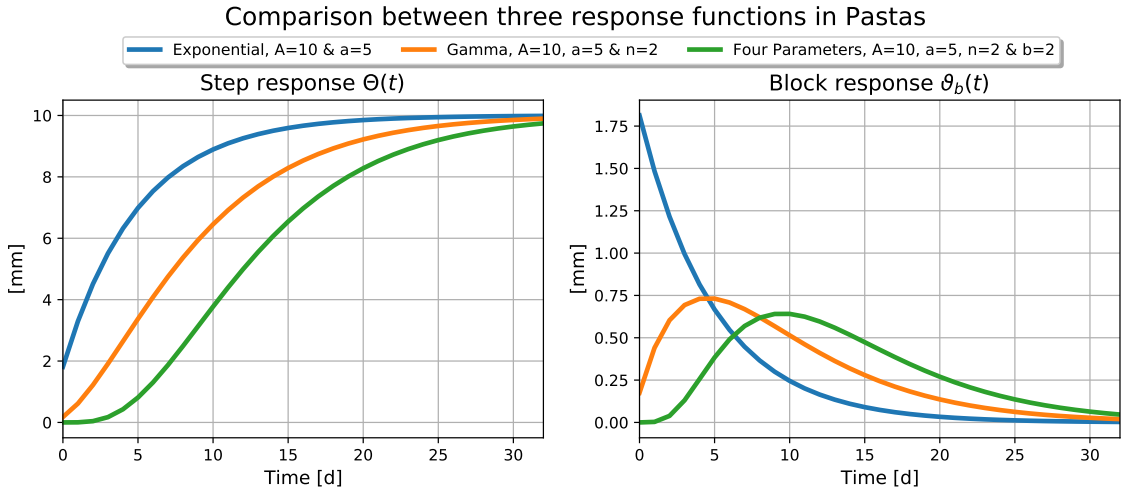

Figure 4.2: The exponential, gamma and four-parameters response functions available in the TFN model Pastas with some random parameters. Note that the parameters are used for the step response function, not the block response.

response function of the can take the exact shape, the fit of the TFN model should be perfect (as shown in section 2.2.2) if there is no noise. To achieve the same effect of a good fit, the recharge can be modelled and used as an input stress in the TFN model. In Pastas there are two options to estimate the recharge, a linear model and a nonlinear model which are described in subsections 4.2.1 and 4.2.2 respectively.

4.2.1 The linear model

The linear model approximates the groundwater recharge R as the precipitation surplus. The recharge is a linear combination of the rainfall $P(t)$ and potential evaporation $E_p(t)$:

$$R(t) = P(t) - fE_p(t) \tag{4.5}$$

where f is called the evaporation factor (Collenteur et al., 2019). This parameter is optimised between 0 and 2 and determines the ratio between the effect of the precipitation and potential evaporation.

Writing the recharge as a linear combination of the precipitation and evaporation comes from the water balance of the unsaturated zone where the recharge can be formulated from all the other fluxes in the unsaturated zone (de Ridder & Boonstra, 1994):

$$R = P - R_o - E_s - E_t - E_i - \frac{\Delta S_u}{\Delta t} \tag{4.6}$$

where R is the recharge, P is the precipitation, R_o is the amount of runoff, E_s is the soil evaporation, E_t is the transpiration, E_i is the interception evaporation and $\frac{\Delta S_u}{\Delta t}$ is the change in storage in the unsaturated zone. All dimensions are [L/T]. The linear recharge model is based on the following approximation: there is no runoff, all the evaporation fluxes can be summed and reduced by a constant (f) and, there is no storage in the unsaturated zone.

4.2.2 The nonlinear (FLEX) model

The FLEX model, as described by Collenteur; et al. (2021), is a nonlinear recharge model with two storage zones as seen in 4.3. The two storage zones are an interception zone and a root zone reservoir. The water balance for the interception reservoir

is written as:

$$\frac{\Delta S_i}{\Delta t} = P - E_i - P_e \tag{4.7}$$

where P_e is the effective precipitation that goes to the root zone. The interception evaporation E_i is equal to the maximum potential evaporation $k_v E_p (= E_{max})$ (energy-limited) or the amount of water available S_i (water-limited). The water balance for the unsaturated zone reservoir is written as:

$$\frac{dS_r}{dt} = P_e - E_{s,t} - R \tag{4.8}$$

where $E_{s,t}$ is the combined evaporation flux constituting of both soil evaporation and transpiration which is:

$$E_{s,t} = (E_{max} - E_i) \min\left(1, \frac{S_r}{l_p S_{r,max}}\right) \tag{4.9}$$

The recharge from the root zone is calculated as:

$$R = K_s \left(\frac{S_r}{S_{r,max}}\right)^{\gamma} \tag{4.10}$$

The nonlinear FLEX recharge model has six parameters of which three are commonly estimated. The fixed values or the boundaries for the parameters are presented in Table 4.1. The list below describes the (physical) meaning of each of the parameters.

- $S_{r,max}$ is the maximum storage capacity of the root zone reservoir [L]
- l_p determines at what fraction of $S_{r,max}$ the evaporation flux is limited by the availability of soil water [-]
- γ is a parameter that determines how nonlinear the recharge is with respect to the saturation of the root zone [-]
- $S_{i,max}$ is the maximum storage capacity of the interception zone reservoir [L]
- K_s is the saturated hydraulic conductivity [L/T]
- k_v is the vegetation coefficient for the maximum evaporation [-]

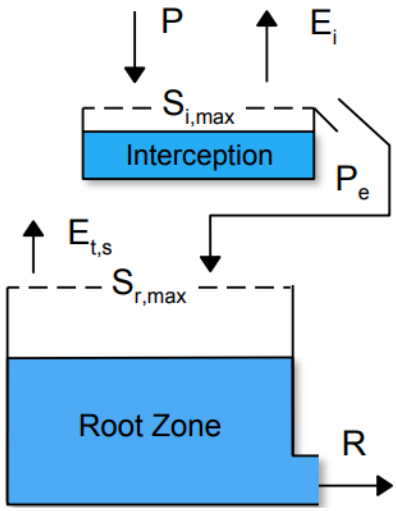

Figure 4.3: FLEX model systematisation of the groundwater system according from Collenteur; et al. (2021)

Table 4.1: The parameters in the FLEX model and their fixed values or the range of possible values.

Parameter	Fixed	Value (range)
$S_{r,max}$ [mm]	No	1e-5 - 1e3
l_p [-]	Yes	0.25
γ [-]	No	1e-5 - 50
$S_{i,max}$ [mm]	Yes	2
K_s [mm/d]	No	1 - 1e4
k_v [-]	Yes	1

4.3 TFN Modelling on Synthetic Time Series with an Unsaturated Zone

Synthetic time series with HYDRUS-1D are created for the five different soil types: Loamy Sand, Sand, Sandy Silt, Clay and Silty Loam. Seven increasingly deeper drainage levels d are considered: -100, -150, -200, -250, -300, -400, -500cm. All simulations have a surface layer boundary condition at the top with no runoff. The bottom boundary condition is set to a constant pressure head (of 20 cm) with a drainage resistance of 46.82 days. The synthetic time series for the groundwater table are modelled for 1999-2020 (22 years) with 1999 to 2001 the warm-up period, 2002 till 2017 the calibration period and 2018 till 2020 the validation period.

The synthetic time series for the groundwater table can be seen in C.1. The maximum water balance error calculated by HYDRUS-1D for the simulations is 30cm which relates to an average error 14mm per simulation year. Some of these time series can be deemed more realistic than others. Especially for the Silty Loam time series a lot of ponding is observed. For the Silty Loam HYDRUS-1D simulations runoff was allowed if more than 2cm of ponding occurred. These groundwater table time series are highly variable and additionally three clear outliers were removed and filled with interpolated values. Even though the time series for Silty Loam are questionable, we do take them into account since they might still give information on the highly variable groundwater tables in low permeable soils.

The TFN model is varied in the selection of the recharge model (linear or nonlinear) and the three response functions (exponential, gamma or four-parameters). The TFN model uses nonlinear least squares as an objective function to calibrate the modelled groundwater table to the synthetic groundwater table during the calibration period. Least squares finds a local minimum of a cost function with bounds on the parameters (Table 4.1) (Virtanen et al., 2020).

The calibration is done in two runs. In the first run the parameters for the response function and recharge model are optimised without the noise model. The optimal parameters found in this run are then fed back as initial values into a second run with noise model. This way we improve the initial parameters for the second run, increasing the final model fit. The value for the parameter $S_{r,max}$ of the FLEX model is fixed after the first optimisation without the noise model. All the other parameters, including the drainage level d, are again optimised in the second run.

In the following subsections the results are discussed of the TFN models using the linear and nonlinear recharge model. The results discussed below are based on Tables 4.2 - 4.7 which show the EVP and RMSE for the linear and nonlinear recharge models on both the calibration and validation period.

Table 4.2: The EVP [%] for five soil profiles using the exponential response function with the linear and FLEX recharge model. Both the calibration and validation period are shown and the rows indicate the drainage level d [cm]. The text in blue is the best fit per the soil profile.

Profile	B02 LoamySand				B05 Sand				B07 SandySilt				B10 Clay				B14 SiltyLoam			
Recharge	Linear		FLEX		Linear		FLEX		Linear		FLEX		Linear		FLEX		Linear		FLEX	
Cal/Val	Cal	Val	Cal	Val	Cal	Val	Cal	Val	Cal	Val	Cal	Val	Cal	Val	Cal	Val	Cal	Val	Cal	Val
-100cm	60.6	71.9	91.1	90.5	32.1	46.1	92.5	93.9	67.2	81.1	87.7	85.8	44.4	42.9	86.2	88.5	40.2	44.1	74.0	76.3
-150cm	29.9	42.7	91.3	93.7	9.7	15.9	75.7	74.3	59.8	74.0	88.8	89.7	34.1	31.3	80.9	71.9	27.0	30.1	55.7	44.7
-200cm	17.8	27.5	75.0	77.7	4.3	6.7	67.1	70.5	25.9	37.3	90.2	92.7	27.5	47.7	68.1	83.7	20.2	23.3	53.4	61.4
-250cm	7.9	12.1	73.4	77.5	6.5	9.2	70.9	80.9	10.7	15.3	78.5	78.7	34.3	15.0	65.0	28.2	19.9	20.8	50.4	58.5
-300cm	4.3	6.0	72.9	79.2	9.9	12.6	72.1	83.4	7.1	9.5	79.8	84.0	35.1	29.5	63.0	52.7	18.9	13.7	42.4	37.2
-400cm	12.6	15.1	69.0	80.2	16.6	19.0	76.0	81.5	16.2	18.0	84.0	87.9	11.3	14.3	74.1	79.7	21.8	12.7	74.4	51.8
-500cm	14.1	16.2	69.3	73.8	14.5	15.9	72.9	74.1	17.7	18.9	84.2	80.2	10.5	12.3	68.6	77.3	16.0	21.4	69.7	80.0

Table 4.3: The EVP [%] for five soil profiles using the gamma response function with the linear and FLEX recharge model. Both the calibration and validation period are shown and the rows indicate the drainage level d [cm]. The text in blue is the best fit per the soil profile.

Profile	B02 LoamySand				B05 Sand				B07 SandySilt				B10 Clay				B14 SiltyLoam			
Recharge	Linear		FLEX		Linear		FLEX		Linear		FLEX		Linear		FLEX		Linear		FLEX	
Cal/Val	Cal	Val	Cal	Val	Cal	Val	Cal	Val	Cal	Val	Cal	Val	Cal	Val	Cal	Val	Cal	Val	Cal	Val
-100cm	77.9	77.2	91.0	89.9	60.9	59.6	85.3	83.9	81.3	86.5	87.6	85.4	53.3	49.3	86.2	88.6	49.5	50.2	74.3	76.4
-150cm	42.3	43.8	95.6	96.6	52.8	59.6	93.6	94.4	70.7	78.4	88.8	89.8	38.5	29.4	80.7	69.5	32.0	34.0	59.6	43.2
-200cm	30.5	36.9	92.9	94.9	47.5	61.1	94.2	95.9	36.9	42.5	92.4	93.1	28.7	40.1	71.4	83.1	20.0	23.7	56.0	65.0
-250cm	21.4	30.6	88.9	91.5	63.2	71.4	93.2	96.3	26.2	36.7	92.5	92.7	35.7	14.3	61.0	25.6	18.7	17.8	53.2	59.3
-300cm	25.2	36.5	86.5	91.8	65.5	67.4	91.6	95.7	38.2	49.1	92.4	92.6	37.2	26.9	65.0	52.7	18.9	12.7	43.3	37.4
-400cm	39.8	41.0	81.3	89.5	66.1	61.1	89.0	92.4	61.0	53.3	92.4	93.9	36.6	36.4	77.6	82.8	49.6	25.3	74.0	53.6
-500cm	47.9	45.2	75.6	84.5	65.2	61.6	87.7	81.6	68.6	55.8	88.0	88.7	34.0	33.8	75.1	80.6	52.4	43.1	71.0	88.4

Table 4.4: The EVP [%] for five soil profiles using the four parameters response function with the linear and FLEX recharge model. Both the calibration and validation period are shown and the rows indicate the drainage level d [cm]. The text in blue is the best fit per the soil profile.

Profile	B02 LoamySand				B05 Sand				B07 SandySilt				B10 Clay				B14 SiltyLoam			
Recharge	Linear		FLEX		Linear		FLEX		Linear		FLEX		Linear		FLEX		Linear		FLEX	
Cal/Val	Cal	Val	Cal	Val	Cal	Val	Cal	Val	Cal	Val	Cal	Val	Cal	Val	Cal	Val	Cal	Val	Cal	Val
-100cm	82.2	82.5	91.1	90.2	90.6	90.7	93.1	93.4	83.7	89.4	86.4	85.4	57.5	52.0	86.2	88.6	51.9	52.8	74.3	76.5
-150cm	63.2	67.6	96.1	96.9	56.3	72.2	97.0	98.0	73.0	81.5	88.8	89.8	41.6	32.9	81.0	71.5	34.7	37.0	59.7	44.7
-200cm	37.2	55.2	93.3	95.1	58.2	75.6	94.7	96.8	73.0	76.7	93.8	95.2	31.3	45.0	72.4	84.0	23.1	27.8	56.8	65.2
-250cm	37.5	56.0	88.2	91.6	65.6	77.0	92.2	96.5	44.5	63.2	95.8	97.1	37.5	15.7	59.8	24.7	21.5	23.5	53.3	59.8
-300cm	45.9	58.3	86.7	92.4	67.3	74.2	90.8	96.2	59.5	70.5	95.4	97.1	38.9	29.6	66.1	53.2	19.4	14.7	43.6	38.0
-400cm	51.0	55.9	80.6	91.1	67.5	68.5	90.8	90.9	65.5	65.3	94.0	96.4	47.4	50.5	78.3	85.8	49.5	27.6	75.7	52.2
-500cm	48.3	53.3	75.6	84.5	64.4	65.6	89.6	82.0	65.5	61.6	92.2	91.7	46.3	50.1	76.0	83.6	52.1	44.9	71.6	86.1

4.3.1 Different Recharge Models

The FLEX recharge model almost always leads to a better fit in terms of RMSE and EVP. The validation period is often even better for the than the calibration period. This is remarkable but can be explained by the long calibration period and the generally good model structure. Especially the nonlinear recharge model performs better during the validation periods.

Figure 4.5 shows TFN model simulation for the groundwater table of the silty loam soil with a drainage level of -200cm. It shows a good performance of the nonlinear recharge model (EVP = 90 %) and is typical for the general appearance. The nonlinear recharge model performs well since the root zone storage becomes zero during summer. This results in zero recharge and no further drop in the head. Most of the peaks are captured better by the nonlinear recharge model as well. For the exponential response function, adequate TFN models are already obtained compared to the four parameters response function which has two more parameters.

The linear recharge model does not give a good model for this scenario with the exponential response function (EVP = 36 %). The linear recharge model with the four parameters response function gives a much better model (EVP = 73 %) than the one with the exponential response function. However the linear TFN model obtained is still worse than the nonlinear recharge model. This can be explained by the better model structure of the nonlinear recharge model. The linear recharge model keeps applying a recharge flux therefore undershooting the groundwater table in the sum-

Table 4.5: The RMSE [mm] for five soil profiles using the exponential response function with the linear and FLEX recharge model. Both the calibration and validation period are shown and the rows indicate the drainage level d [cm]. The text in blue is the best fit per the soil profile.

Profile	B02 LoamySand				B05 Sand				B07 SandySilt				B10 Clay				B14 SiltyLoam			
Recharge	Linear		FLEX		Linear		FLEX		Linear		FLEX		Linear		FLEX		Linear		FLEX	
Cal/Val	Cal	Val	Cal	Val	Cal	Val	Cal	Val	Cal	Val	Cal	Val	Cal	Val	Cal	Val	Cal	Val	Cal	Val
-100cm	33.7	28.2	16.0	17.0	32.8	32.0	10.9	11.1	40.1	29.1	24.6	26.2	86.5	80.2	43.2	36.6	197.0	181.5	129.8	119.2
-150cm	29.1	27.2	10.3	9.0	26.9	28.8	13.9	15.9	32.1	26.0	17.0	16.9	66.9	74.4	36.0	47.4	210.0	207.3	163.5	183.8
-200cm	24.8	24.7	13.7	13.7	22.7	26.1	13.2	14.5	30.5	30.9	11.1	10.6	58.3	37.0	38.6	20.6	181.8	185.1	138.9	130.7
-250cm	22.6	24.4	12.2	12.3	21.1	24.9	10.8	10.7	26.8	29.9	13.1	14.9	39.6	84.3	28.9	77.1	183.7	197.5	144.6	142.3
-300cm	20.7	23.8	11.0	11.2	20.6	24.3	9.7	9.6	23.6	27.7	10.8	11.4	32.9	46.4	24.8	37.6	104.2	173.6	87.8	147.2
-400cm	18.9	22.2	10.0	10.2	14.4	19.3	7.7	9.2	21.9	25.5	7.6	8.7	26.4	31.7	14.2	15.4	40.4	80.0	23.1	59.3
-500cm	14.6	19.9	8.6	11.1	13.0	18.5	7.3	10.3	14.1	19.2	6.1	9.6	22.6	29.1	13.3	14.8	31.6	33.7	19.0	21.6

Table 4.6: The RMSE [mm] for five soil profiles using the gamma response function with the linear and FLEX recharge model. Both the calibration and validation period are shown and the rows indicate the drainage level d [cm]. The text in blue is the best fit per the soil profile.

Profile	B02 LoamySand				B05 Sand				B07 SandySilt				B10 Clay				B14 SiltyLoam			
Recharge	Linear		FLEX		Linear		FLEX		Linear		FLEX		Linear		FLEX		Linear		FLEX	
Cal/Val	Cal	Val	Cal	Val	Cal	Val	Cal	Val	Cal	Val	Cal	Val	Cal	Val	Cal	Val	Cal	Val	Cal	Val
-100cm	25.3	25.4	16.2	17.4	24.9	28.0	15.2	17.9	30.3	24.6	24.7	26.6	79.3	75.5	43.2	36.5	181.1	171.1	129.2	118.9
-150cm	26.4	26.9	7.3	6.7	19.4	19.9	7.2	7.4	27.4	23.7	16.9	16.8	64.6	75.3	36.2	49.4	202.6	200.8	156.1	186.1
-200cm	22.8	23.1	7.3	6.5	16.7	16.6	5.5	5.4	28.1	29.8	9.8	10.6	57.8	39.4	36.6	20.9	181.9	184.0	135.0	124.5
-250cm	20.9	21.6	7.9	7.6	12.4	13.1	5.2	4.7	24.3	25.9	7.7	8.9	39.2	84.6	30.5	78.5	185.0	200.7	140.3	140.9
-300cm	18.3	19.4	7.7	7.0	11.5	13.4	5.3	4.8	19.0	20.4	6.6	7.9	32.4	47.2	24.2	37.6	104.1	174.4	87.1	147.1
-400cm	14.6	17.6	7.7	7.4	9.2	14.1	5.3	6.0	13.0	17.0	5.2	6.1	22.3	27.4	13.3	14.2	32.4	74.8	23.3	58.2
-500cm	11.2	16.4	7.7	8.5	8.6	14.0	4.9	8.4	8.6	15.1	5.3	7.1	19.3	25.2	11.8	13.7	23.8	30.0	18.6	13.5

Table 4.7: The RMSE [mm] for five soil profiles using the four parameters response function with the linear and FLEX recharge model. Both the calibration and validation period are shown and the rows indicate the drainage level d [cm]. The text in blue is the best fit per the soil profile.

Profile	B02 LoamySand				B05 Sand				B07 SandySilt				B10 Clay				B14 SiltyLoam			
Recharge	Linear		FLEX		Linear		FLEX		Linear		FLEX		Linear		FLEX		Linear		FLEX	
Cal/Val	Cal	Val	Cal	Val	Cal	Val	Cal	Val	Cal	Val	Cal	Val	Cal	Val	Cal	Val	Cal	Val	Cal	Val
-100cm	22.7	22.3	16.1	17.2	12.2	13.5	10.4	11.6	28.3	21.8	25.8	26.6	75.6	73.5	43.2	36.5	176.7	166.7	129.1	118.8
-150cm	21.1	20.6	6.9	6.3	18.7	16.5	4.9	4.4	26.3	22.0	16.9	16.8	62.9	73.5	35.9	47.7	198.5	196.5	155.9	183.7
-200cm	21.6	19.5	7.1	6.5	14.8	13.3	5.3	4.7	18.4	19.1	8.8	9.0	56.7	37.9	36.0	20.3	178.4	180.0	133.7	124.1
-250cm	18.6	17.3	8.1	7.6	11.9	12.0	5.6	4.6	21.1	19.5	5.8	5.8	38.6	84.0	31.0	78.9	181.7	195.6	140.1	140.0
-300cm	15.5	16.0	7.7	6.8	10.9	11.9	5.5	4.6	15.3	15.6	5.2	5.1	31.9	46.5	23.8	37.4	103.8	172.9	86.9	146.3
-400cm	12.9	15.5	7.9	6.8	9.0	13.3	4.8	6.4	12.0	14.6	4.6	4.8	20.3	25.1	13.0	12.9	32.5	74.4	22.5	59.2
-500cm	11.2	17.0	7.7	8.5	8.6	13.6	4.5	8.3	9.0	15.6	4.3	6.1	17.4	23.2	11.6	12.6	23.9	30.0	18.4	16.1

mers.

There is one groundwater table time series where the EVP and RMSE give a better performance for the linear recharge model. This is the case for the sandy silt profile at a shallow drainage level of -100cm. In Figure 4.4 the TFN model is shown for the sandy silt profile with the shallow drainage level of -100cm. The linear recharge model performs about the same as the FLEX recharge model. For this simulation in the dry summer of 2018 the head is estimated significantly better by the linear model than the nonlinear model. That is because the drop in head during this summer is significant.

All the simulations for the groundwater table (between 2016 and 2019) can be found in appendices D - H.

4.3.2 Difference in Soil Type

For the coarser grained, higher permeable soils loamy sand, sand and sandy silt the FLEX model performs relatively well. Also the linear model with the four-parameters response function can give decent results for these models. The finer grained, low permeable soil types, clay and silty loam are more difficult to simulate. Silty loam shows the worst results for both recharge models. An important factor for this is the limited infiltration capacity of these soils. In the synthetic time series for these soil types we observe ponding and large fluctuations in the groundwater table. Also the behaviour of the silty loam groundwater time series can be disputed for not being

realistic enough. Both the linear and nonlinear recharge model do not account for ponding.

4.3.3 Difference in Unsaturated Zone Thickness

The drainage level is the level to which the head returns under hydrostatic, equilibrium conditions without any fluxes from the top or bottom of the profile. Vice versa the thickness of the unsaturated zone is the negative value of the drainage level since the surface is taken at 0 cm. For the simulations the drainage levels were between -100 cm and -500 cm. Simulations with a drainage level above -100 cm were not done since HYDRUS-1D has convergence problems for those models. The deeper simulations at -400 and -500 cm show a low variation in the groundwater table.

If the drainage level increases, the RMSE generally decreases. However this does not necessarily mean that the fit is better, because the EVP generally decreases with a deeper drainage level. The decrease in RMSE with a deeper drainage level can be explained with the lower variation of the groundwater table time series.

In Figures B.1, B.2, B.3 the EVP is plotted against the drainage level for the exponential, gamma and four-parameters response function respectively. The EVP of the nonlinear recharge model generally decreases a little bit with increasing depth of the drainge level but maintains a relatively high EVP of $> 70\%$. The EVP of the linear recharge model is still high for a shallow drainage level but with increasing depth the EVP is low. The use of the gamma and four-parameters response functions increase the EVP of the linear recharge model with depth. This confirms the explanation of section 4.1 that the response function can account for the dispersion effect in the unsaturated zone.

In general we see the same trends between the response functions. However, for both recharge models, the four-parameters function response function almost always gives the best value for the RMSE and EVP for both the linear and nonlinear model. The differences generally small for the nonlinear recharge model. The question is if two extra of the four parameters response function, compared to the exponential response function, are proportional to the small increase in the goodness-of-fit.

4.3.4 Difference in Estimating Recharge Flux

The performance of the recharge models in estimating the recharge flux is discussed in this subsection. This comparison is the same as Collenteur; et al. (2021). Note that the model is still calibrated on the groundwater table, but from the optimal parameters found for the recharge model we obtain an estimate of the recharge. We can compare the modelled recharge to the recharge found with HYDRUS-1D. In theory we can take the recharge flux from any discretised cell, at any depth in our 1D soil column from HYDRUS-1D as the recharge flux. The vertical flux varies in the HYDRUS-1D soil column but, the recharge flux is relatively constant for the deeper cells, so the recharge flux is taken from the bottom cell in the soil column.

The values for the EVP and RMSE for the linear and nonlinear recharge fluxes during the calibration period are presented in Tables 4.8 - 4.10. From these tables we see that the linear recharge model has a EVP of zero for the estimation of the recharge. The EVP is always zero which means that the mean of the synthetic recharge would be a better estimate. Also the RMSE is generally bad for the linear recharge model. The highly variable pattern of the linear recharge model dos not correspond to the more smooth recharge found in the HYDRUS-1D. The nonlinear recharge model gives a better estimate for the daily recharge flux.

In Figure B.4 we do see that the yearly cumulative recharge can also be estimated relatively well by the linear recharge model for the shallow drainage levels for some

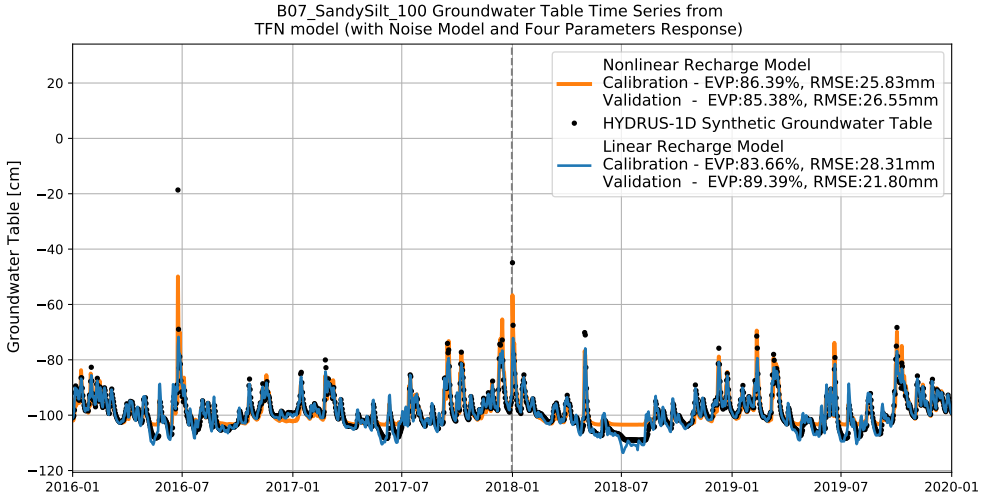

Figure 4.4: Model for which the linear recharge model performs good. 2016-2017 are part of the calibration period, 2018-2019 are part of the validation period.

soil types. For the deeper drainage levels, most models using linear recharge give a poor estimate for the recharge due to the f parameter hitting the optimisation bound of -2. This gives a negative yearly sum of recharge which does not happen in the HYDRUS-1D simulations. When using another response function than the exponential response function this problem disappears as can be seen in Figures B.5 and B.6.

The nonlinear recharge model performs better than the linear model in estimating the recharge flux. For deeper drainage levels the nonlinear recharge model does not perform that well anymore due to a variation which is too low. However the cumulative recharge is in the same range as the HYDRUS-1D.

Interesting is the fact that, in order to get the best estimate of the recharge flux, the exponential response function gives the best RMSE and EVP. This corresponds to the theory that the gamma and four-parameters response functions incorporate some unsaturated zone process. If one would want to obtain the actual recharge, the response of the saturated zone would is exponential response function as shown in section 2.2.1. Note that this is then at the location of $\frac{x}{L} = \frac{11}{40}$.

4.3.5 Difference in Estimating the Actual Evaporation Flux

In this subsection we to compare the ability of the recharge models to simulate evaporation reduction. This is done by looking at the ratio between the potential and actual evaporation, E_a/E_p which is always between 0 and 1. From HYDRUS-1D we do not take into account the interception evaporation since it is modelled as a threshold. To obtain the actual evaporation flux from HYDRUS-1D we add soil evaporation and transpiration. The potential evaporation is the sum of $E_{t,p}$ and $E_{s,p}$ from Equations 3.7 and 3.8.

The linear recharge model has a factor f which is multiplied with the potential evaporation flux. This constant is sometimes referred to as the evaporation factor since it limits the effect of the potential evaporation flux for the entire simulation. However, since the parameter is constant it does not take into account the seasonal dependence (Obergfell et al., 2019). Furthermore, the main purpose of this parameter is to determine the ratio between the effect of precipitation and evaporation, instead of identifying the evaporation reduction. That is why we omit this parameter from

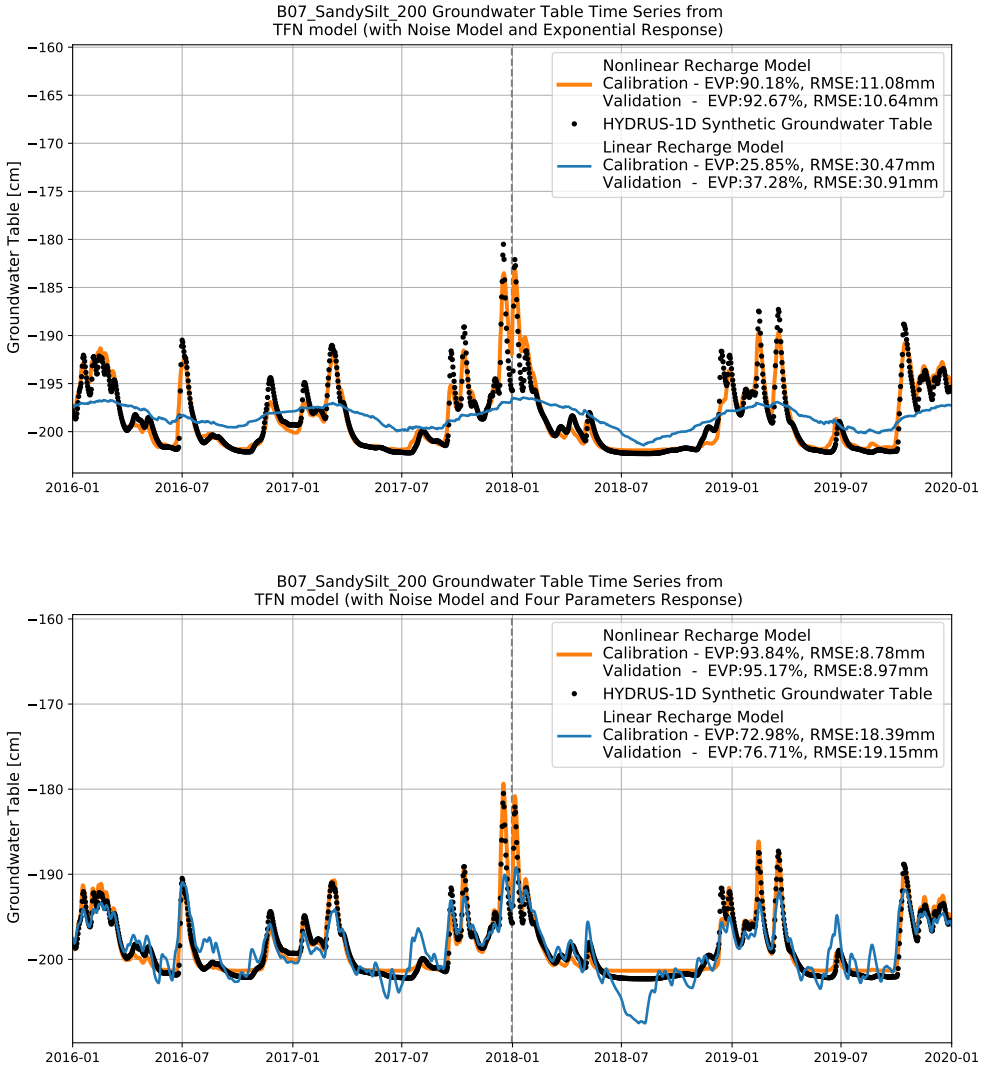

Figure 4.5: TFN model for which the nonlinear recharge model performs good. 2016-2017 are part of the calibration period, 2018-2019 are part of the validation period.

Table 4.8: The RMSE [cm] and EVP for the comparison of the synthetic recharge with the linear and FLEX recharge. The TFN model uses the exponential response function. The metrics are computed on the calibration period. The rows indicate the drainage level from the soil profile.

Profile	B02 LoamySand				B05 Sand				B07 SandySilt				B10 Clay				B14 SiltyLoam			
Recharge	Linear		FLEX		Linear		FLEX		Linear		FLEX		Linear		FLEX		Linear		FLEX	
Metric	EVP	RMSE	EVP	RMSE	EVP	RMSE	EVP	RMSE	EVP	RMSE	EVP	RMSE	EVP	RMSE	EVP	RMSE	EVP	RMSE	EVP	RMSE
-100cm	0.0	4.9	73.2	1.3	0.0	5.9	79.2	1.0	0.0	4.8	50.3	2.0	0.0	4.7	46.4	1.8	0.0	4.9	63.4	1.3
-150cm	0.0	5.6	82.0	0.6	0.0	6.0	70.0	0.7	0.0	5.1	52.4	1.4	0.0	5.0	0.0	1.9	0.0	5.1	71.5	0.9
-200cm	0.0	6.0	70.5	0.6	0.0	6.1	61.2	0.6	0.0	5.9	76.3	0.8	0.0	5.1	0.0	2.5	0.0	5.1	73.1	0.7
-250cm	0.0	6.1	54.4	0.7	0.0	6.1	54.7	0.6	0.0	6.0	72.7	0.6	0.0	5.1	0.0	1.5	0.0	5.1	69.6	0.6
-300cm	0.0	6.1	39.2	0.7	0.0	6.1	50.1	0.5	0.0	6.0	69.3	0.5	0.0	5.1	50.3	0.8	0.0	5.2	49.8	0.7
-400cm	0.0	6.1	35.6	0.6	0.0	6.2	7.5	0.7	0.0	6.1	46.0	0.5	0.0	6.1	42.8	0.7	0.0	6.1	25.6	0.6
-500cm	0.0	6.2	0.0	0.7	0.0	6.2	0.0	0.7	0.0	6.1	11.8	0.6	0.0	6.1	30.9	0.6	0.0	6.1	23.6	0.5

Table 4.9: The RMSE [cm]and EVP for the comparison of the synthetic recharge with the linear and FLEX recharge. The TFN model uses the gamma response function. The metrics are computed on the calibration period. The rows indicate the drainage level from the soil profile.

Profile	B02 LoamySand				B05 Sand				B07 SandySilt				B10 Clay				B14 SiltyLoam			
Recharge	Linear		FLEX		Linear		FLEX		Linear		FLEX		Linear		FLEX		Linear		FLEX	
Metric	EVP	RMSE	EVP	RMSE	EVP	RMSE	EVP	RMSE	EVP	RMSE	EVP	RMSE	EVP	RMSE	EVP	RMSE	EVP	RMSE	EVP	RMSE
-100cm	0.0	4.9	73.2	1.3	0.0	5.3	13.5	1.7	0.0	4.8	50.2	2.0	0.0	4.7	46.4	1.8	0.0	4.9	60.7	1.3
-150cm	0.0	5.2	38.6	1.2	0.0	5.2	0.0	1.8	0.0	5.1	53.1	1.4	0.0	5.0	6.5	1.8	0.0	5.1	62.5	1.0
-200cm	0.0	5.2	0.0	1.6	0.0	5.1	0.0	1.7	0.0	5.3	20.1	1.3	0.0	5.1	0.0	1.7	0.0	5.1	62.8	0.8
-250cm	0.0	5.2	0.0	1.6	0.0	5.0	0.0	1.6	0.0	5.2	18.2	1.0	0.0	5.1	0.0	1.8	0.0	5.1	66.3	0.7
-300cm	0.0	5.1	0.0	1.1	0.0	5.0	0.0	1.1	0.0	5.1	5.5	0.9	0.0	5.1	0.0	1.5	0.0	5.1	48.3	0.7
-400cm	0.0	5.0	0.0	1.1	0.0	5.1	0.0	1.1	0.0	5.1	0.0	0.9	0.0	5.1	0.0	0.9	0.0	5.1	26.3	0.6
-500cm	0.0	5.1	0.0	1.2	0.0	5.1	0.0	3.5	0.0	5.1	0.0	1.0	0.0	5.0	0.0	1.0	0.0	5.2	0.0	0.6

Table 4.10: The RMSE [cm] and EVP for the comparison of the synthetic recharge with the linear and FLEX recharge. The TFN model uses the four parameter response function. The metrics are computed on the calibration period. The rows indicate the drainage level from the soil profile.

Profile	B02 LoamySand				B05 Sand				B07 SandySilt				B10 Clay				B14 SiltyLoam			
Recharge	Linear		FLEX		Linear		FLEX		Linear		FLEX		Linear		FLEX		Linear		FLEX	
Metric	EVP	RMSE	EVP	RMSE	EVP	RMSE	EVP	RMSE	EVP	RMSE	EVP	RMSE	EVP	RMSE	EVP	RMSE	EVP	RMSE	EVP	RMSE
-100cm	0.0	4.9	73.0	1.3	0.0	5.1	4.8	1.8	0.0	4.8	49.9	2.0	0.0	4.7	46.3	1.8	0.0	4.9	61.1	1.3
-150cm	0.0	5.1	32.8	1.2	0.0	5.2	0.0	1.8	0.0	5.1	52.5	1.4	0.0	5.0	6.4	1.8	0.0	5.1	67.7	1.0
-200cm	0.0	5.2	0.0	1.6	0.0	5.1	0.0	1.7	0.0	5.1	5.1	1.4	0.0	5.1	0.0	1.8	0.0	5.1	63.2	0.8
-250cm	0.0	5.1	0.0	1.7	0.0	5.0	0.0	1.7	0.0	5.2	0.0	1.4	0.0	5.1	0.0	2.0	0.0	5.1	63.3	0.7
-300cm	0.0	5.1	0.0	1.6	0.0	5.0	0.0	1.2	0.0	5.1	0.0	1.0	0.0	5.1	0.0	1.7	0.0	5.1	44.5	0.7
-400cm	0.0	5.0	0.0	1.1	0.0	5.1	0.0	2.7	0.0	5.1	0.0	1.0	0.0	5.0	0.0	1.0	0.0	5.1	3.5	0.7
-500cm	0.0	5.1	0.0	1.2	0.0	5.1	0.0	3.6	0.0	5.1	0.0	1.1	0.0	5.0	0.0	1.1	0.0	5.2	0.0	0.6

the linear recharge model from this comparison.

For the nonlinear model we take the actual evaporation flux from the root zone storage as calculated with Equation 4.9. The potential flux for the root zone storage is $E_{max} - E_i$ from this equation.

Figure B.7 and B.8 show the results for a dry and wet year respectively for all the soil types. It is observed in general that HYDRUS-1D is able to handle sharper drops in evaporation since the evaporation only takes place from the upper 15 cm (root depth) of the soil profile. If there is enough water present in the upper 15 cm the ratio between E_a and E_p is 1. This is easier to achieve than for the root zone storage of the FLEX model to fill up entirely, especially if it is empty. The bucket framework of the FLEX model is a bit slower in that sense, compared to the HYDRUS-1D model.

Between the soil types we see that, especially for the Silty Loam, with a low permeability and a lot of ponding, the estimates for the evaporation reduction are the worst, mainly during the wet years. This is confirmed by the EVP which shown in the Figures as well.

In general the EVP is relatively low (maximum of 66%). However we do see that, especially in the dry year, the FLEX model does show some of the same behaviour as found in HYDRUS-1D. For the gamma and four-parameters response functions, we generally see the same performance.

4.4 Findings of Chapter 4

The nonlinear recharge model almost always performs better than the linear recharge model when prediction synthetic groundwater table time series created with HYDRUS-1D for all our soil types and drainage levels. The fluctuations of the groundwater system are captured well by the nonlinear recharge model. The undershooting of the groundwater table plateau is not observed during the summer since the nonlinear recharge model stops applying a recharge flux due to the root zone storage.

5 | Conclusions & Discussion

The main goal of this research was to assess the performance of the nonlinear recharge model in the TFN model and compare it to the linear recharge model. Additionally, the conditions under which the nonlinear recharge model performs better needed to be defined. The research questions were:

R.Q. 1 What lower boundary condition can be used for a one-dimensional model to generate realistic synthetic time series of the groundwater table?

R.Q. 2 How does the unsaturated zone affect the nonlinear behaviour of the groundwater table?

R.Q. 3 How does the TFN model, using the linear or nonlinear recharge model, perform in modelling synthetic groundwater table time series created with an unsaturated zone model?

R.Q. 4 When is it recommended to use the linear or nonlinear recharge model when doing groundwater table time series analysis using TFN modelling?

First a summary is given to the answers on the first two research questions which were answered in Chapters 2 and 3.

In section 2.3 we saw that a one-dimensional model can be used for creating synthetic time series if we use a drainage resistance as a boundary condition that is plausible in relation to a two-dimensional domain. A one-dimensional model of a soil profile will be most similar to a Kraijenhoff van de Leur system at distance fraction of $\frac{5}{1000}$ and $\frac{11}{40}$ (and due to symmetry at $\frac{29}{40}$ & $\frac{995}{1000}$) of a domain length. When creating time series for the groundwater table using HYDRUS-1D we use a boundary condition with a constant pressure head and a drainage resistance of 46.82 days. This is because we find this drainage resistance gives the most similar response for the Kraijenhoff van de Leur polder system at $\frac{x}{L} = \frac{11}{40}$ in Swifterbant, Flevoland. This way we can make time series which are relatively realistic with a one-dimensional unsaturated zone model.

In section 3.3 we saw that the water content of the unsaturated zone can have a large influence on the recharge and eventually the behaviour of the groundwater table. A change in the saturation degree of the unsaturated zone has a large effect on the (amount of) water that flows to the groundwater table, but also on the amount of water that is evaporated. Additionally, doubling the amount of precipitation does not mean that the response of the groundwater table doubles. This is because water flows faster through the unsaturated zone if the unsaturated zone becomes more wet in the case of a larger precipitation event.

A large assumption of this research is that our one-dimensional unsaturated zone model is a good and realistic enough, white box model to obtain an answer on the third and fourth question. We know that 2D or 3D unsaturated zone models would be give more realistic groundwater simulations than the one-dimensional model used in this study. Horizontal flow, which plays an important role in groundwater systems, would be taken into account with 2D and 3D models. However, all of the unsaturated

zone models solve Richards' equation since it is known to describe variably saturated flow. And we know from section 3.3 that we can simulate the nonlinear processes present in the unsaturated zone with the 1D model. That is why we think the findings of this study are adequate to answer the third and fourth research question.

To answer the third research question, 35 different synthetic time series for the groundwater table were created using HYDRUS-1D. These time series were modelled using the transfer function noise model using both the linear and nonlinear recharge model. The danger of the nonlinear recharge model is that the larger number of parameters may lead to to overparameterisation compared to the linear model (which in turn may be oversimplified with only one parameter). A model with more parameters and flexibility has a behaviour which is less dependent on the model structure. This makes it more difficult to check whether we are getting the right answer for the right reason (Kirchner, 2006). From Perrin et al. (2001) we know that a model with a higher number of parameters generally performs better during the the calibration phase. But during the validation phase the model shows results which are as good as the models with a lower number of parameters. This can be explained by the complex models tending to be less robust for different scenarios. That is why we split the resulting time series in a calibration and validation period. This is done in accordance with the statement of Kirchner (2006) that the calibration and validation data sets should represent conditions which are different enough. The different conditions are ensured by enclosing the relatively dry summer of 2018 in the validation period. With all this in mind we draw the three main conclusions.

The first conclusion is that the TFN model that uses the linear recharge model performs virtually always worse (34/35 validation period and 35/35 calibration periods) than the nonlinear recharge model when estimating synthetic groundwater table time series created with HYDRUS-1D. However, when the drainage level is shallow (in our case -100 down to -150cm), the linear recharge model can give a good EVP (>70%) for coarser, more permeable soils. This can be explained by the observation that groundwater uptake (upwards recharge) is a more important process when the unsaturated zone is shallow, compared to deeper drainage levels. Even though the linear recharge model can give sufficient goodness-of-fit values, it still undershoots the groundwater table levels in summer which is one of the common issues raised by (Peterson & Western, 2014). The incorporation of the dispersion of the unsaturated zone with the gamma and four-parameters significantly improves the performance of all TFN models using the linear recharge model.

The second conclusion is that the TFN model with the nonlinear recharge model shows a better EVP and RMSE than the linear model for 34 out of 35 of the HYDRUS-1D. The fluctuations of the groundwater system are captured well by the nonlinear recharge model. The undershooting of the groundwater table plateau is not observed during the summer since the nonlinear recharge model stops simulating an evaporation and recharge flux. This is because the actual evaporation simulated by the model is limited by the availability of soil moisture. There is a decrease in the performance of the nonlinear recharge model visible with decreasing saturated conductivity and grain size. This can be attributed to ponding and the largely fluctuating behaviour of the groundwater table in these soils.

The third conclusion is that the nonlinear recharge model is able to simulate the recharge flux and evaporation reduction relatively well. These two processes are the main source of non-linearity in the HYDRUS-1D simulations. As an estimator of the recharge, the nonlinear recharge model describes the fluctuations of the recharge better than the linear recharge model. Even though it is currently a limitation that the nonlinear recharge model does not simulate groundwater uptake (upwards recharge). To get an accurate estimate of the recharge flux when using the nonlinear recharge model it is advised to always use the exponential response function. From a theoretical point of view this would be better because the response of the groundwater table

to recharge should be instantaneous. Also the goodness-of-fit metrics are better for the exponential response function compared to other response functions when estimating the recharge flux.

To give an answer on research question 4, the nonlinear model is always the best option when modelling synthetic groundwater table time series created with HYDRUS-1D. The addition of the nonlinear recharge model to the TFN model creates better estimates for the groundwater tables from an unsaturated zone models. Moreover, the complex unsaturated zone processes and fluxes are described relatively well by the nonlinear recharge model.

It is known that many heterogeneous and complex processes in watersheds can be described by incorporating a simple model for the collection, storage and release of water (McDonnell et al., 2007). In this study we also find that these concepts work when using the FLEX nonlinear recharge model in our grey box TFN model. Shifting the TFN model a bit more to white in the grey scale of models (Fig. 1.1), allows us to describe the non-linearity, introduced by Richards' equation in HYDRUS-1D, better. This way we find a better alternative to the linear recharge model in describing the complexity of the groundwater system, enabling us in making the right predictions for the right process reasons (Collenteur; et al., 2021; McDonnell et al., 2007). We do find however that upwards recharge due to groundwater uptake plays an important role in HYDRUS-1D soil profile models with a groundwater table shallower than 200cm. This is currently not implemented in the nonlinear recharge model and is an omission of a process found in the unsaturated zone model.

6 Limitations & Recommendations

In this chapter some of limitation and the subsequent recommendations are mentioned. These recommendations would improve the answers on the research questions of this research and could lead to new research topics.

6.1 Unsaturated Zone Model HYDRUS-1D

In this research, the time series for the head are created with HYDRUS-1D which is a one-dimensional model. The one-dimensional model is not able to incorporate multi-dimensional processes that affect the groundwater such as horizontal flow. In chapter 2 we showed that a one-dimensional model can be related to a two-dimensional model, but there is always an error while doing this. A two- or three-dimensional model should be able to incorporate groundwater processes more realistically. To include horizontal groundwater flow, in future research it would be better to use HYDRUS-2D or HYDRUS-3D.

A simplification currently is the use of a homogeneous soil profile in the HYDRUS-1D model. In reality, soils always consist of multiple layers. With the large range of soil types from the Staring series in Heinen et al. (2020) it is relatively simple to implement non-homogeneous soils in HYDRUS-1D. Two approaches could be used. The first approach would be to add more layers to the HYDRUS-1D profile such that we obtain a profile with two or three layers (excluding the bottom clay layer). The second approach would be to recreate a soil sample from the field. If there is a groundwater measurement location nearby, the time series for the head created could be calibrated.

The first approach is the simplest since it does not account for the complexity of the subsurface. The problem however would be still the same as the current research with the question how accurate a one-dimensional homogeneous model is to test these performance of the recharge models. The second approach could give a more satisfactory answer given that it can be calibrated to a measured time series. However to calibrate this model and can be a lot of trouble, not to mention the numerical complexity of a multilayered model. Even though this would be solved by HYDRUS-1D.

HYDRUS-1D also gives the option to simulate dual-porosity and dual-permeability to simulate preferential flow. Dual-porosity models assume that there is no water flow in the matrix, such that water flow is restricted to the macro-pores (Simunek et al., 2003). Dual-permeability models allow for water flow in the matrix as well, solving two flow equations separately (Simunek et al., 2009). The main disadvantage of dual-porosity and dual-permeability models is that they require many more input parameters to characterise the soil system than for instance the van Genuchten soil model. Generally, these parameters are not known and difficult to measure. From

field observations we do know that preferential flow does occur so it would be good to test the performance of time series models on time series created with dual-porosity or dual-permeability models.

Additional options available in the HYDRUS-1D model would be to incorporate hysteresis. Hysteresis would add the effect of wetting and draining on the relationship between the water content and pressure head. If this option does not give additional numerical complexity it could be useful to test the effect on the time series for the groundwater table.

Another option would be to change the root uptake with a root growth model. This way the root depth increases in summer and decreases in winter. Another change would be to use the Feddes root uptake model. Even though it gives more numerical complexity than the van Genucten root uptake model, during near saturation situations the Feddes model would give more realistic values for the root uptake (Simunek et al., 2009).

6.2 Improving the Nonlinear Recharge Model

From the HYDRUS-1D recharge simulation, and from reality we know that groundwater uptake (upwards recharge) is possible. It would be a valuable addition to the nonlinear recharge model to implement this process. This could be done in a few ways:

- Subtracting the 'unused' part of the potential evaporation from the recharge flux. A possible pitfall however would be that the nonlinear model starts to show the same problem as the linear model where during summers too much evaporation is possible. To avoid this we could use a parameter to introduce evaporation reduction in time. However this parameter would be constant for the simulation period.
- Creating a groundwater reservoir in the FLEX model from which water can flow towards the root zone reservoir. This way the amount of groundwater uptake through time would be limited by the amount of water available in the groundwater reservoir.

6.3 Improving the Linear Recharge Model

What is observed in summer, is that the linear recharge model estimates the groundwater head to drop lower than is observed in reality. A possible solution for this would be to make the parameter f time dependent such that during these period the parameter becomes smaller and the effect of evaporation becomes lower. This could be done by estimating it on a seasonally or monthly basis. This would not be too difficult to test since the observed head time series do carry information of time. An alternative would be to estimate the parameter f after the groundwater head passes a certain threshold value.

Estimate the actual evaporation instead of using the potential evaporation with a crop factor. Radar soil moisture data should make it easier to estimate reliable time series for evaporation (and groundwater recharge) (Bouaziz et al., 2020).

6.4 Using HYDRUS-1D as a Recharge Model

HYDRUS-1D itself could also be used as a recharge model. This model would have a twelve parameters that have to be estimated (for a homogeneous soil). The van Genuchten soil parameters, the drainage resistance of the bottom clay layer and

the parameters for root depth and uptake. However due to the added numerical complexity and number of parameters this option would not have the preference.

6.5 Measured Time Series

The groundwater table in the Netherlands, especially in the western part, is most of the time relatively shallow, within 1.2m below the surface (Dufour, 2000). For the rest of the Netherlands it is usually within 4m below the surface. Research from Zaadnoordijk et al. (2019) showed that with a linear recharge model, most of the time a potentially useful TFN model can be constructed. The research also showed that in areas in the Netherlands with a deeper groundwater table, most linear recharge time series models are rejected. It would be useful to investigate the use of the nonlinear recharge model on a large scale with measured time series, similar to the research from Zaadnoordijk et al. (2019). That could give a more comprehensive answer on the general applicability of the nonlinear recharge model in time series analysis.

In reality, groundwater measurements are time series for the hydraulic head. There can be differences between the groundwater table and the head. In HYDRUS-1D we generally find a groundwater table that is higher than the head, especially in finer-grained soils. The head in this case is taken above the bottom clay layer. When taking the head as input for our time series model the TFN model performance generally improves, especially for finer grained soils.

6.6 Objective Function

For this report the nonlinear least squares is used as an objective function in the solver. Without the noise model the residuals are minimised by the solver. With the noise model the noise is minimised by the solver.

When using another objective function than nonlinear least squares the goodness-of-fit metrics as reported in Tables 4.3 - 4.7 could be slightly different. However the answers on the research questions would not be very different. The fact that the goodness-of-fit metrics do not become much worse when optimising the model while applying a noise model confirm this thought.

It could be wise however to use different objective functions to solve the model to see how the outcome changes. Goodness-of-fit metrics such as the AIC and BIC could also be used in the future. These metrics give an indication of both the fit and the model complexity (in terms of model parameters) (von Asmuth et al., 2021). However, before these can be interpreted you need to comply with the assumptions of white noise ($v(t)\ N(0, \sigma^2)$).

References

Allen, R., Pereira, L., Raes, D., & Smith, M. (1998). Crop evapotranspiration. guidelines for computing crop water requirements. FAO Irrigation and Drainage Paper, 56.

Bakker, M., Maas, K., & von Asmuth, J. R. (2008). Calibration of transient groundwater models using time series analysis and moment matching. Water Resources Research, 44(4). doi: https://doi.org/10.1029/2007WR006239

Bakker, M., & Post, V. A. (2021). Analytical groundwater modeling: Theory and applications using Python. Taylor and Francis. (In Press)

Bakker, M., & Schaars, F. (2019). Solving groundwater flow problems with time series analysis: You may not even need another model. Groundwater, 57(6), 826-833. doi: 10.1111/gwat.12927

Berendrecht, W. L., Heemink, A. W., van Geer, F. C., & Gehrels, J. C. (2006). A nonlinear state space approach to model groundwater fluctuations. Advances in Water Resources, 29(7), 959 - 973. doi: 10.1016/j.advwatres.2005.08.009

Bouaziz, L. J. E., Steele-Dunne, S. C., Schellekens, J., Weerts, A. H., Stam, J., Sprokkereef, E., … Hrachowitz, M. (2020). Improved understanding of the link between catchment-scale vegetation accessible storage and satellite-derived soil water index. Water Resources Research, 56(3), e2019WR026365. doi: 10.1029/2019WR026365

Collenteur, R. A., Bakker, M., Caljé, R., Klop, S. A., & Schaars, F. (2019). Pastas: Open source software for the analysis of groundwater time series. Groundwater, 57(6), 877-885. doi: 10.1111/gwat.12925

Collenteur;, R. A., Bakker, M., Klammler, G., & Birk, A. (2021). Estimation of groundwater recharge from groundwater levels using nonlinear transfer function noise models and comparison to lysimeter data. Hydrology and Earth System Sciences, 25(5), 2931-2949. doi: 10.5194/hess-25-2931-2021

Collenteur, R. A., Vremec, M., & Brunetti, G. (2020). Interfacing FORTAN code with python: an example for the HYDRUS-1D model. EGU General Assembly, 15377.

de Ridder, N., & Boonstra, J. (1994). Analysis of water balances. Drainage Principles and Applications. International Institute for Land Reclamation and Improvement (ILRI), Wageningen, 16, 601-634.

Dufour, F. (2000). Groundwater in the Netherlands. Delft: Netherlands Institute of Applied Geoscience, TNO.

Feddes, R. A., Kabat, P., Van Bakel, P. J. T., Bronswijk, J. J. B., & Halbertsma, J. (1988). Modelling soil water dynamics in the unsaturated zone - state of the art. Journal of Hydrology, 100(1), 69 - 111. doi: 10.1016/0022-1694(88)90182-5

Fenicia, F., Savenije, H. H. G., Matgen, P., & Pfister, L. (2006). Is the groundwater reservoir linear? learning from data in hydrological modelling. Hydrology and Earth System Sciences, 10(1), 139–150. doi: 10.5194/hess-10-139-2006

Field, A. (2017). Discovering statistics using IBM SPSS statistics (Fifth ed.). London: SAGE Publications.

Fitts, C. R. (2013). Groundwater science (Second ed.). Boston: Academic Press. doi: 10.1016/B978-0-12-384705-8.00003-0

Grinevskii, S. O. (2011). Modeling root water uptake when calculating unsaturated flow in the vadose zone and groundwater recharge. Moscow University Geology Bulletin, 66, 189–201. doi: 10.3103/S0145875211030057

Heinen, M., Bakker, G., & Wösten, J. (2020). Waterretentie- en doorlatendheidskarakteristieken van boven- en ondergronden in nederland: de staringreeks: Update 2018 (No. 2978). Wageningen Environmental Research. (Project number: KB-33-001-021) doi: 10.18174/512761

Hipel, K. W., & McLeod, A. I. (1994). Time series modelling of water resources and environmental systems. London: Elsevier Science.

Jackson, E. K., Roberts, W., Nelsen, B., Williams, G. P., Nelson, E. J., & Ames, D. P. (2019). Introductory overview: Error metrics for hydrologic modelling – a review of common practices and an open source library to facilitate use and adoption. Environmental Modelling & Software, 119, 32-48. doi: 10.1016/j.envsoft.2019.05.001

Kirchner, J. W. (2006). Getting the right answers for the right reasons: Linking measurements, analyses, and models to advance the science of hydrology. Water Resources Research, 42(3). doi: 10.1029/2005WR004362

Knotters, M., & Bierkens, M. F. P. (2000). Physical basis of time series models for water table depths. Water Resources Research, 36(1), 181-188. doi: 10.1029/1999WR900288

Kraijenhoff van de Leur, D. A. (1958). A study of non-steady groundwater flow with special reference to a reservoir coefficient. De Ingenieur, 70(19), B87–B94.

Mays, L. W. (2010). Water resources engineering (Second ed.). Hoboken, New Jersey, USA: John Wiley & Sons, Inc.

McDonnell, J. J., Sivapalan, M., Vaché, K., Dunn, S., Grant, G., Haggerty, R., … Weiler, M. (2007). Moving beyond heterogeneity and process complexity: A new vision for watershed hydrology. Water Resources Research, 43(7), W07301. doi: 10.1029/2006WR005467

Neto, D. C., Chang, H. K., & van Genuchten, M. T. (2016). A mathematical view of water table fluctuations in a shallow aquifer in brazil. Groundwater, 54(1), 82-91. doi: 10.1111/gwat.12329

Obergfell, C., Bakker, M., & Maas, K. (2019). Estimation of average diffuse aquifer recharge using time series modeling of groundwater heads. Water Resources Research, 55(3), 2194-2210. doi: 10.1029/2018WR024235

Perrin, C., Michel, C., & Andréassian, V. (2001). Does a large number of parameters enhance model performance? comparative assessment of common catchment model structures on 429 catchments. Journal of Hydrology, 242(3), 275-301. doi: 10.1016/S0022-1694(00)00393-0

Peterson, T. J., & Western, A. W. (2014). Nonlinear time-series modeling of unconfined groundwater head. Water Resources Research, 50(10), 8330-8355. doi: 10.1002/2013WR014800

Schuurmans, J., & Droogers, P. (2010). Penman-monteith referentieverdamping: inventarisatie beschikbaarheid en mogelijkheden tot regionalisatie. STOWA, 37.

Siegel, D. I., & Hinchey, E. J. (2019). Big data and the curse of scale. Groundwater, 57(4), 505-505. doi: 10.1111/gwat.12905

Simunek, J. (2009). Notes on spatial and temporal discretization (when working with hydrus) [Computer software manual].

Simunek, J., Jarvis, N. J., van Genuchten, M. T., & Gärdenäs, A. (2003). Review and comparison of models for describing non-equilibrium and preferential flow and transport in the vadose zone. Journal of Hydrology, 272(1), 14-35. (Soil Hydrological Properties and Processes and their Variability in Space and Time) doi: 10.1016/S0022-1694(02)00252-4

Simunek, J., Šejna, M., Saito, H., Sakai, M., & van Genuchten, M. T. (2009). The HYDRUS-1D software package for simulating the one-dimensional movement of water, heat, and multiple solutes in variably-saturated media (4.08 ed.) [Computer software manual].

Sutanto, S. J., Wenninger, J., Coenders-Gerrits, A. M. J., & Uhlenbrook, S. (2012). Partitioning of evaporation into transpiration, soil evaporation and interception: a comparison between isotope measurements and a hydrus-1d model. Hydrology and Earth System Sciences, 16(8), 2605–2616. doi: 10.5194/hess-16-2605-2012

van Dam, J., & Feddes, R. (2000). Numerical simulation of infiltration, evaporation and shallow groundwater levels with the richards equation. Journal of Hydrology, 233, 72–85. doi: 10.1016/S0022-1694(00)00227-4

van Genuchten, M. T. (1980). A closed-form equation for predicting the hydraulic conductivity of unsaturated soils. Soil Science Society of America Journal, 44(5), 892-898. doi: 10.2136/sssaj1980.03615995004400050002x

van Genuchten, M. T. (1987). A numerical model for water and solute movement in and below the root zone. Research Report No 121, U.S. Salinity laboratory, USDA, ARS, Riverside, California.

Ven, G. A. (1979). Een rekenmodel voor het bescrhijven van de afvoer van de afvoer in het landelijk gebied van de flevopolders (Tech. Rep. No. 12794). Smedinghuis Lelystad: Rijksdienst voor de IJselmeerpolders.

Virtanen, P., Gommers, R., Oliphant, T. E., Haberland, M., Reddy, T., Cournapeau, D., … SciPy 1.0 Contributors (2020). SciPy 1.0: Fundamental Algorithms for Scientific Computing in Python. Nature Methods, 17, 261–272. doi: 10.1038/s41592-019-0686-2

von Asmuth, J., Baggelaar, P., Bakker, M., D., B., Collenteur, R. A., Ebbens, O., … Schaars, F. (2021). Handleiding tijdreeksanalyse. STOWA, 32.

von Asmuth;, J., Bierkens, M. F. P., & Maas, K. (2002). Transfer function-noise modeling in continuous time using predefined impulse response functions. Water Resources Research, 38(12), 23-1-23-12. doi: 10.1029/2001WR001136

von Asmuth;, J. R. (2012). Groundwater system identification through time series analysis (Doctoral dissertation, Delft University of Technology). Retrieved from http://resolver.tudelft.nl/uuid:b6ccd472-9b9d-4810-aa19-3a0b046017e0

von Asmuth, J. R., & Bierkens, M. F. P. (2005). Modeling irregularly spaced residual series as a continuous stochastic process. Water Resources Research, 41(12). doi: 10.1029/2004WR003726

Wang, P., & Pozdniakov, S. P. (2014). A statistical approach to estimating evapotranspiration from diurnal groundwater level fluctuations. Water Resources Research, 50(3), 2276-2292. doi: 10.1002/2013WR014251

Zaadnoordijk, W. J., Bus, S. A., Lourens, A., & Berendrecht, W. L. (2019). Automated time series modeling for piezometers in the national database of the netherlands. Groundwater, 57(6), 834-843. doi: 10.1111/gwat.12819

A Additional Figures Section 3.3

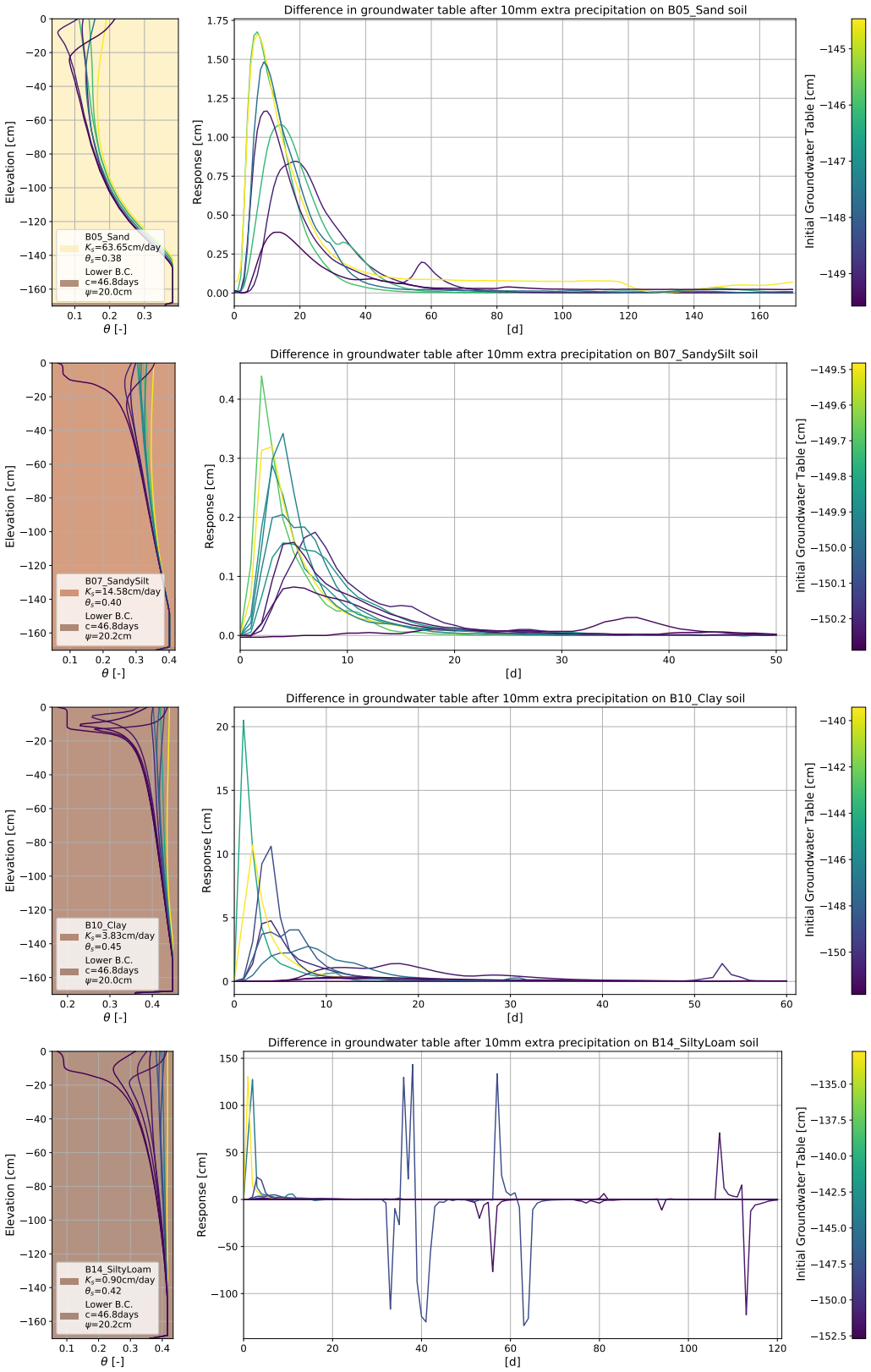

Figure A.1: Change in groundwater table response after 10mm extra precipitation

B Additional Figures Section 4.3

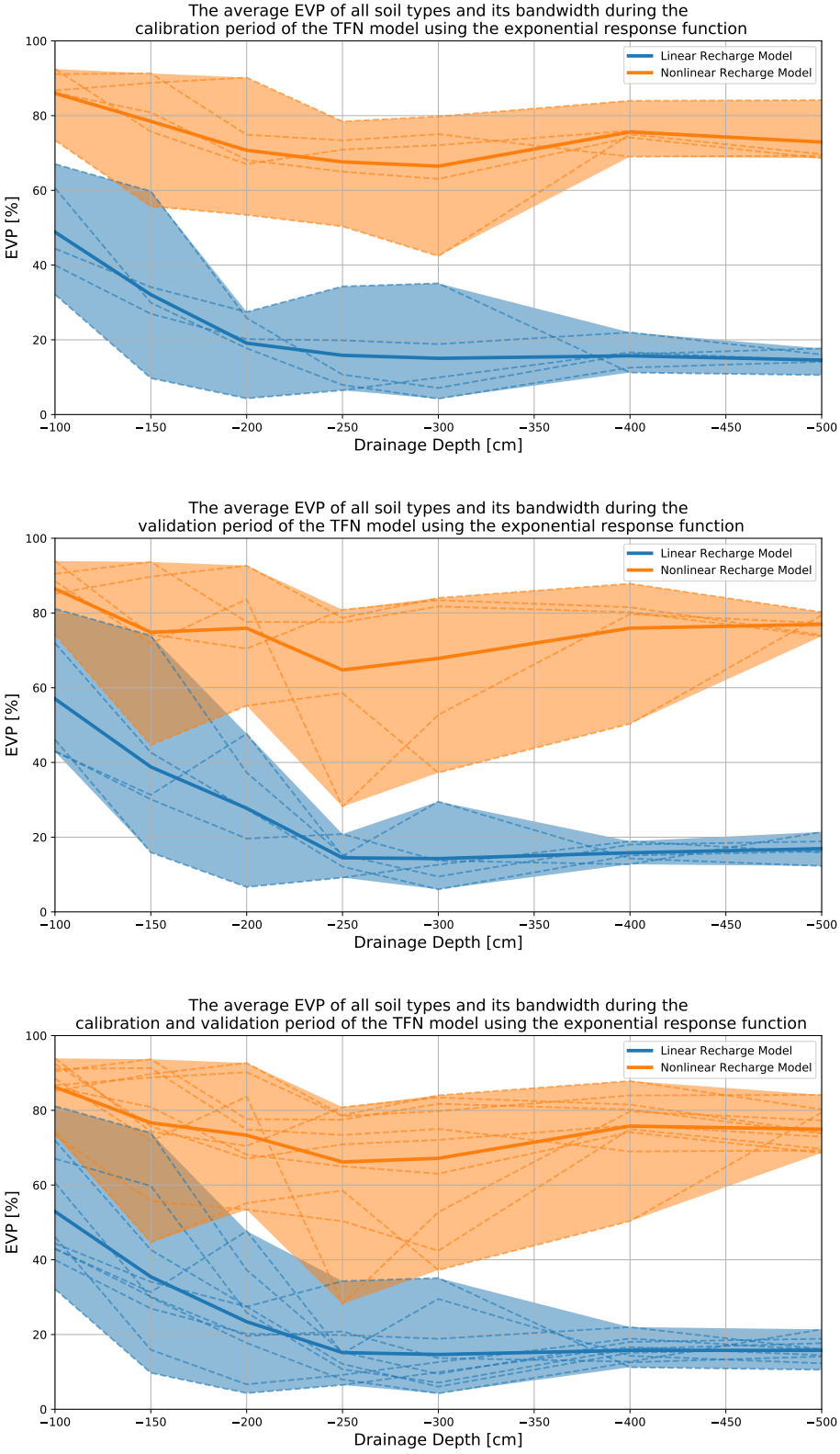

Figure B.1: The average EVP for all soil types against the drainage level for the calibration, validation period. The values for the soil types are visualised as dashed lines. The bandwidth shows the maximum and minimum EVP for any soil type for the specific recharge model. The exponential response function is used in the TFN model.

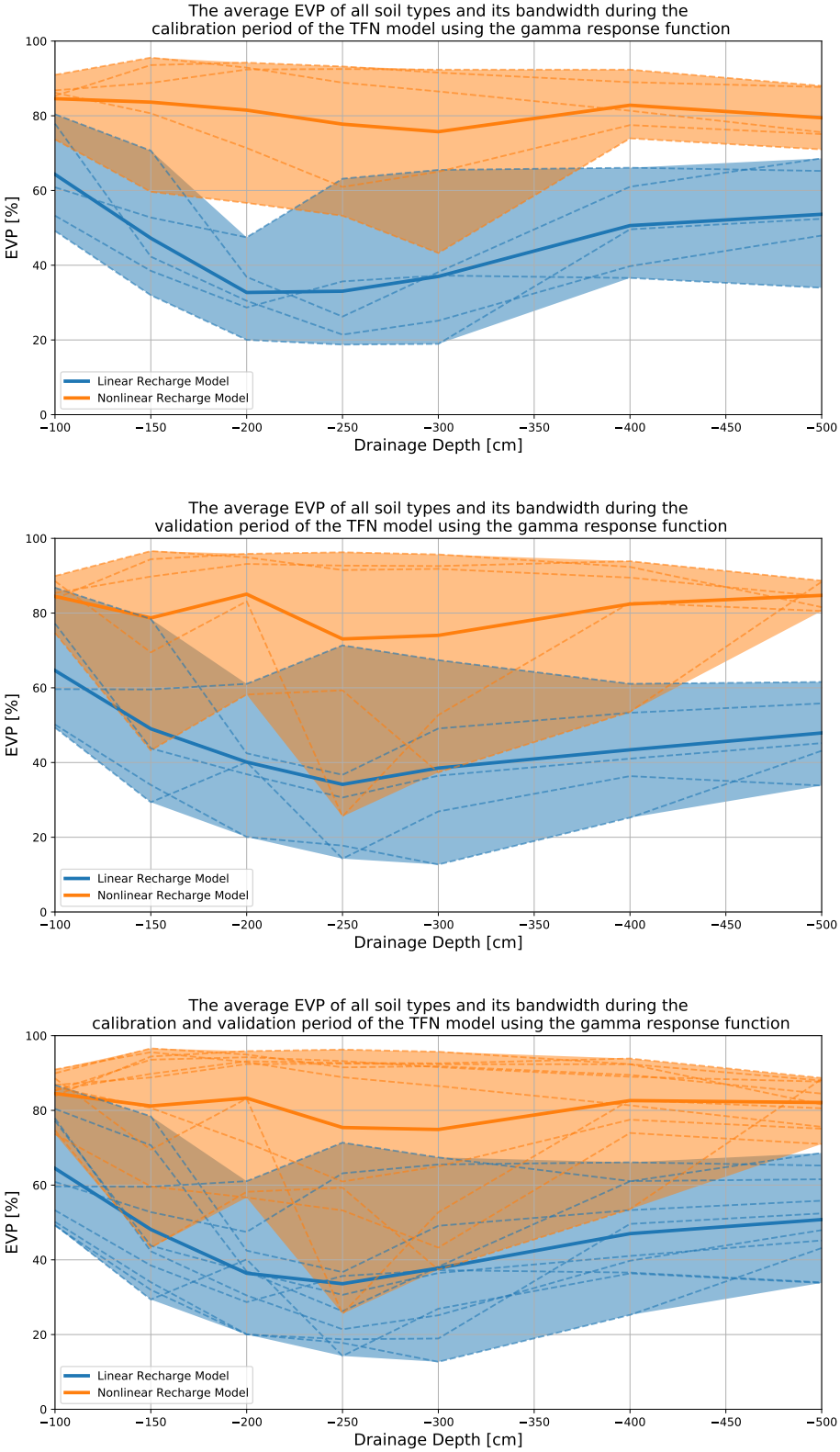

Figure B.2: The average EVP for all soil types against the drainage level for the calibration, validation period. The values for the soil types are visualised as dashed lines. The bandwidth shows the maximum and minimum EVP for any soil type for the specific recharge model. The gamma response function is used in the TFN model.

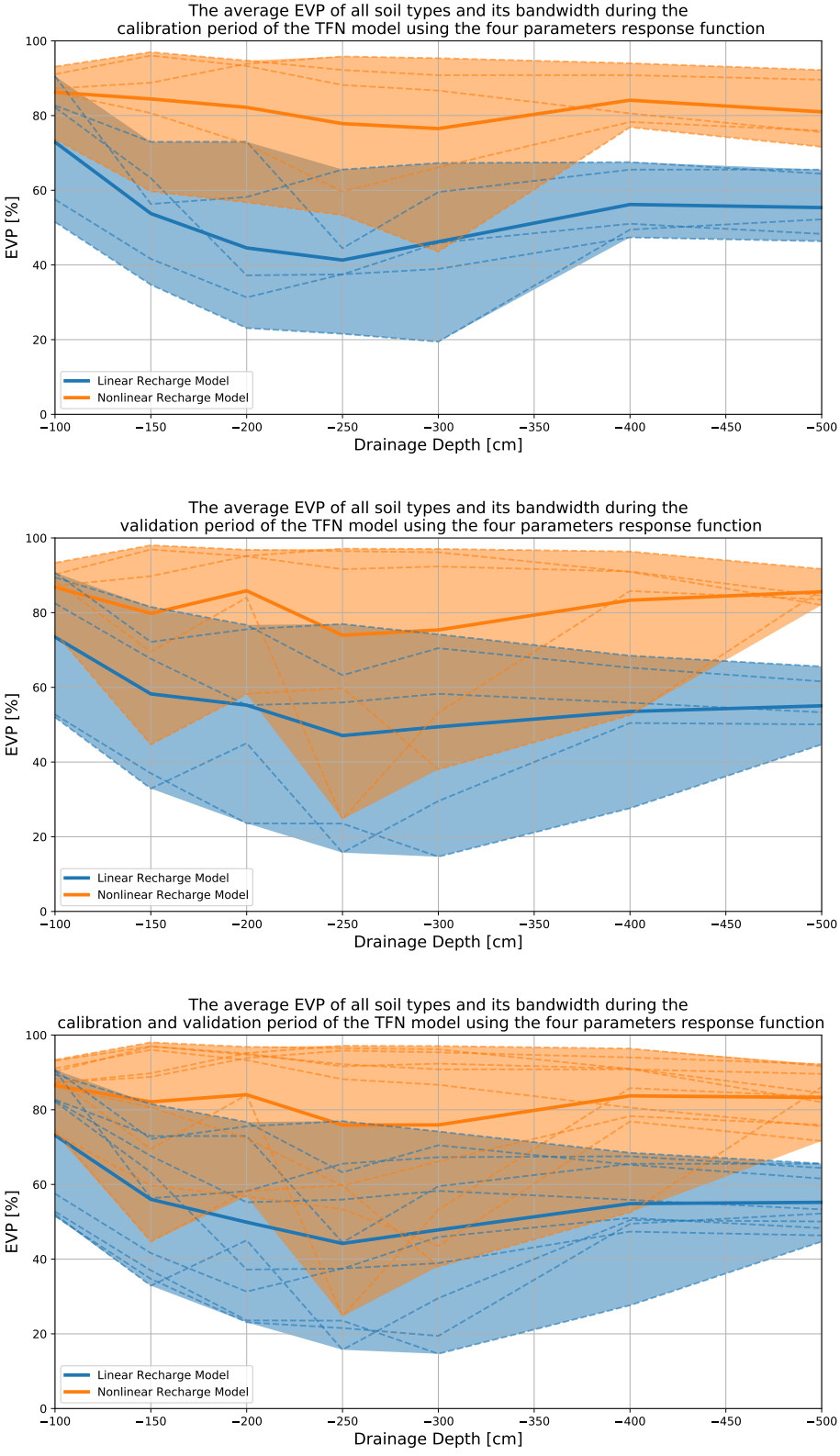

Figure B.3: The average EVP for all soil types against the drainage level for the calibration, validation period. The values for the soil types are visualised as dashed lines. The bandwidth shows the maximum and minimum EVP for any soil type for the specific recharge model. The four-parameters response function is used in the TFN model.

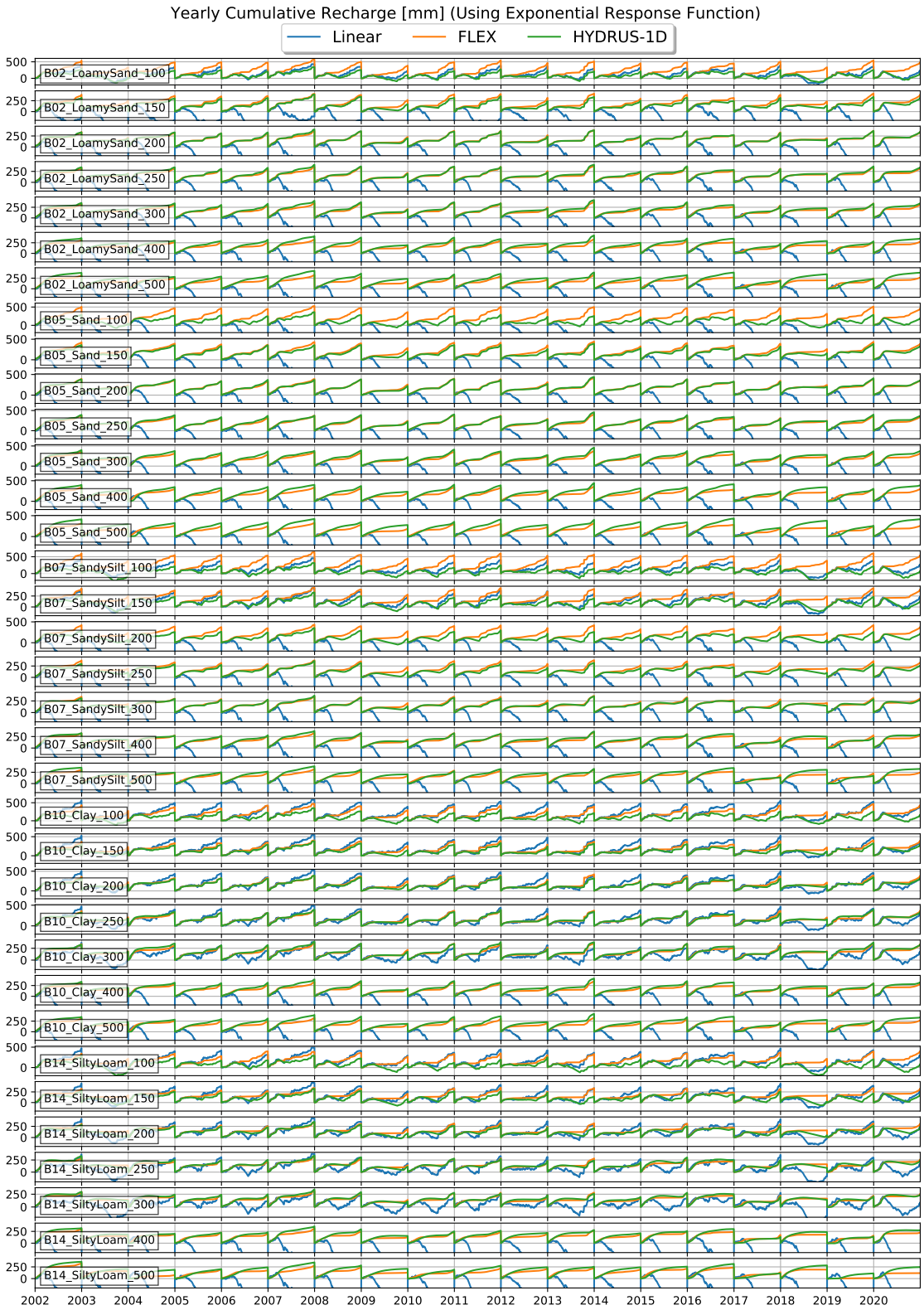

Figure B.4: Yearly Cumulative Recharge. This simulation uses the exponential response function.

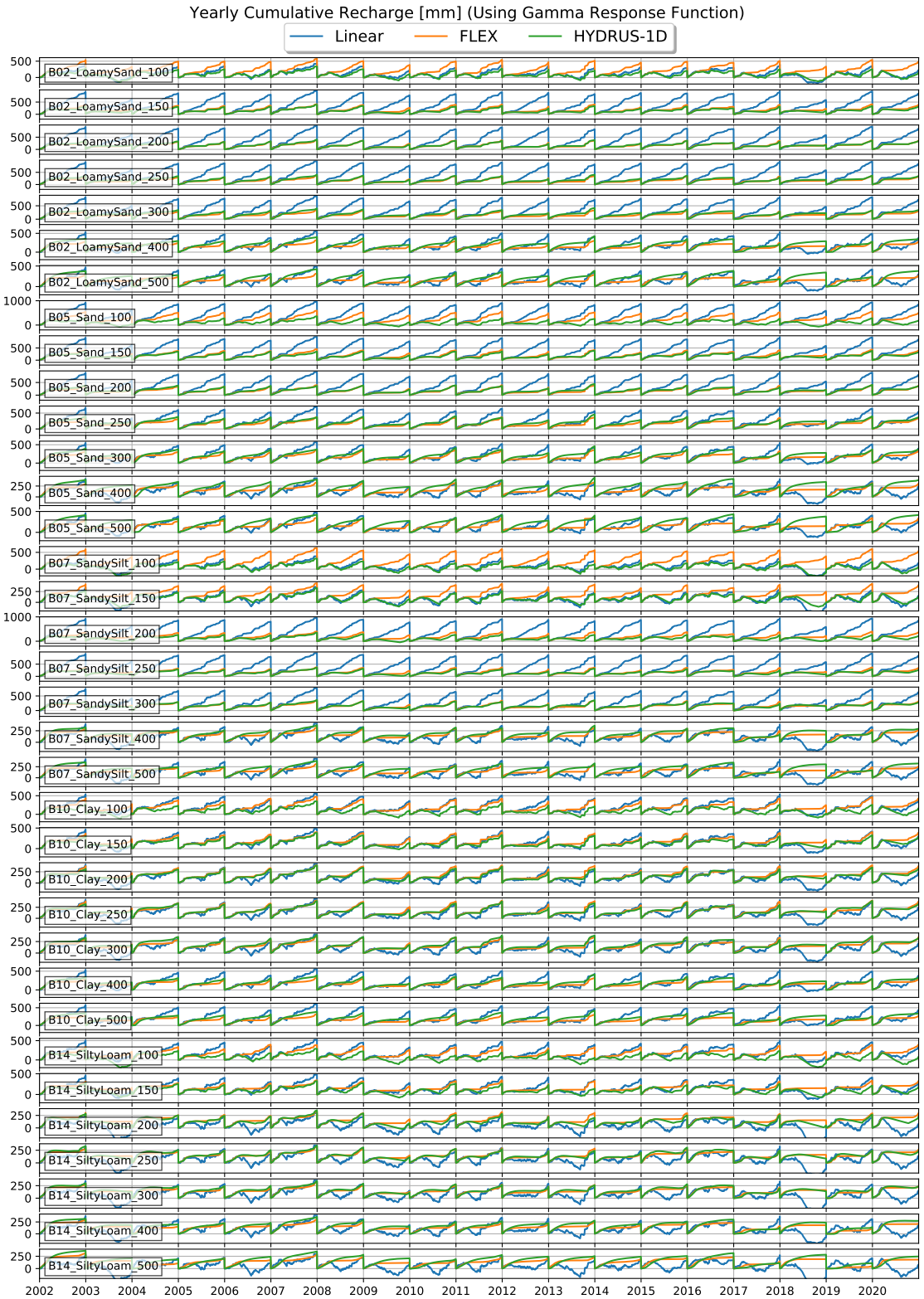

Figure B.5: Yearly Cumulative Recharge. This simulation uses the gamma response function.

Figure B.6: Yearly Cumulative Recharge. This simulation uses the four parameters response function.

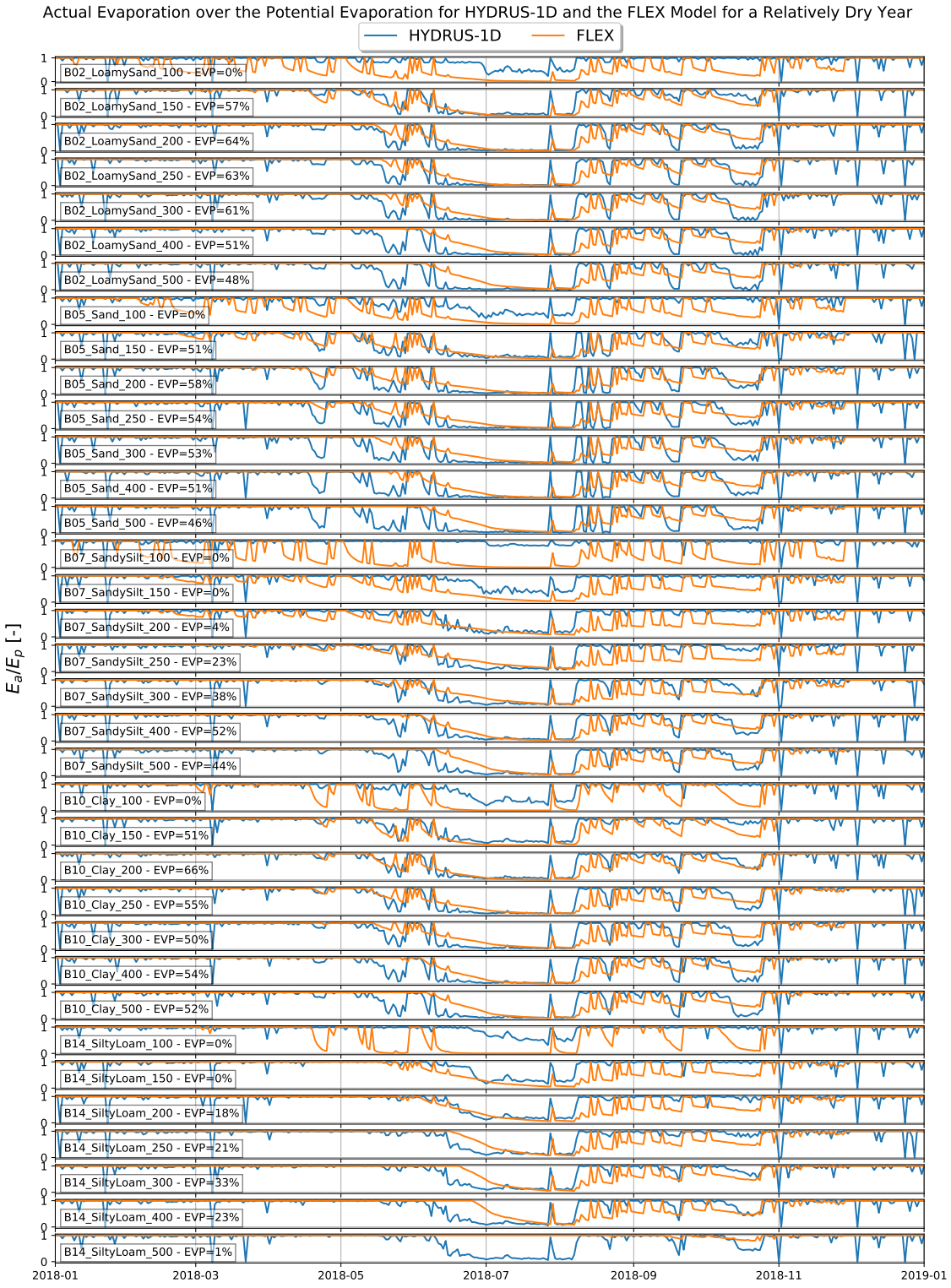

Figure B.7: Actual Evaporation over the Potential Evaporation for HYDRUS-1D and the FLEX Model for a Relatively Dry Year. For every subplot the soil profile, drainage level and EVP is shown. This simulation uses the exponential response function.

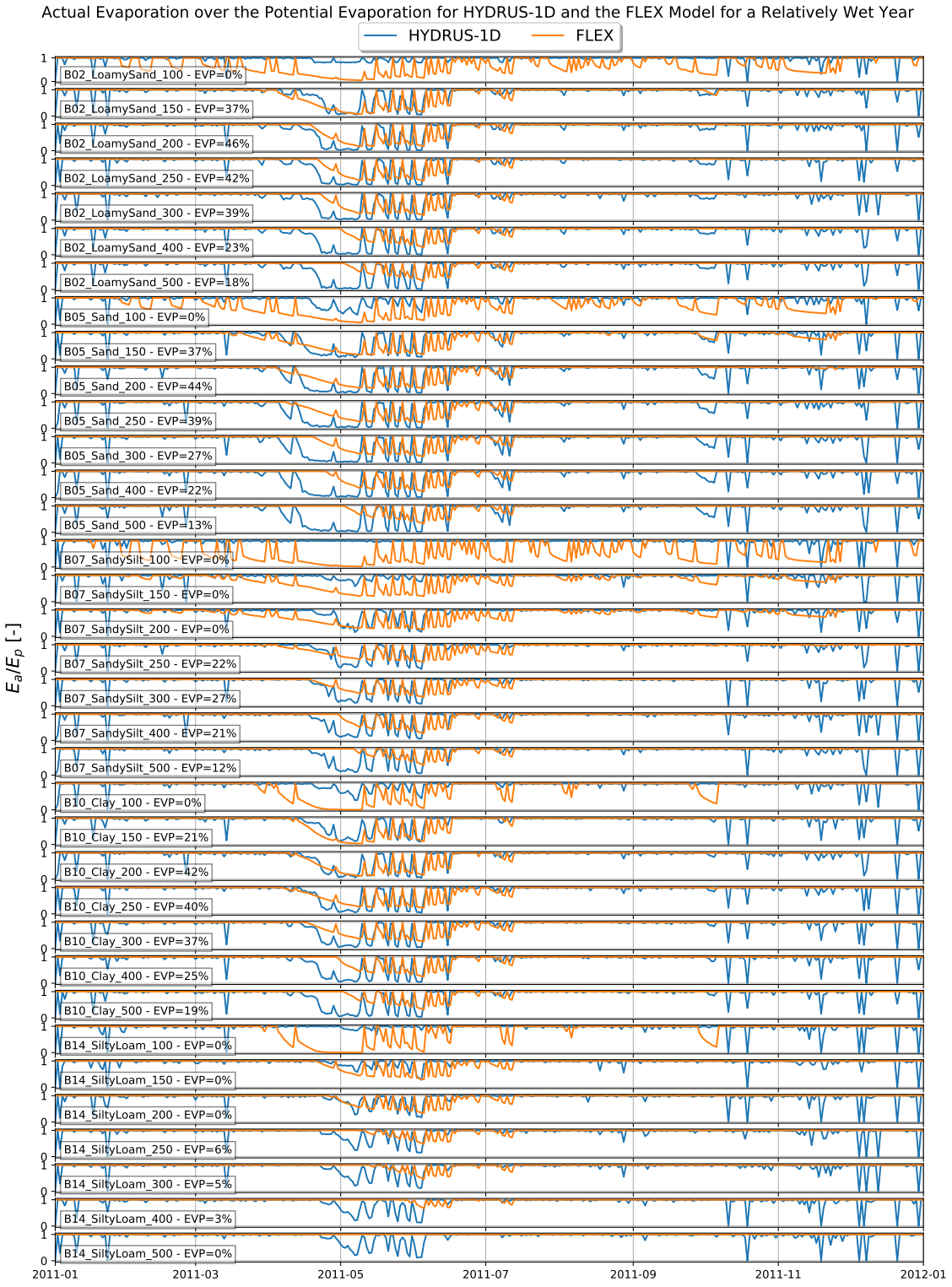

Figure B.8: Actual Evaporation over the Potential Evaporation for HYDRUS-1D and the FLEX Model for a Relatively Wet Year. For every subplot the soil profile, drainage level and EVP is shown. This simulation uses the exponential response function.

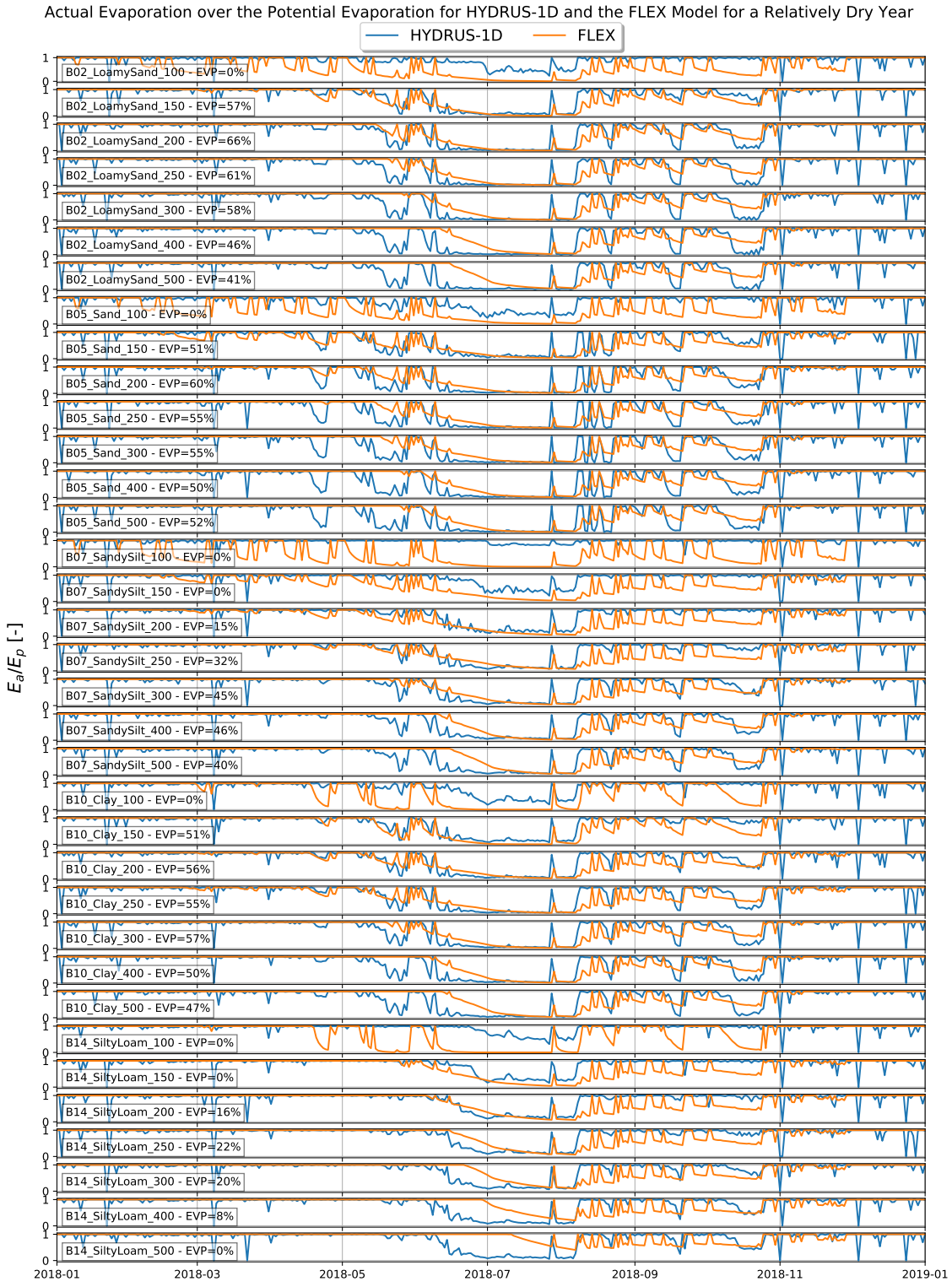

Figure B.9: Actual Evaporation over the Potential Evaporation for HYDRUS-1D and the FLEX Model for a Relatively Dry Year. For every subplot the soil profile, drainage level and EVP is shown. This simulation uses the gamma response function.

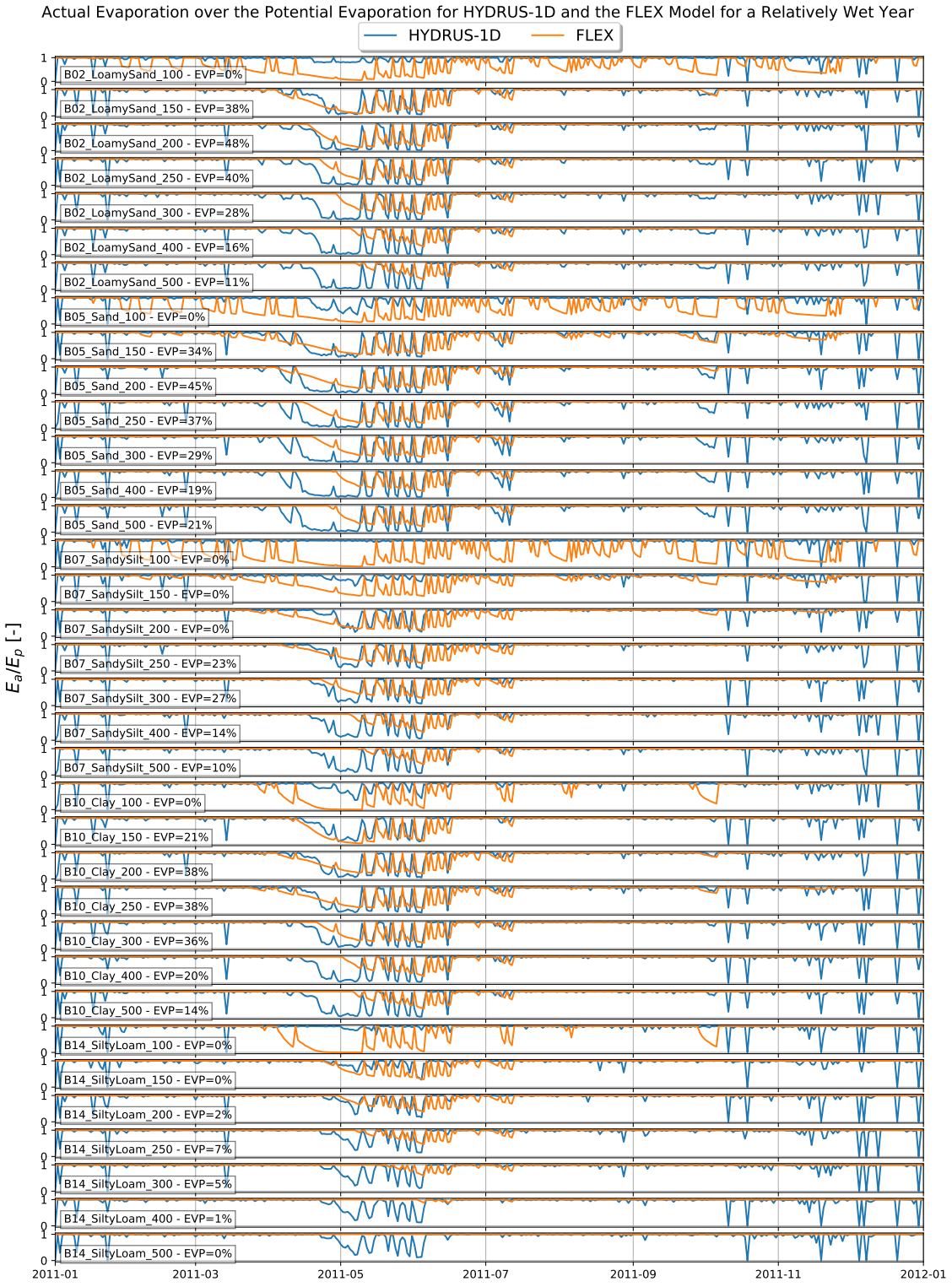

Figure B.10: Actual Evaporation over the Potential Evaporation for HYDRUS-1D and the FLEX Model for a Relatively Wet Year. For every subplot the soil profile, drainage level and EVP is shown. This simulation uses the gamma response function.

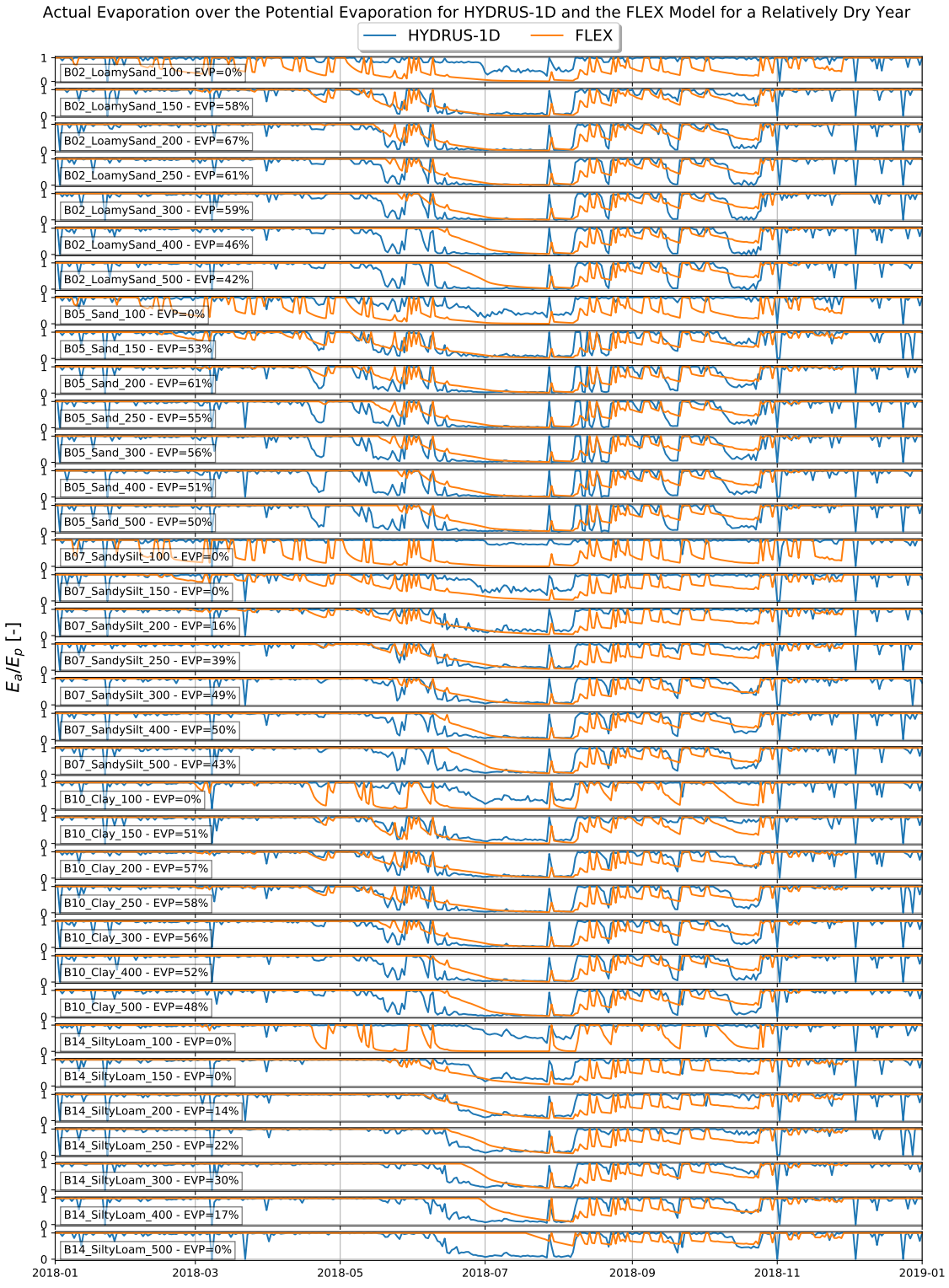

Figure B.11: Actual Evaporation over the Potential Evaporation for HYDRUS-1D and the FLEX Model for a Relatively Dry Year. For every subplot the soil profile, drainage level and EVP is shown. This simulation uses the four parameters response function.

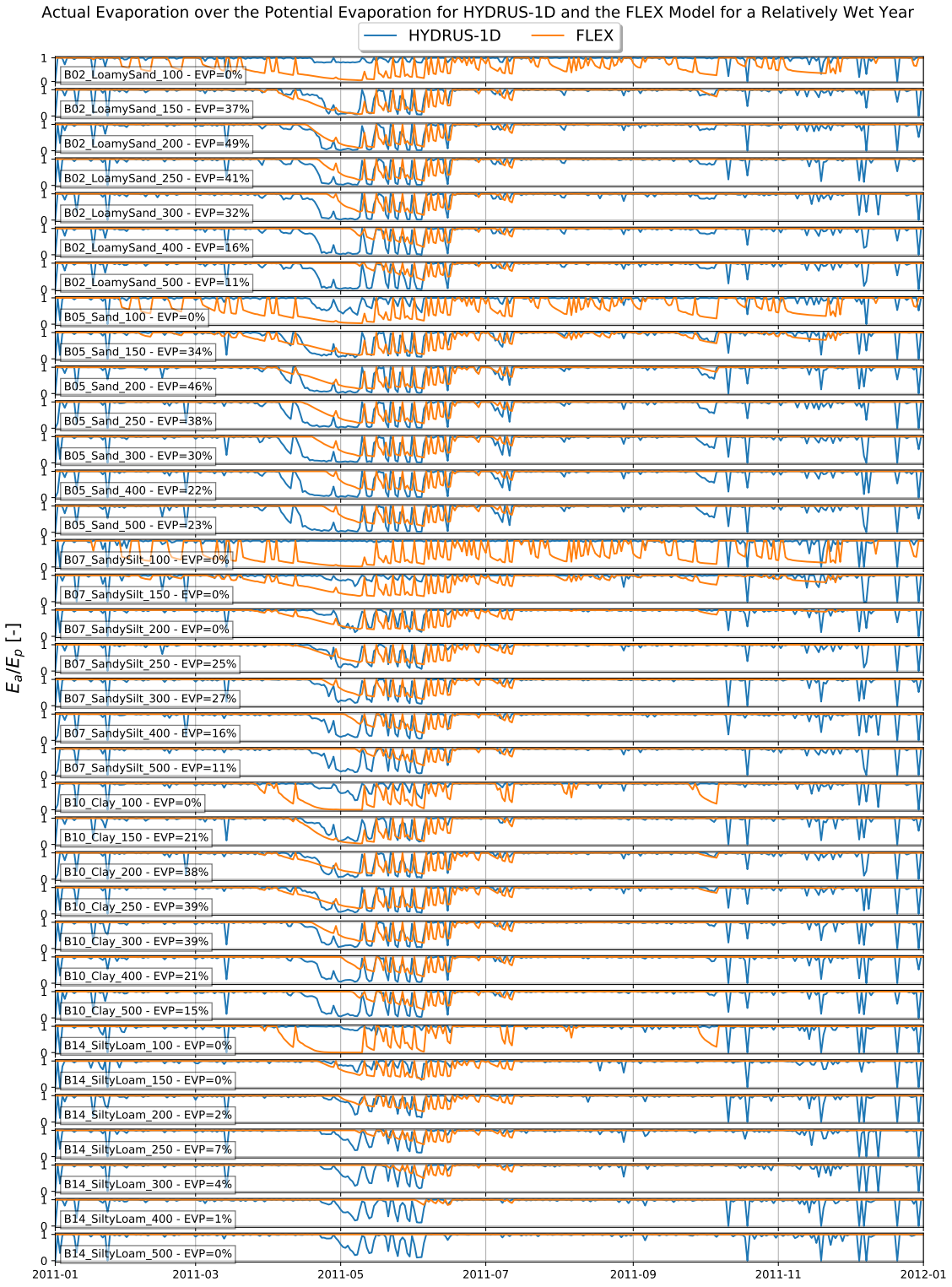

Figure B.12: Actual Evaporation over the Potential Evaporation for HYDRUS-1D and the FLEX Model for a Relatively Wet Year. For every subplot the soil profile, drainage level and EVP is shown. This simulation uses the four parameters response function.

C | HYDRUS-1D Groundwater Table Time Series

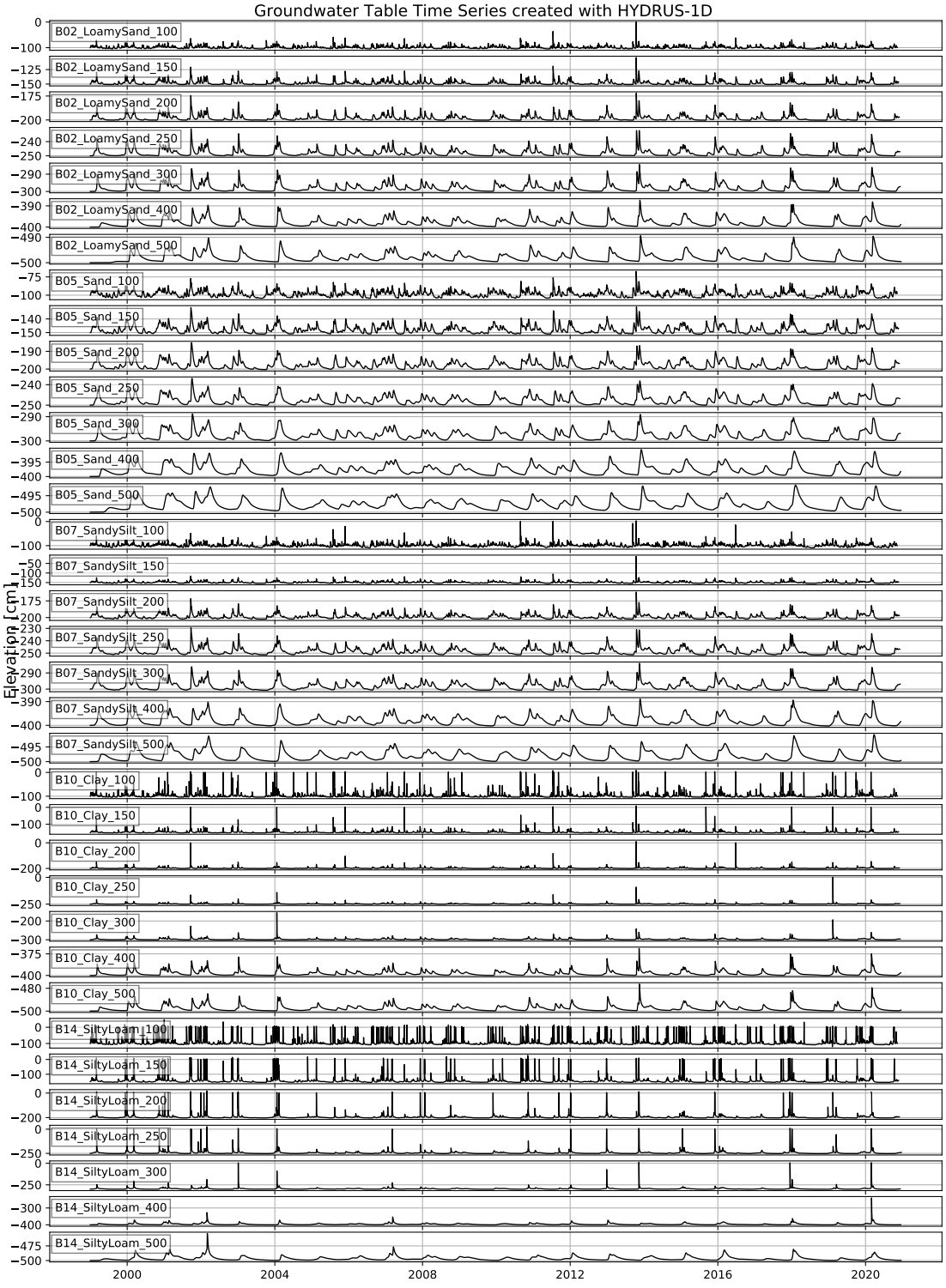

Figure C.1: Groundwater Table Time Series created with HYDRUS-1D

D | TFN Models Loamy Sand

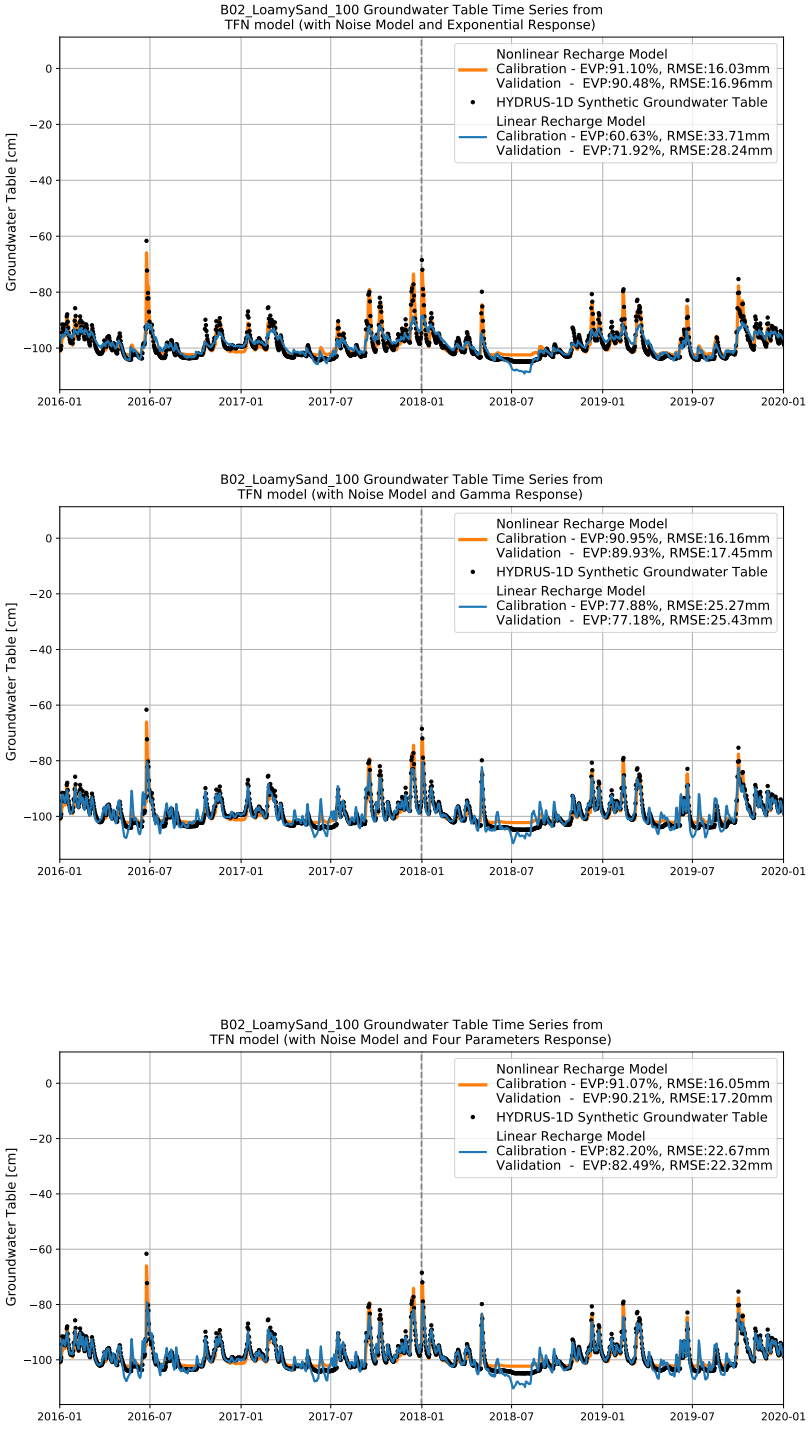

Figure D.1: Loamy Sand -100cm

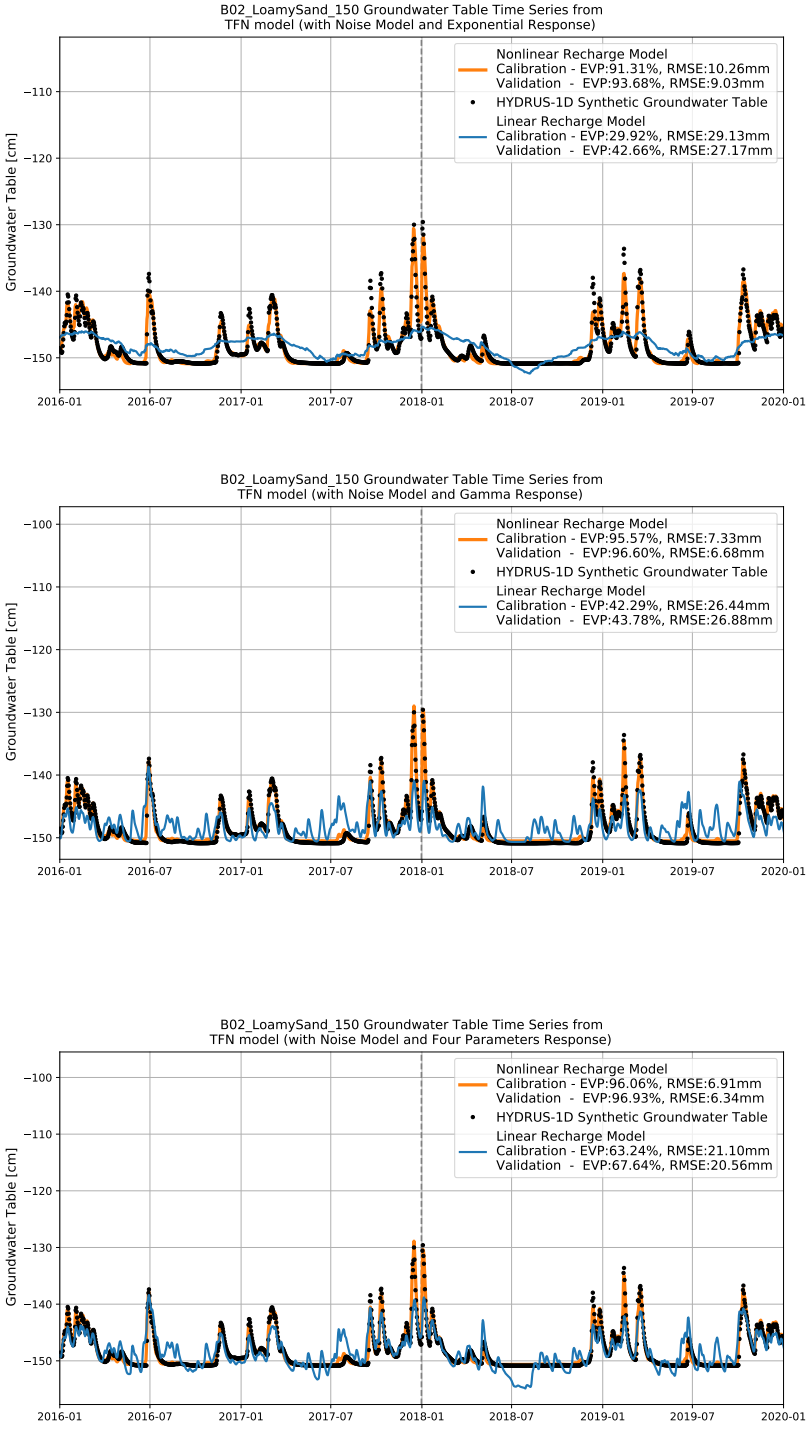

Figure D.2: Loamy Sand -150cm

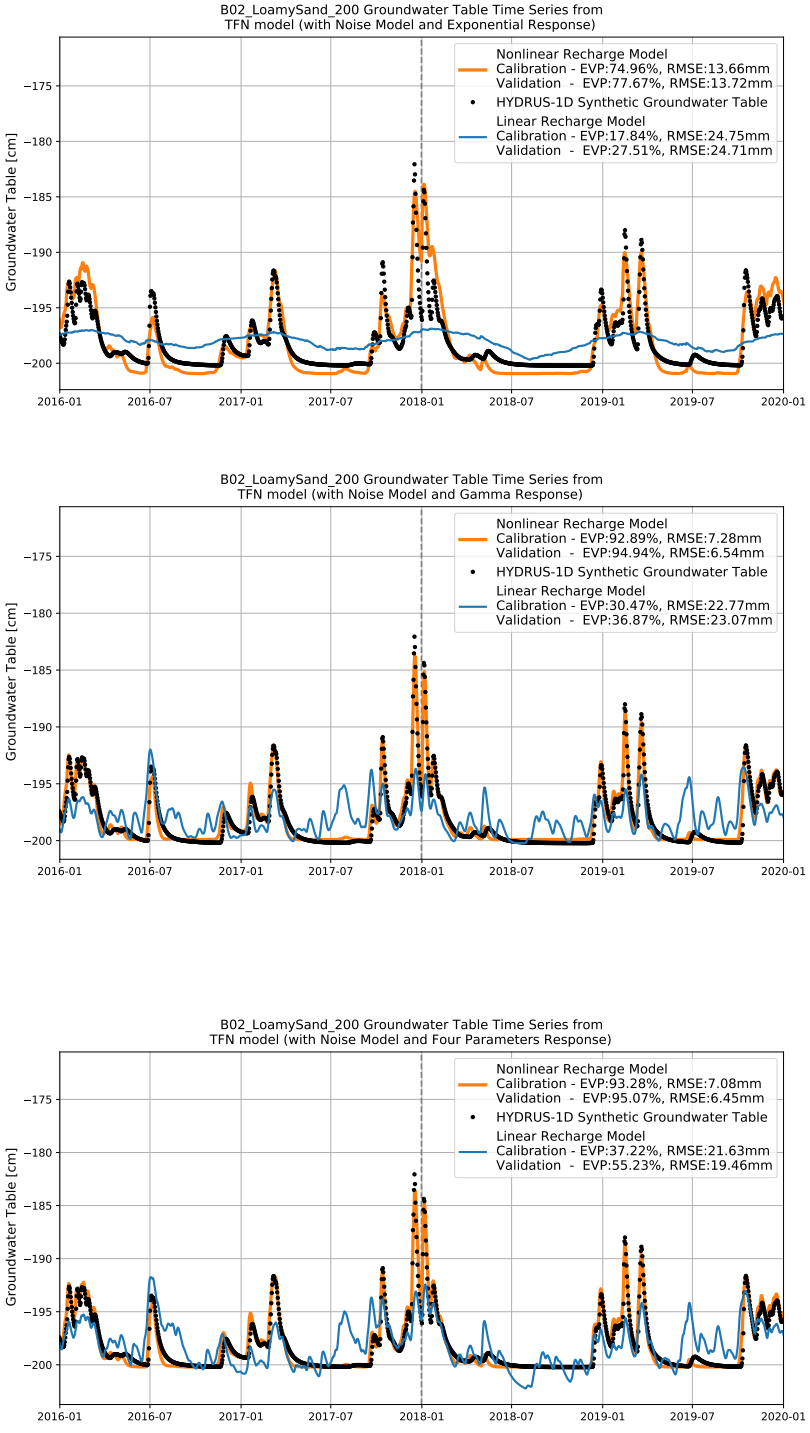

Figure D.3: Loamy Sand -200cm

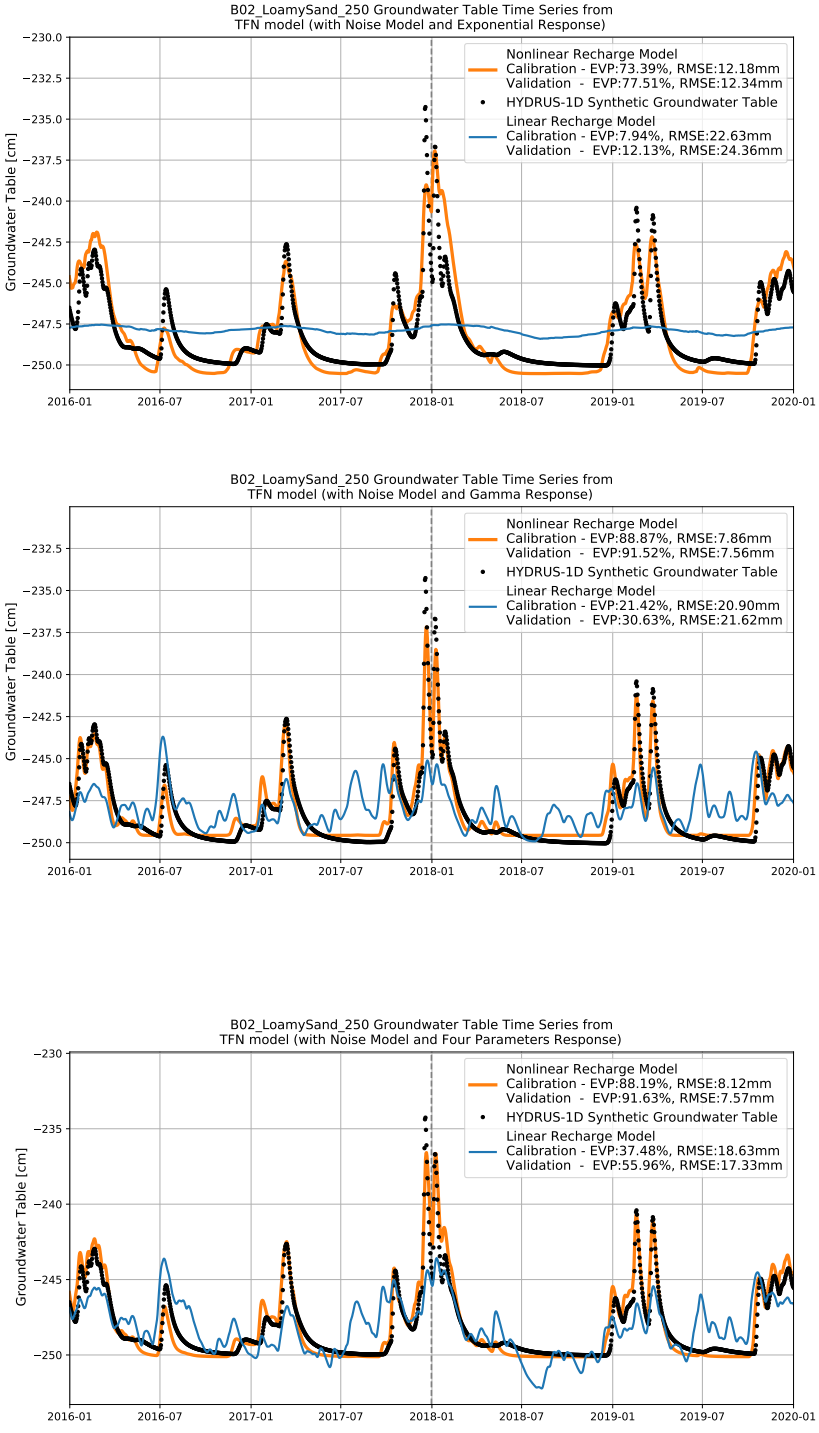

Figure D.4: Loamy Sand -250cm

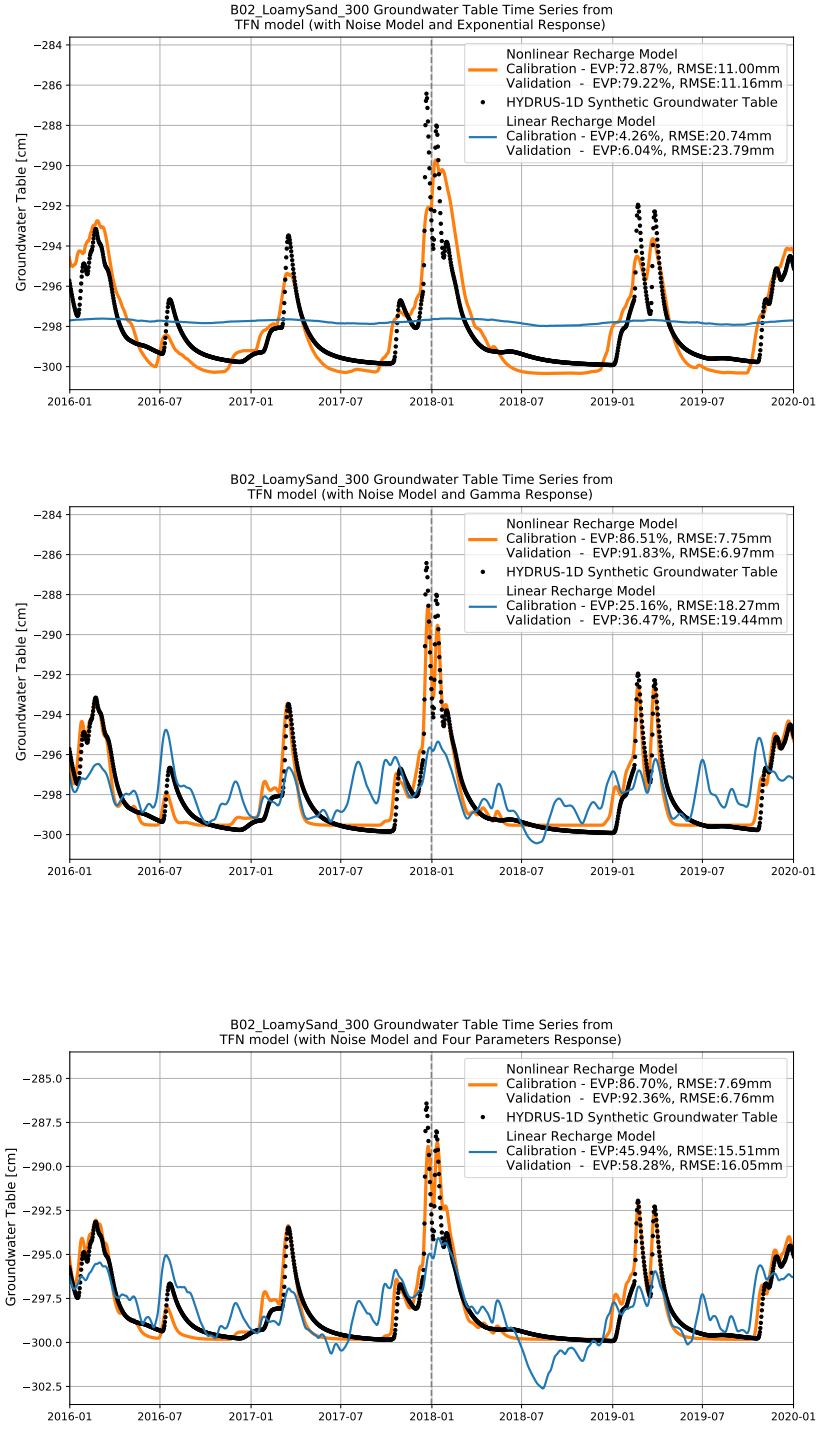

Figure D.5: Loamy Sand -300cm

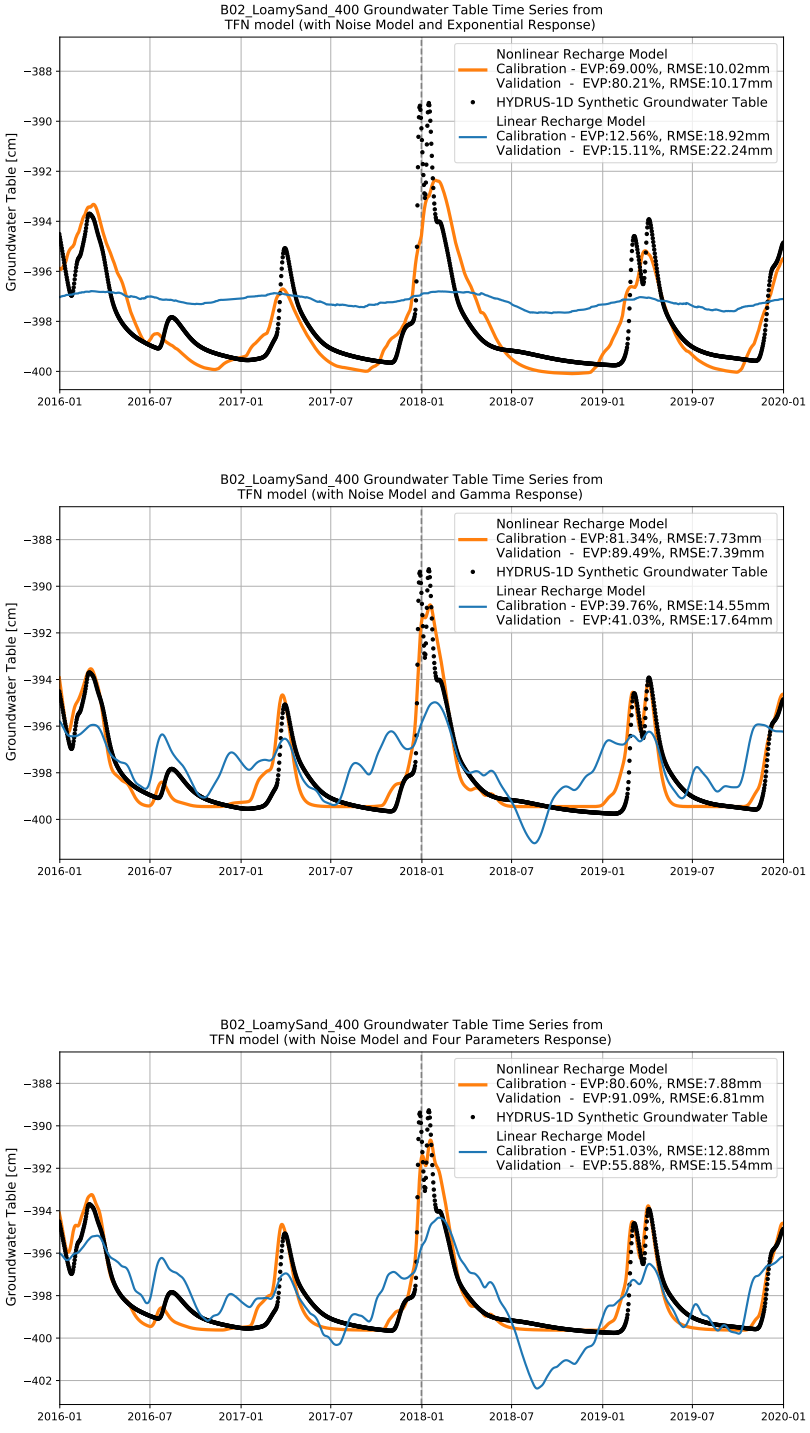

Figure D.6: Loamy Sand -400cm

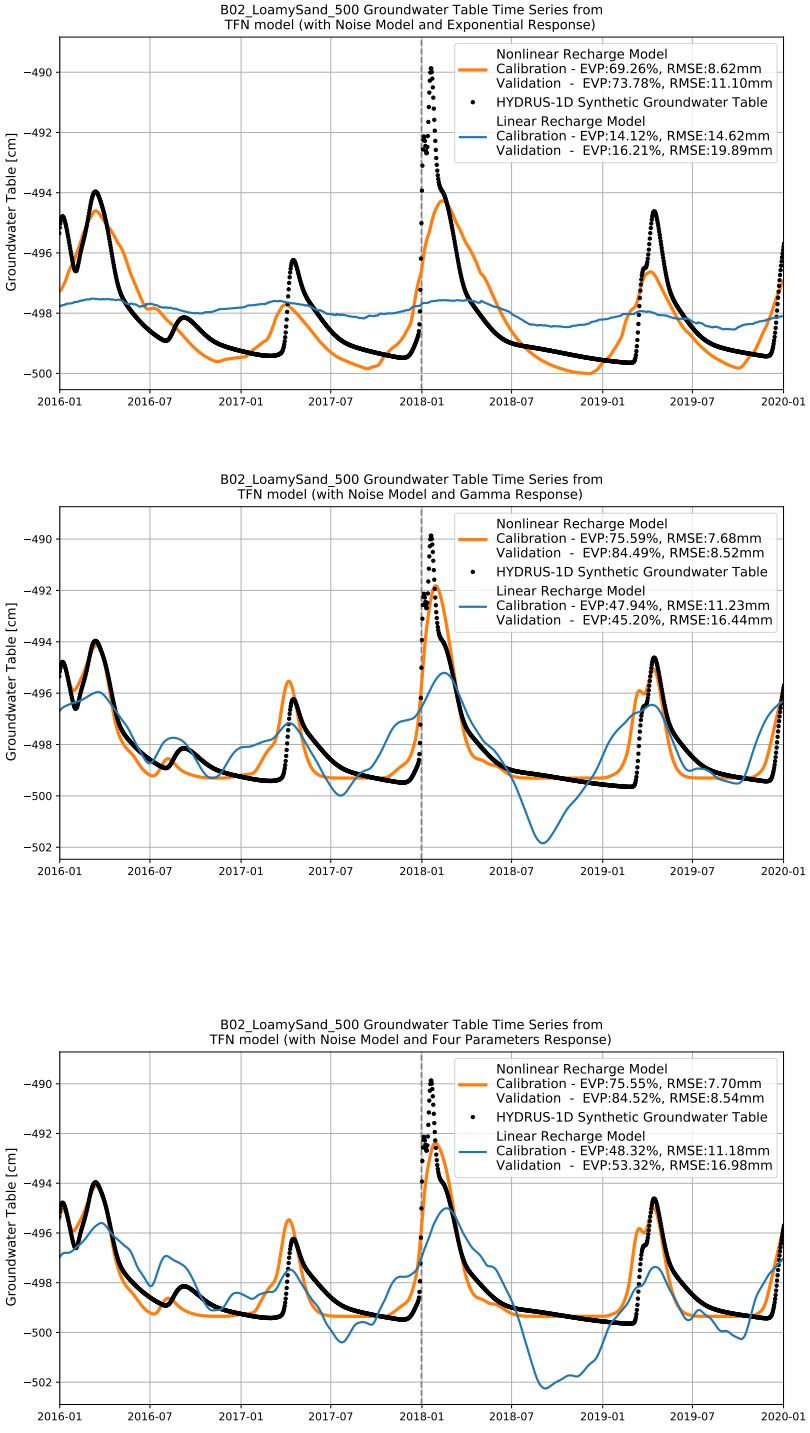

Figure D.7: Loamy Sand -500cm

E | TFN Models Sand

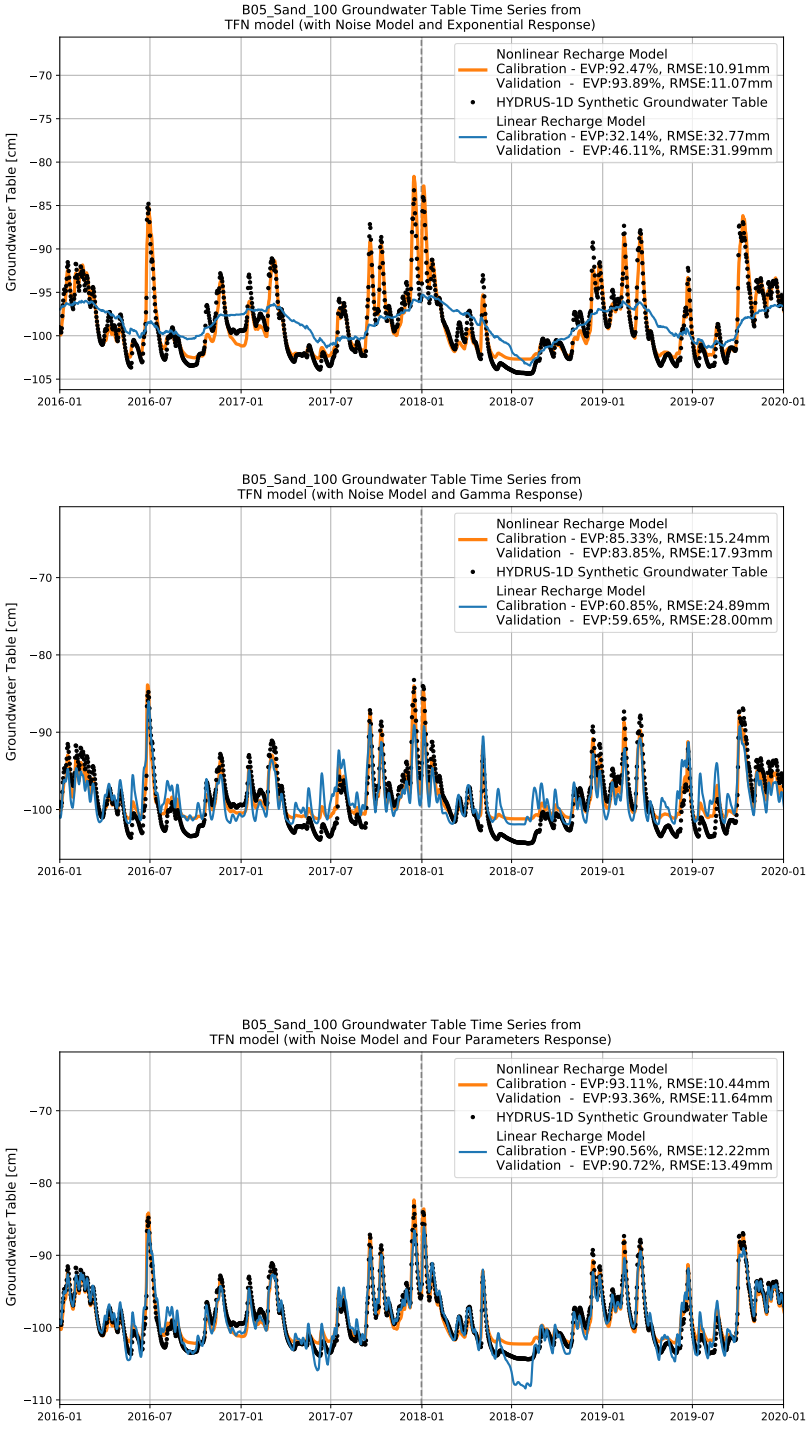

Figure E.1: Sand -100cm

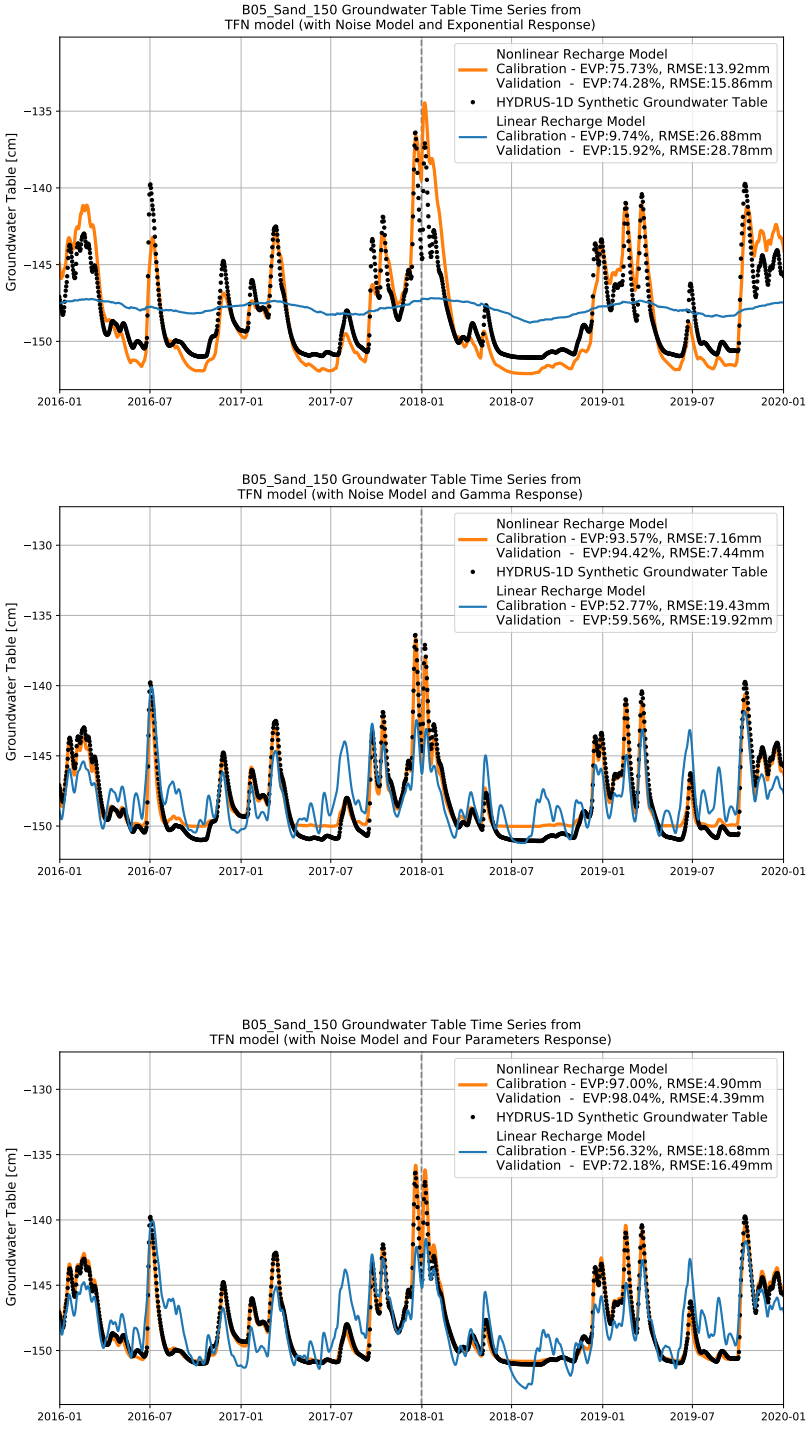

Figure E.2: Sand -150cm

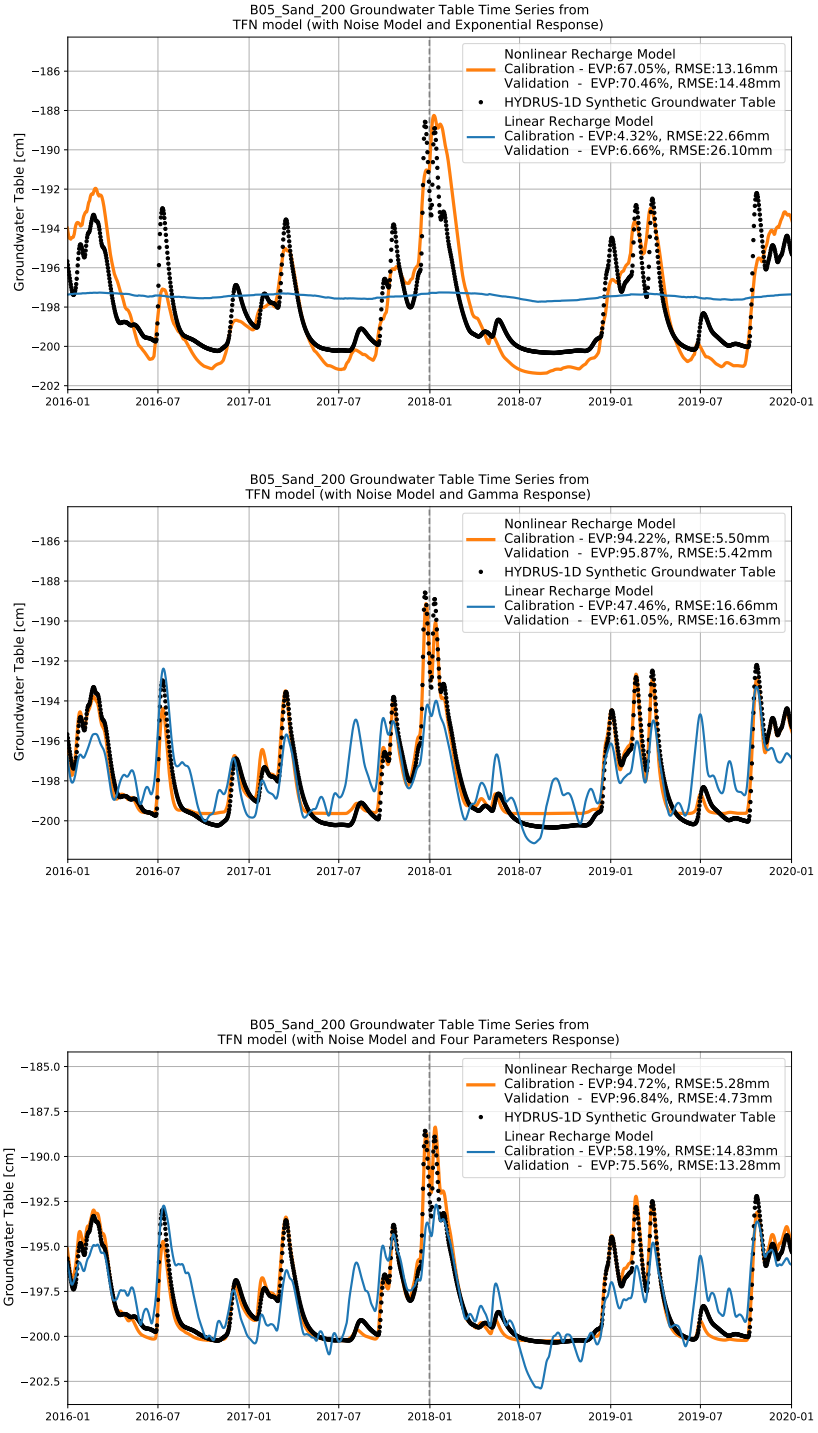

Figure E.3: Sand -200cm

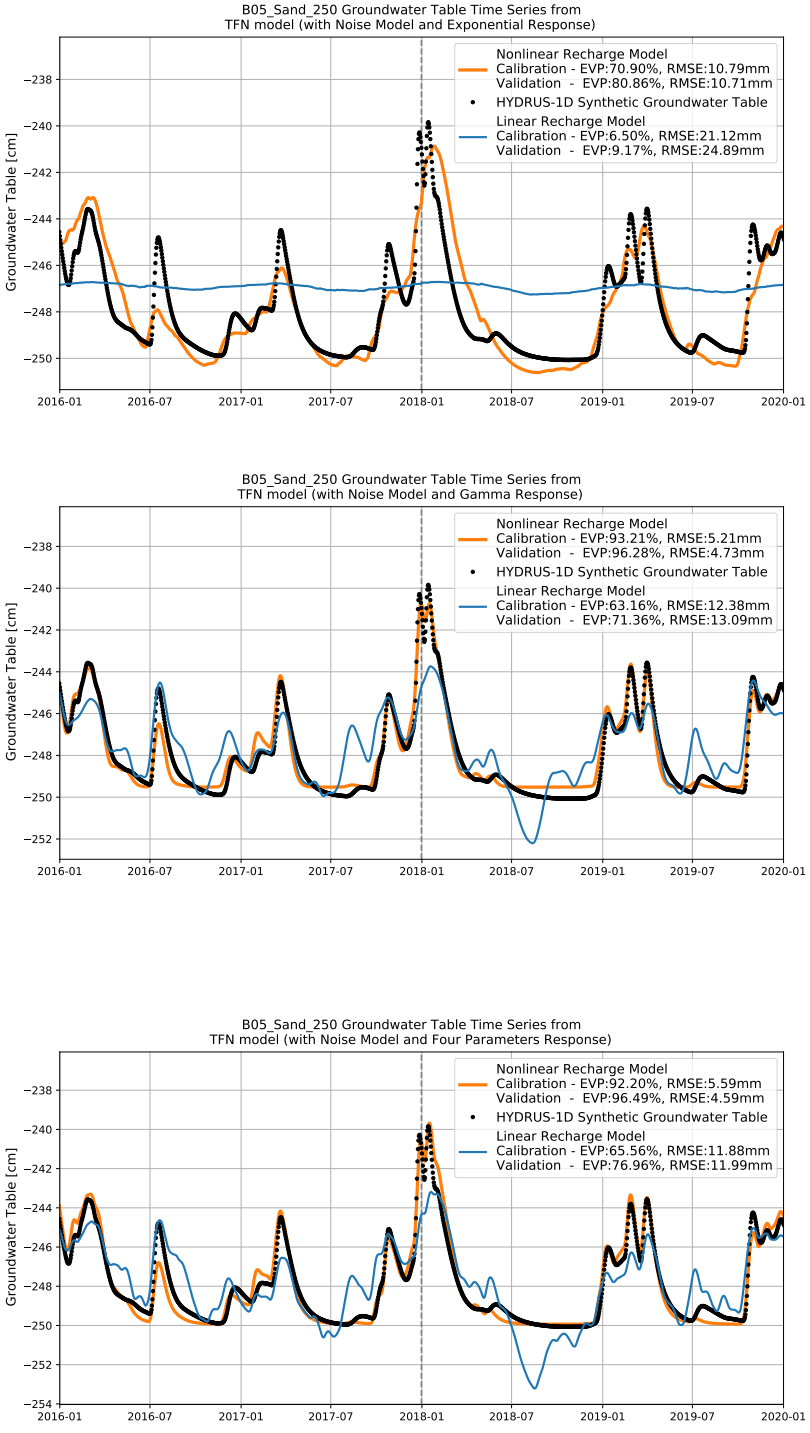

Figure E.4: Sand -250cm

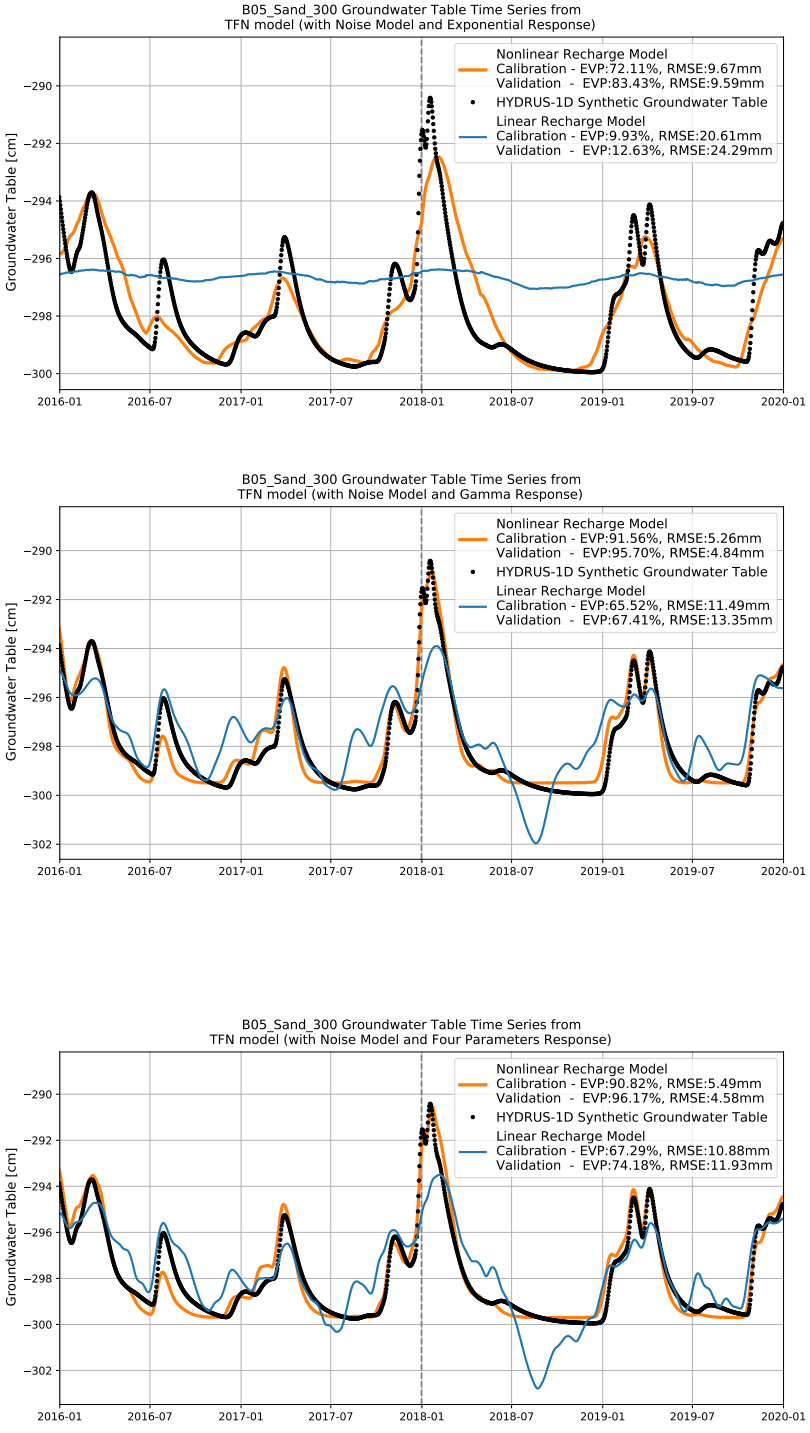

Figure E.5: Sand -300cm

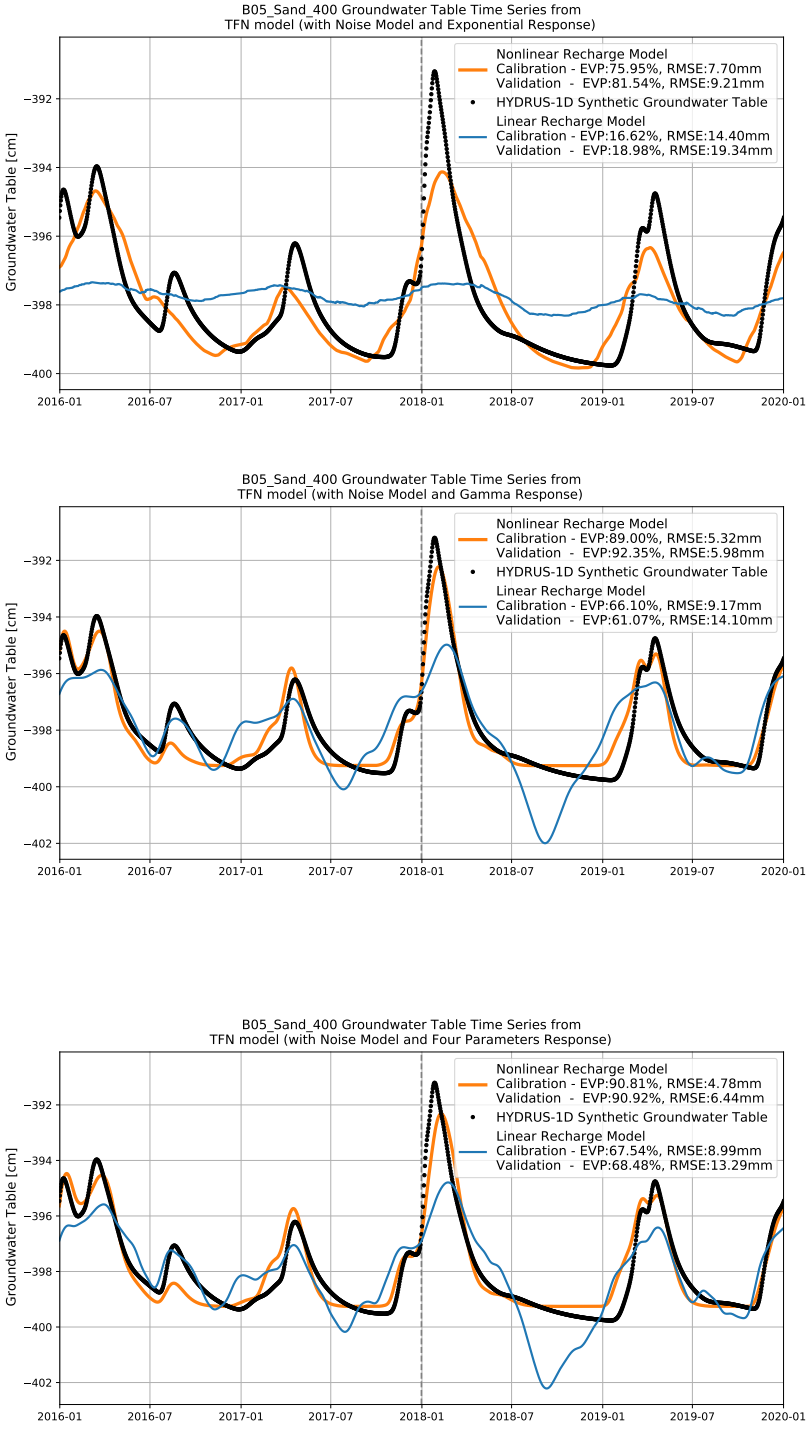

Figure E.6: Sand -400cm

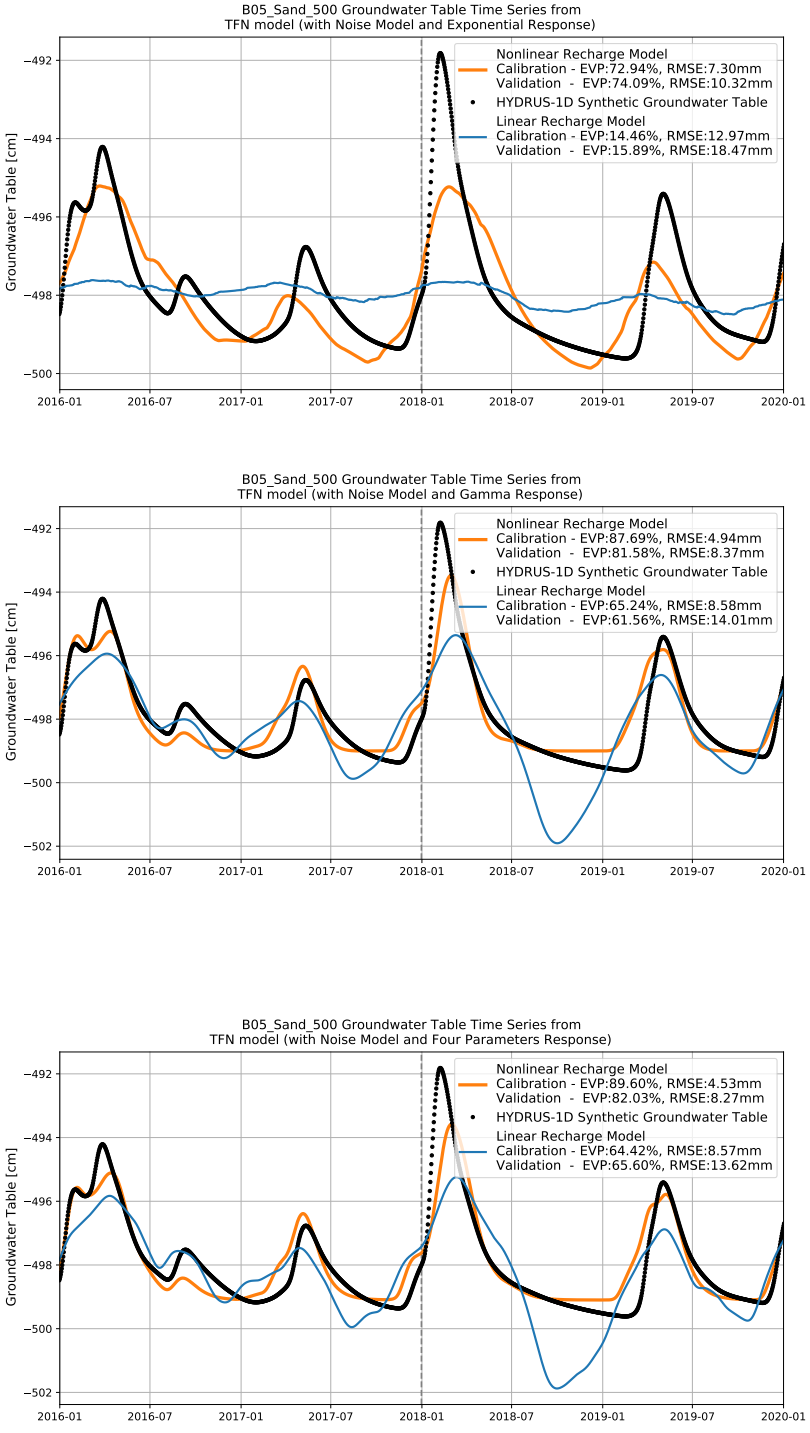

Figure E.7: Sand -500cm

F | TFN Models Sandy Silt

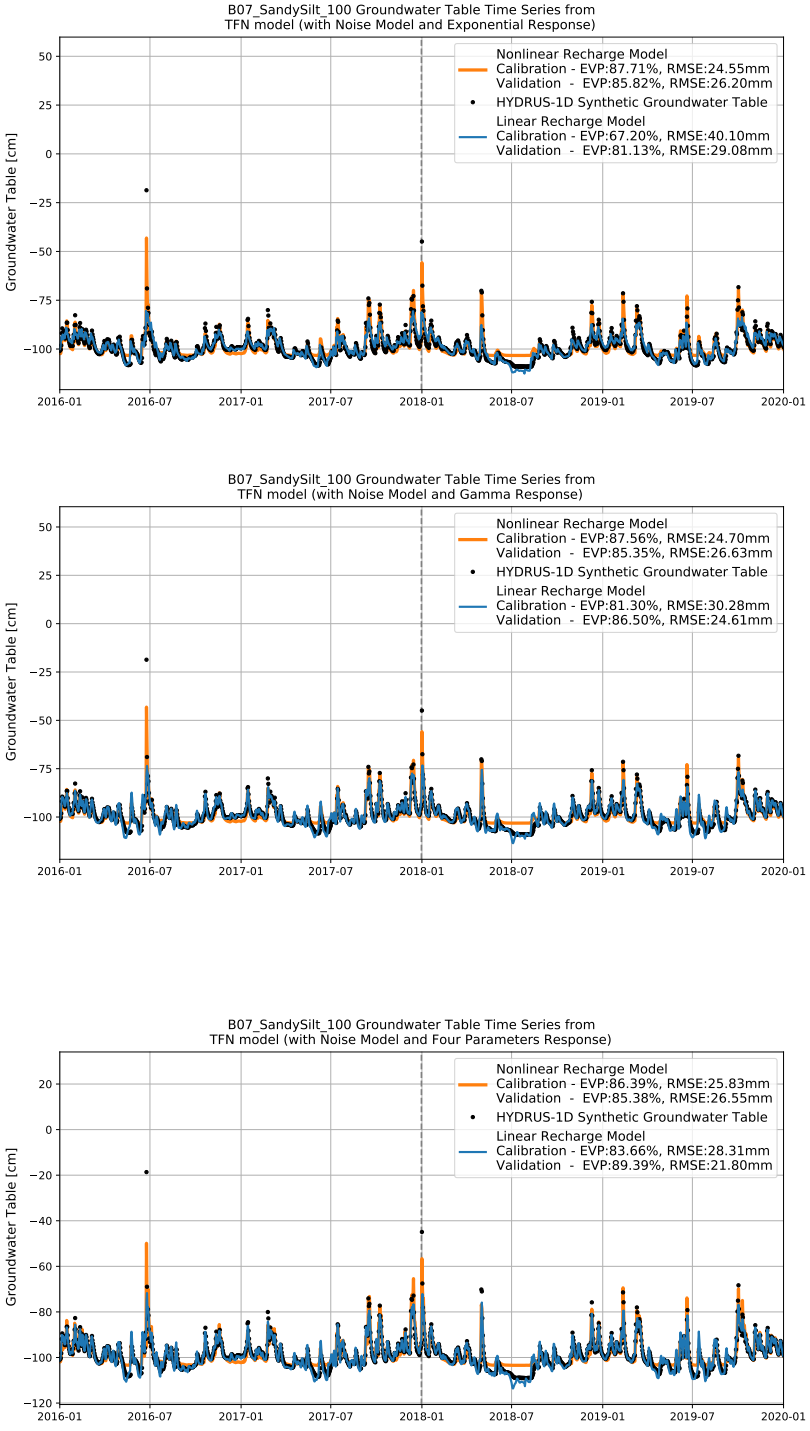

Figure F.1: Sandy Silt -100cm

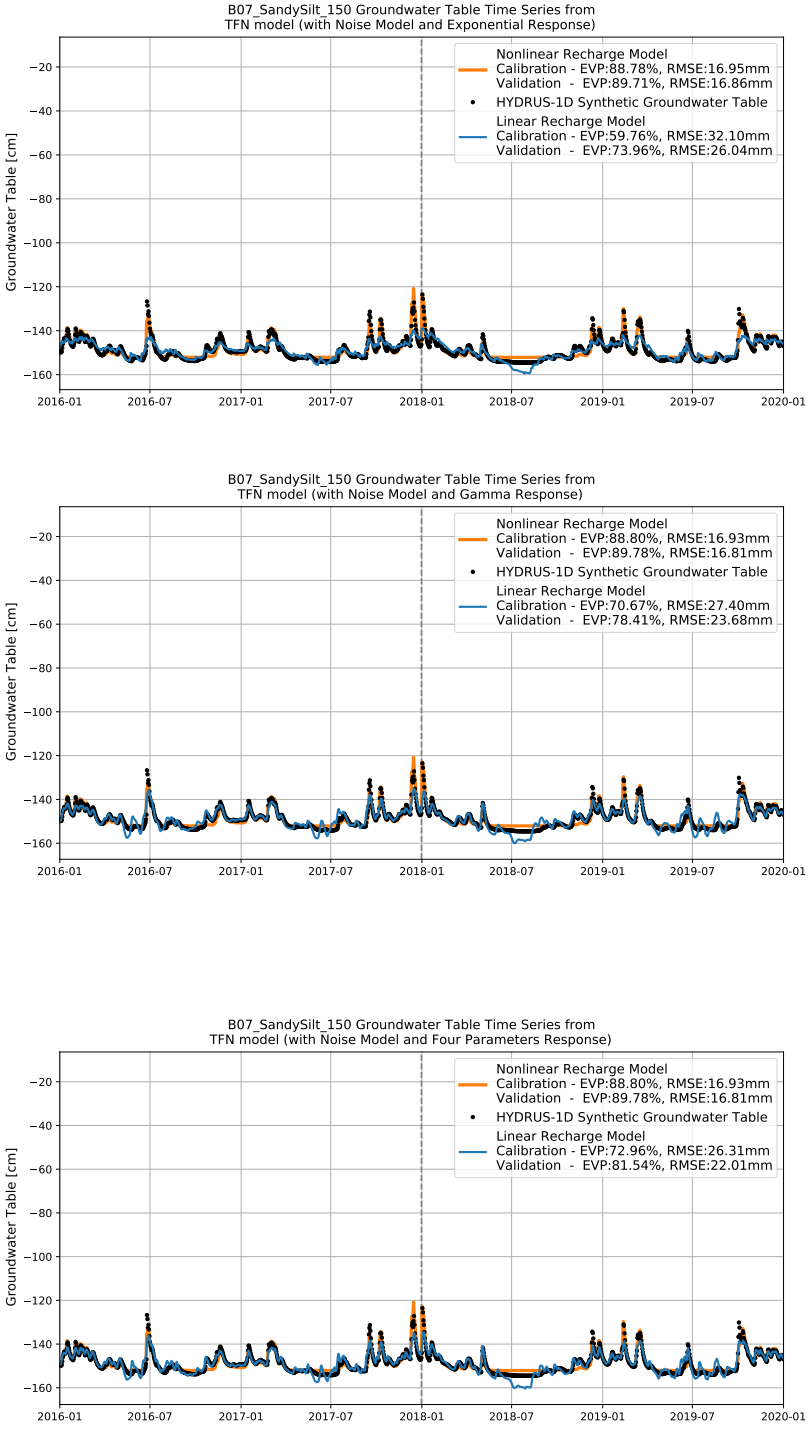

Figure F.2: Sandy Silt -150cm

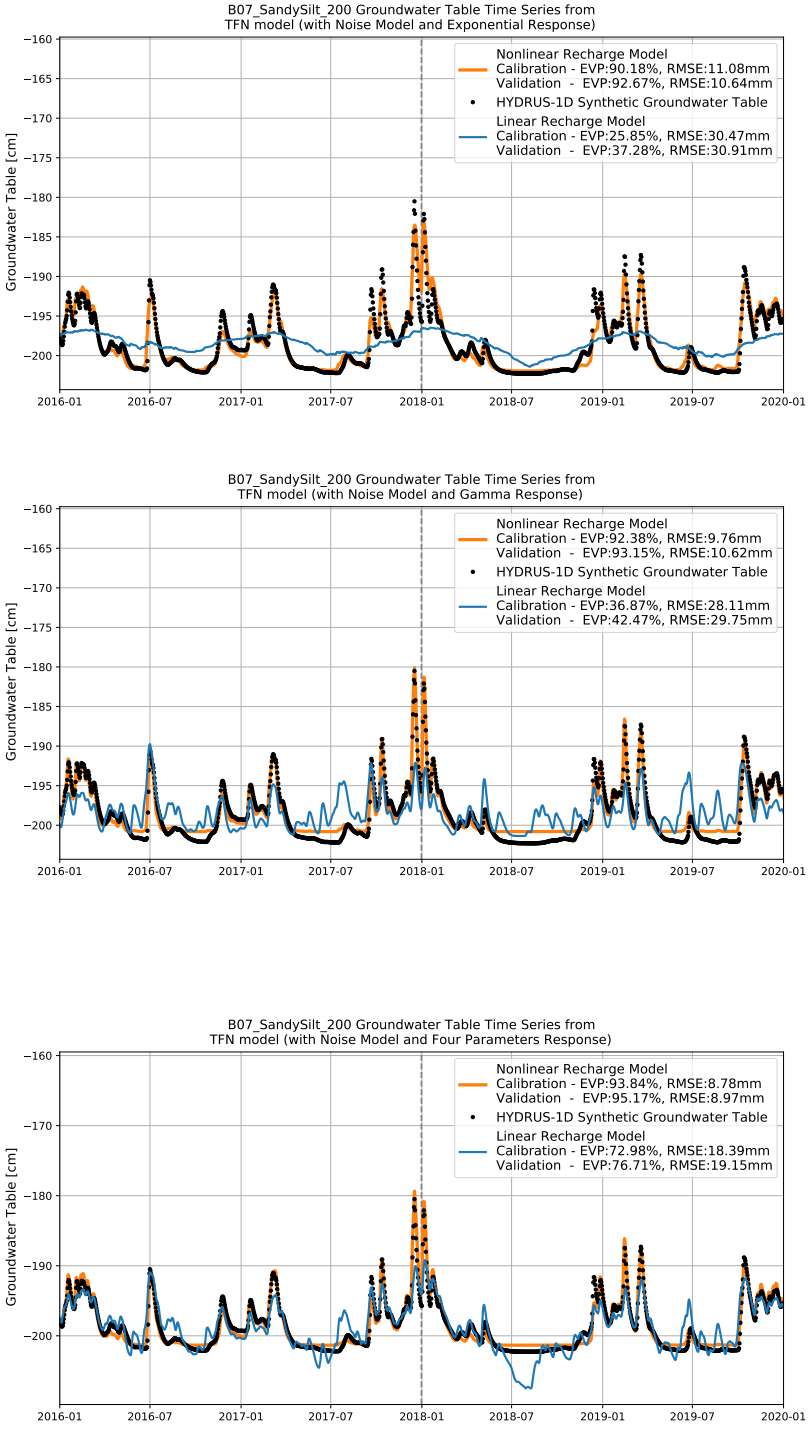

Figure F.3: Sandy Silt -200cm

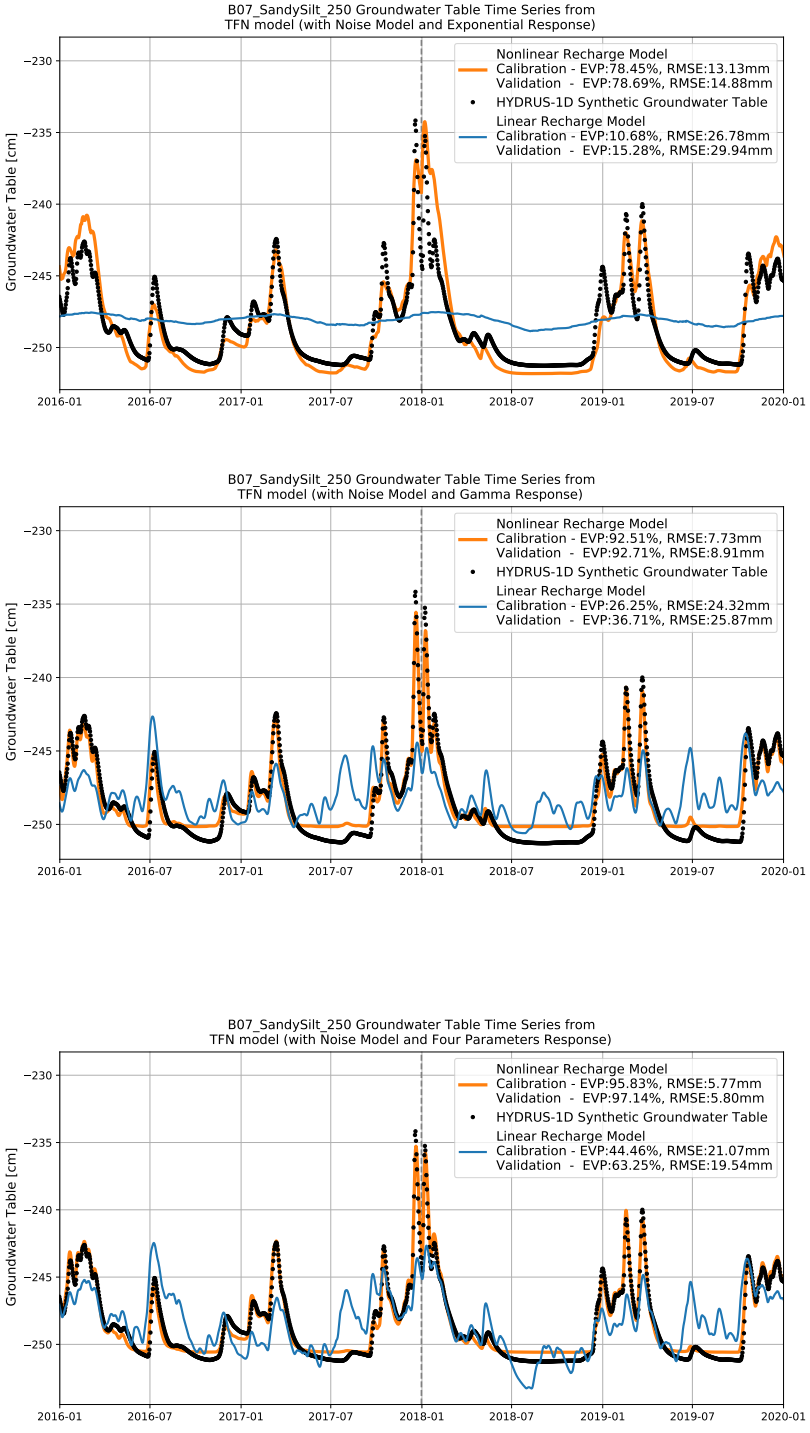

Figure F.4: Sandy Silt -250cm

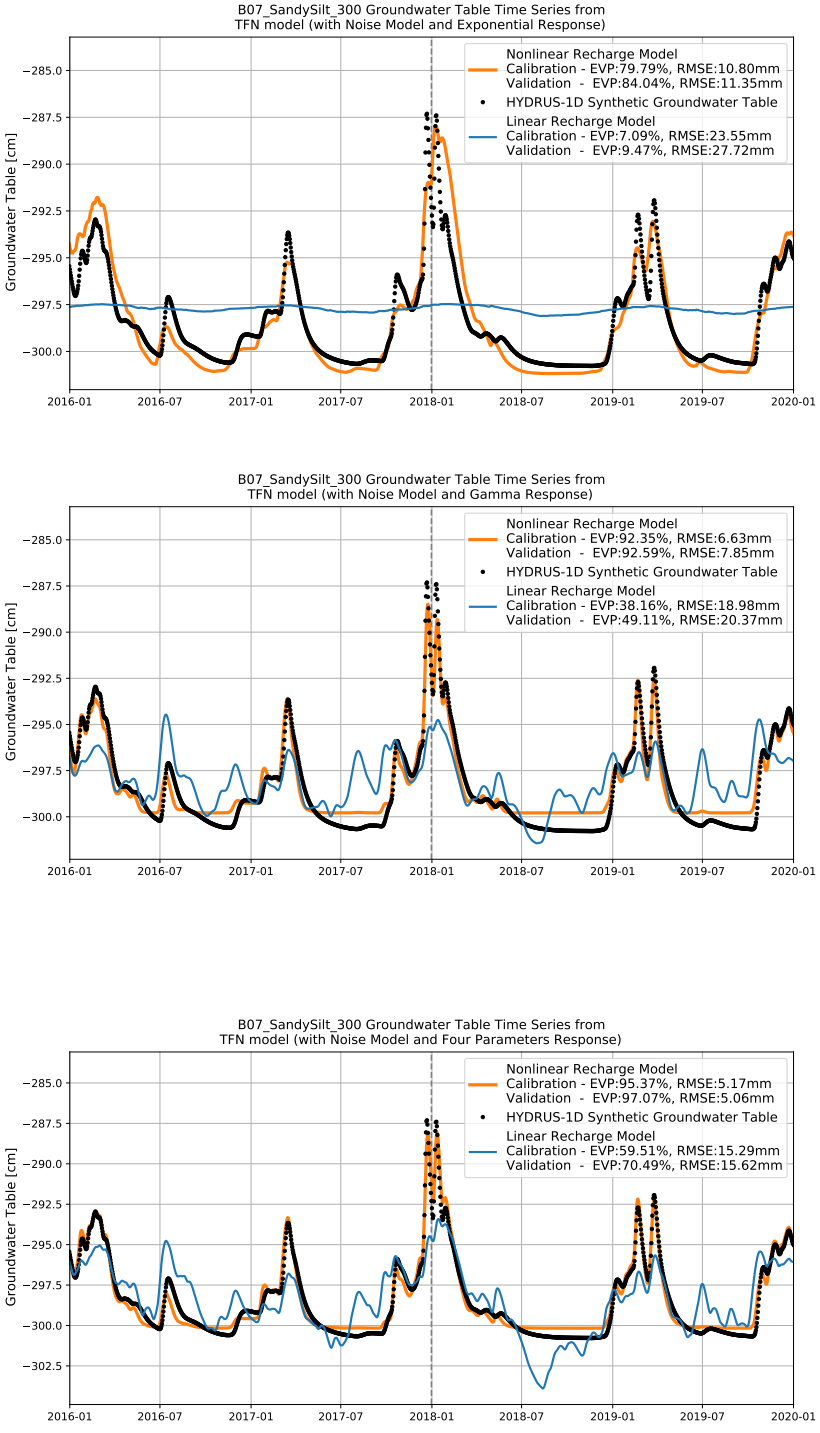

Figure F.5: Sandy Silt -300cm

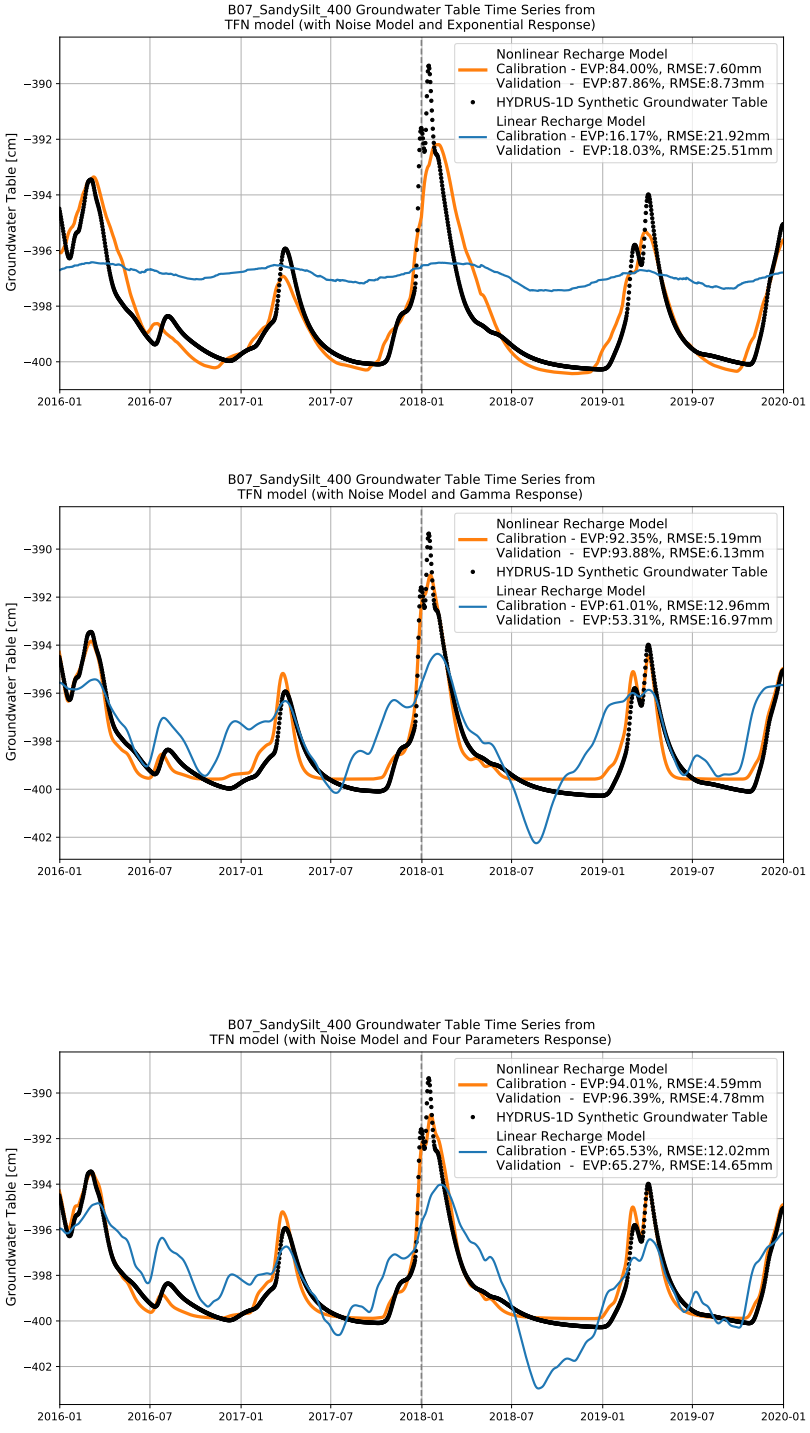

Figure F.6: Sandy Silt -400cm

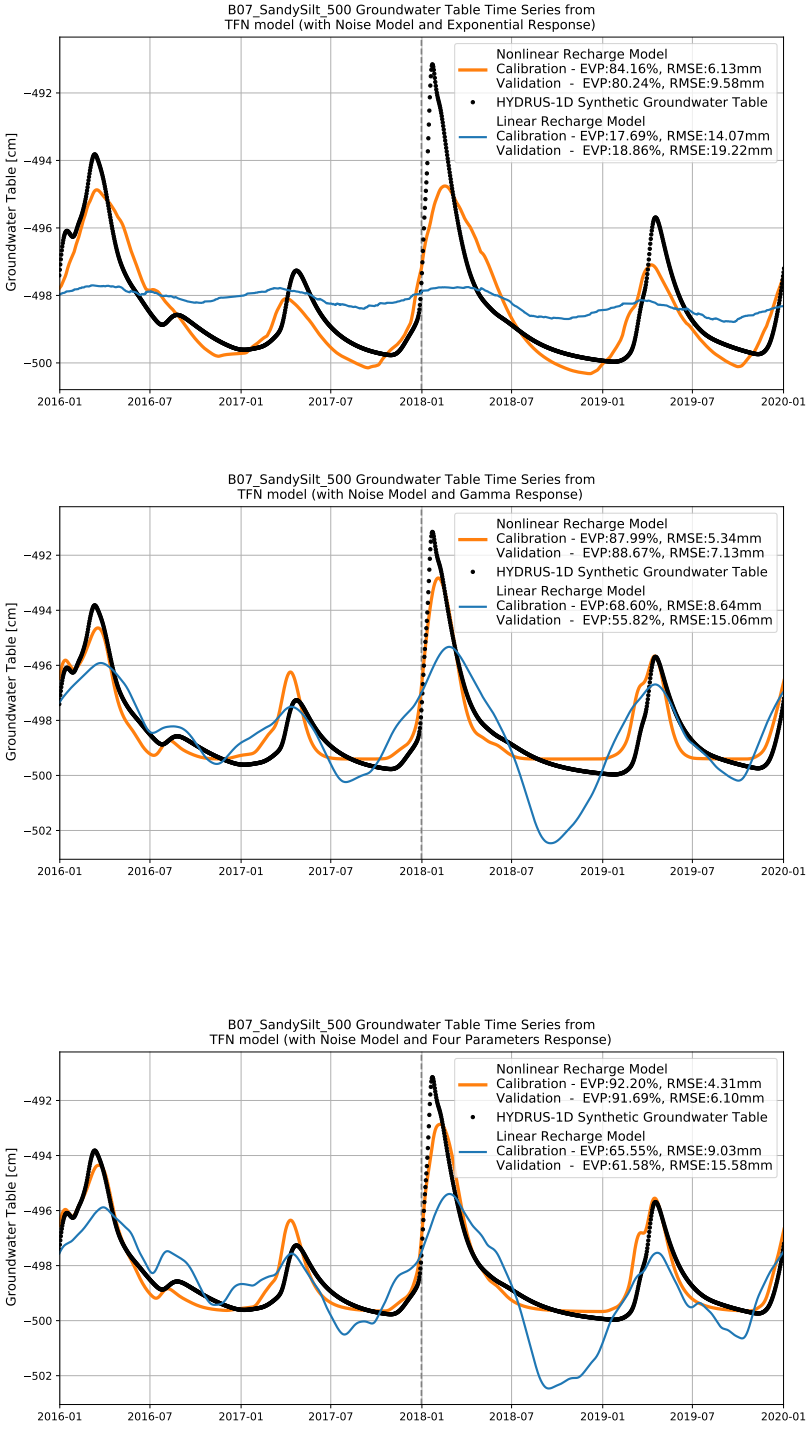

Figure F.7: Sandy Silt -500cm

G | TFN Models Clay

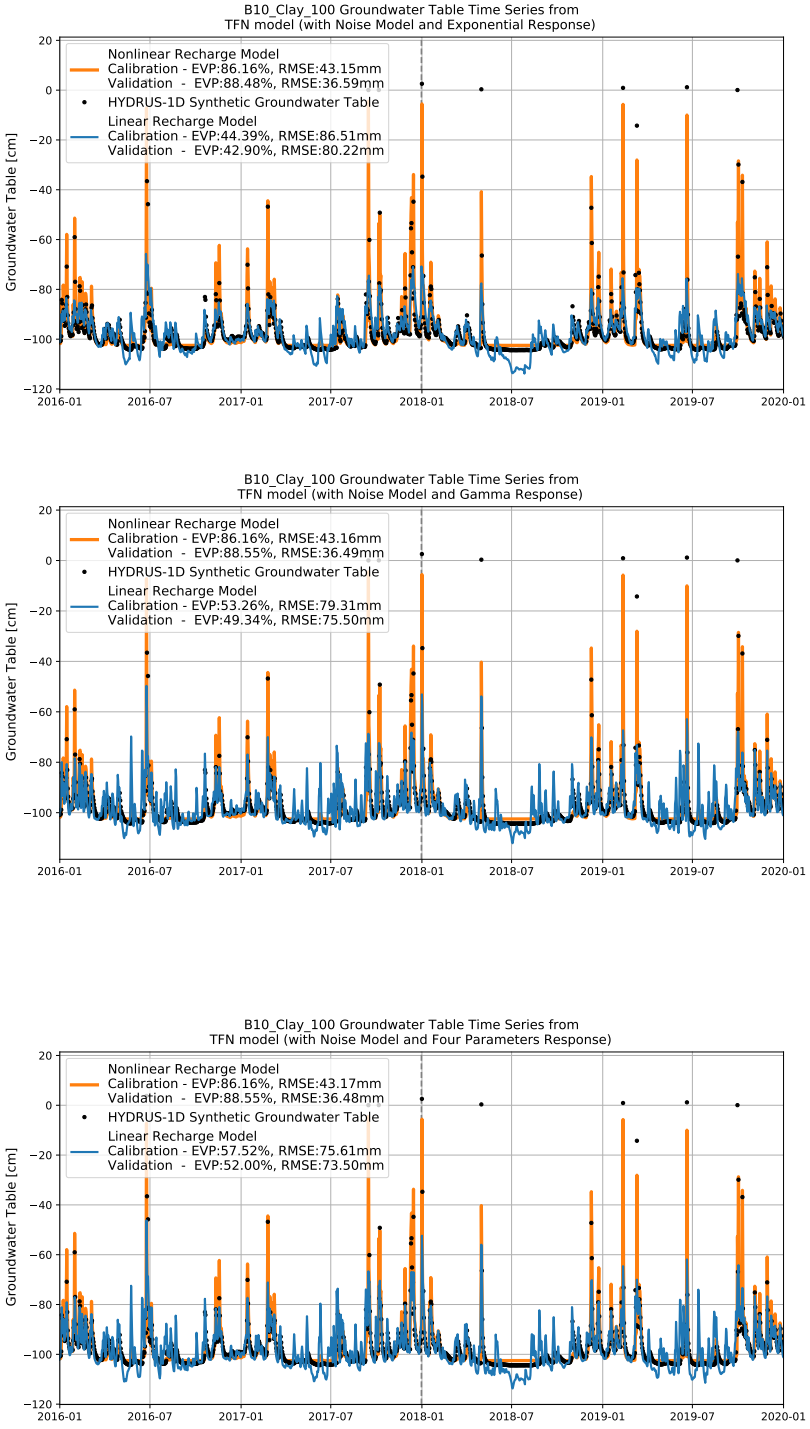

Figure G.1: Clay -100cm

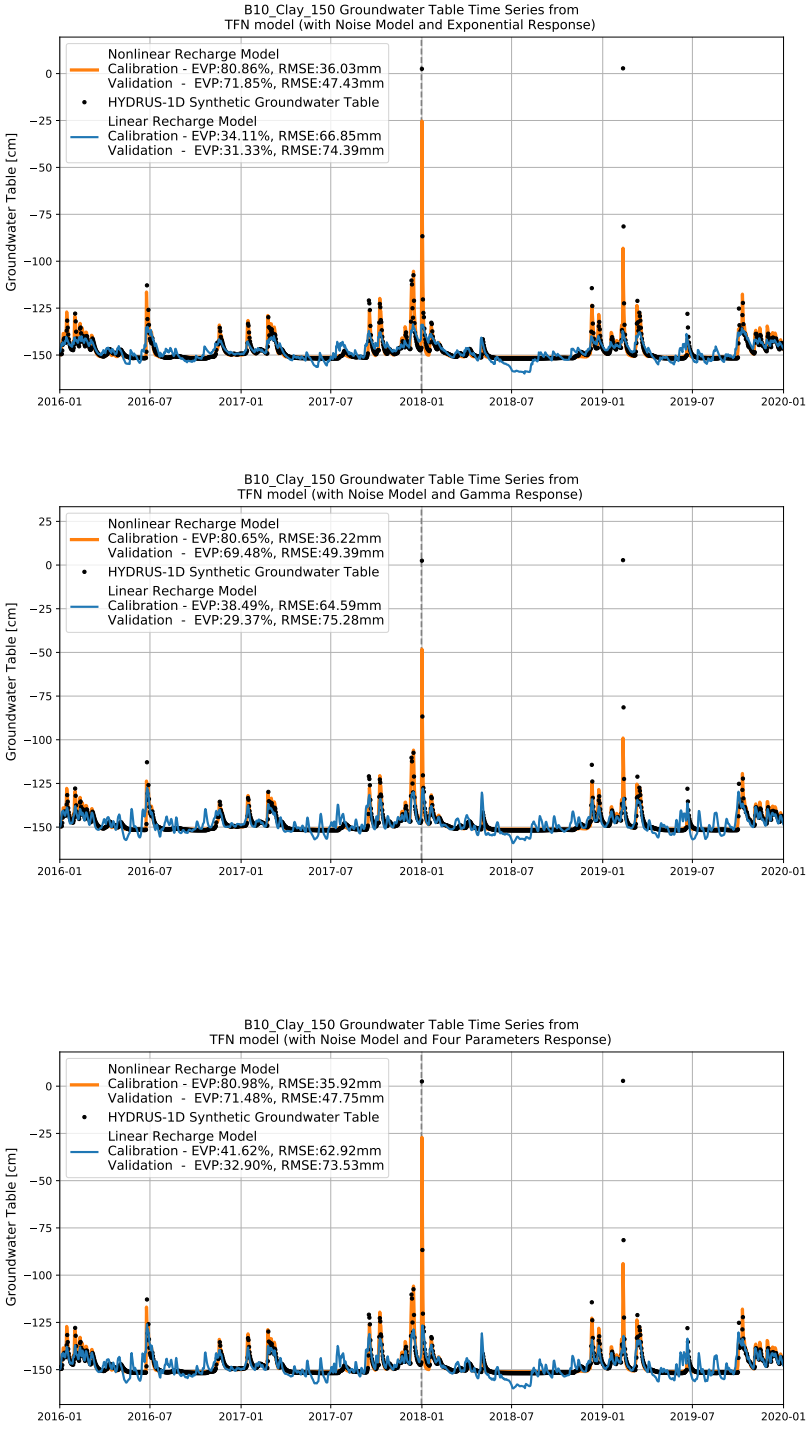

Figure G.2: Clay -150cm

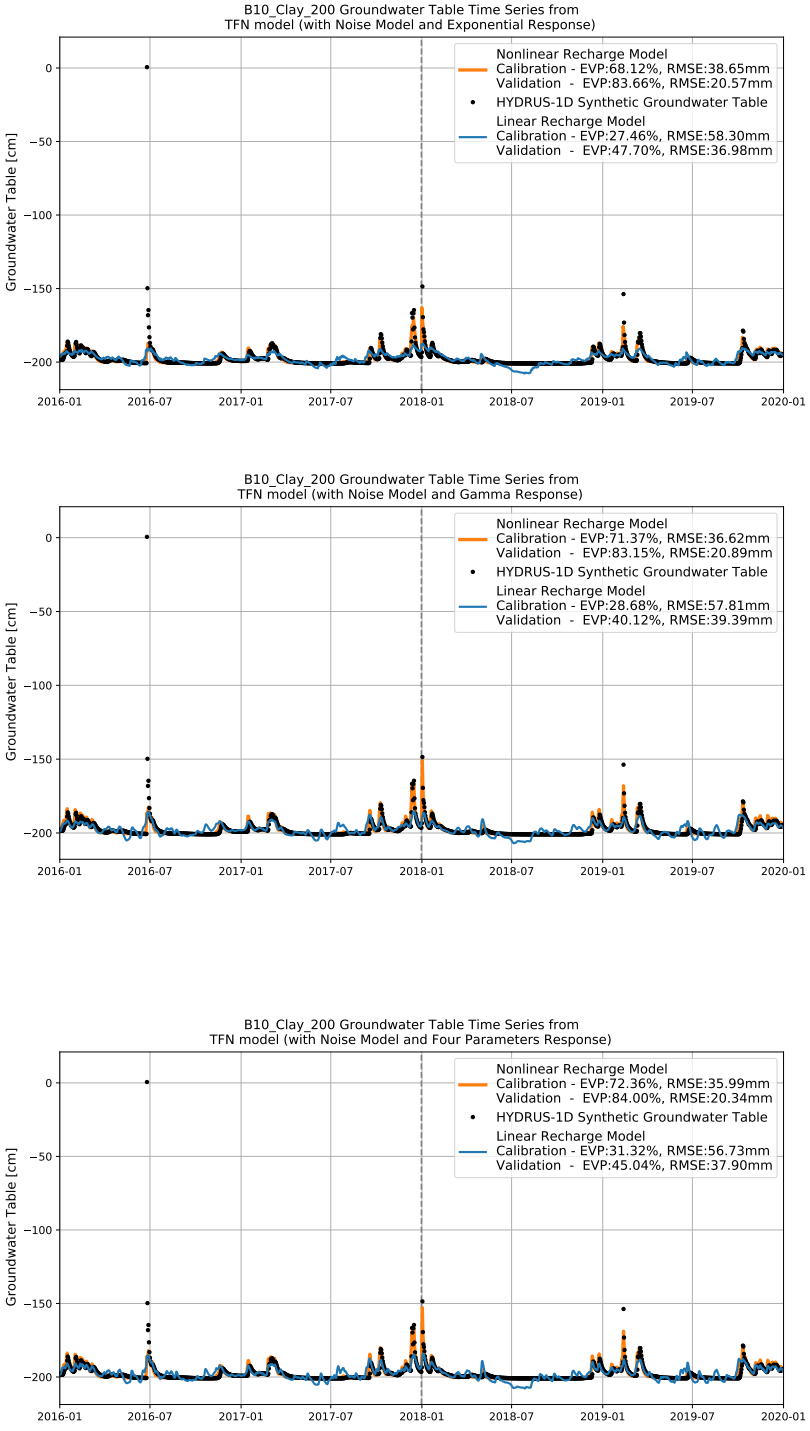

Figure G.3: Clay -200cm

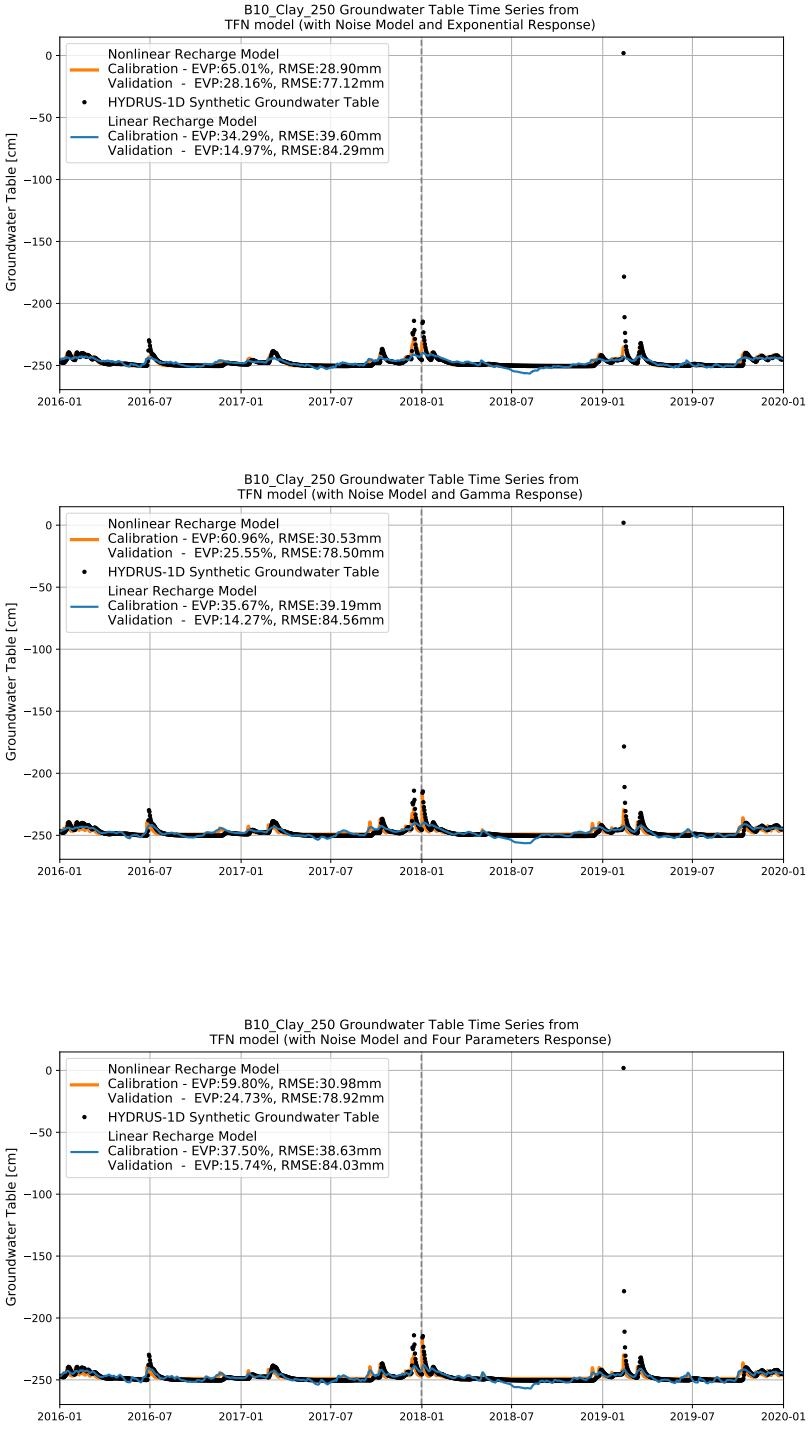

Figure G.4: Clay -250cm

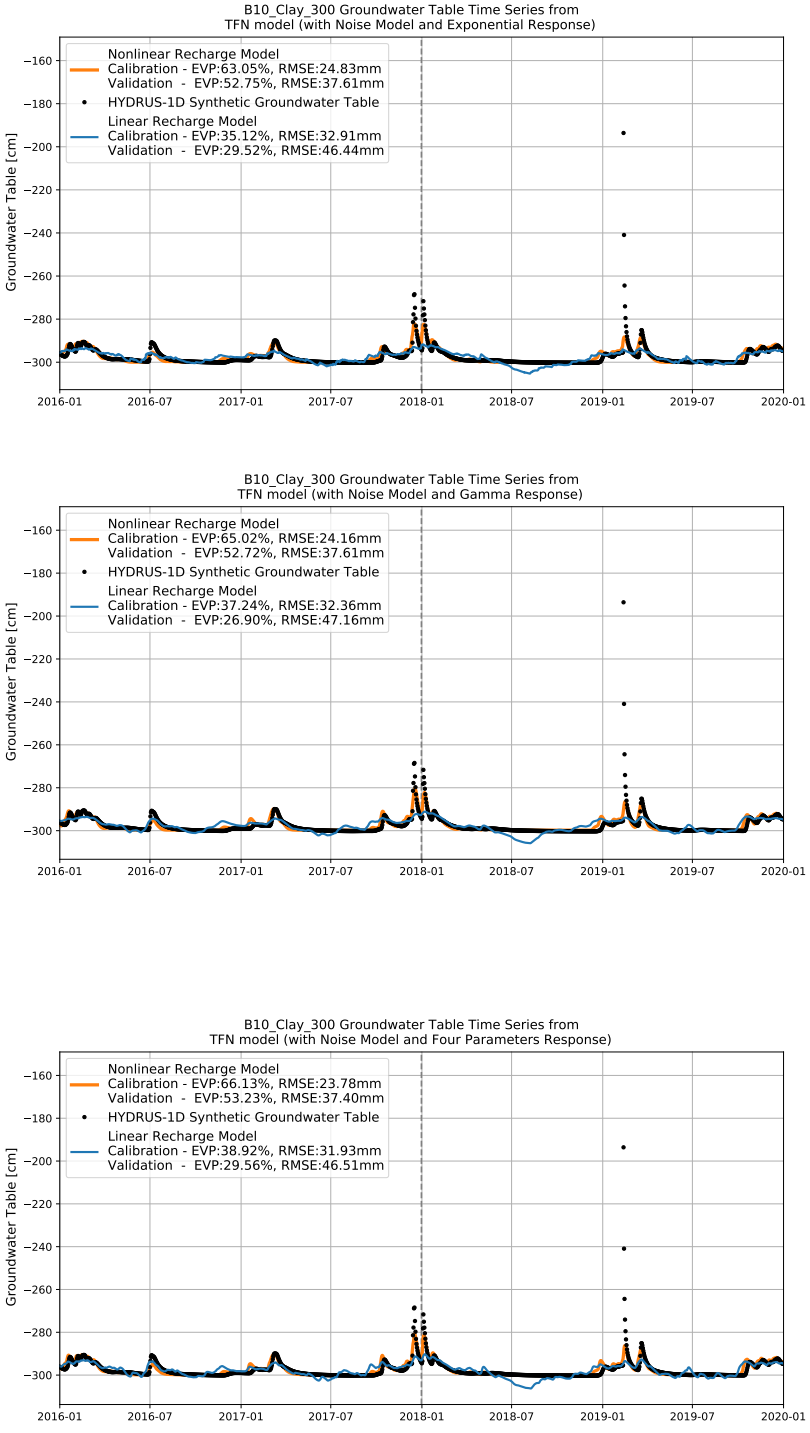

Figure G.5: Clay -300cm

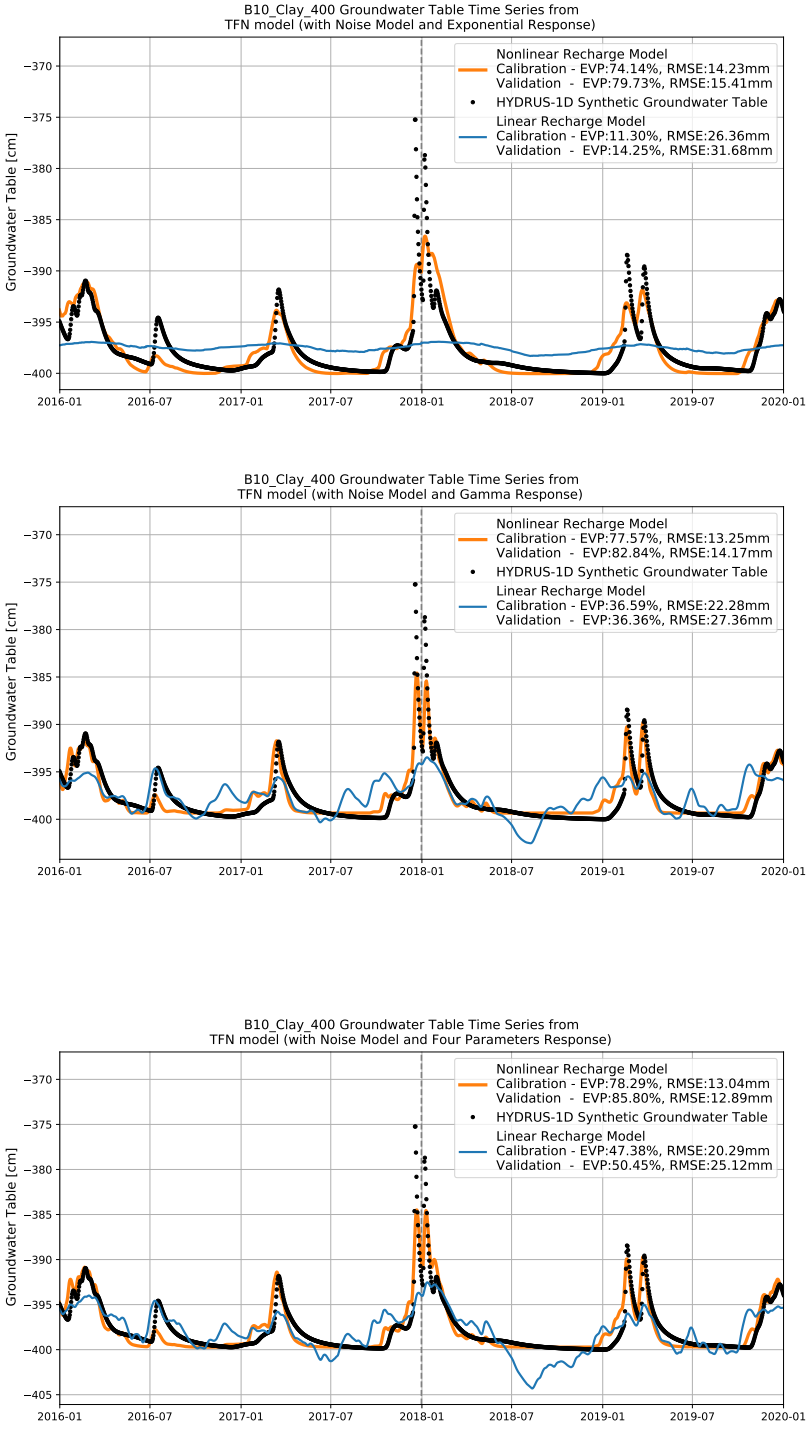

Figure G.6: Clay -400cm

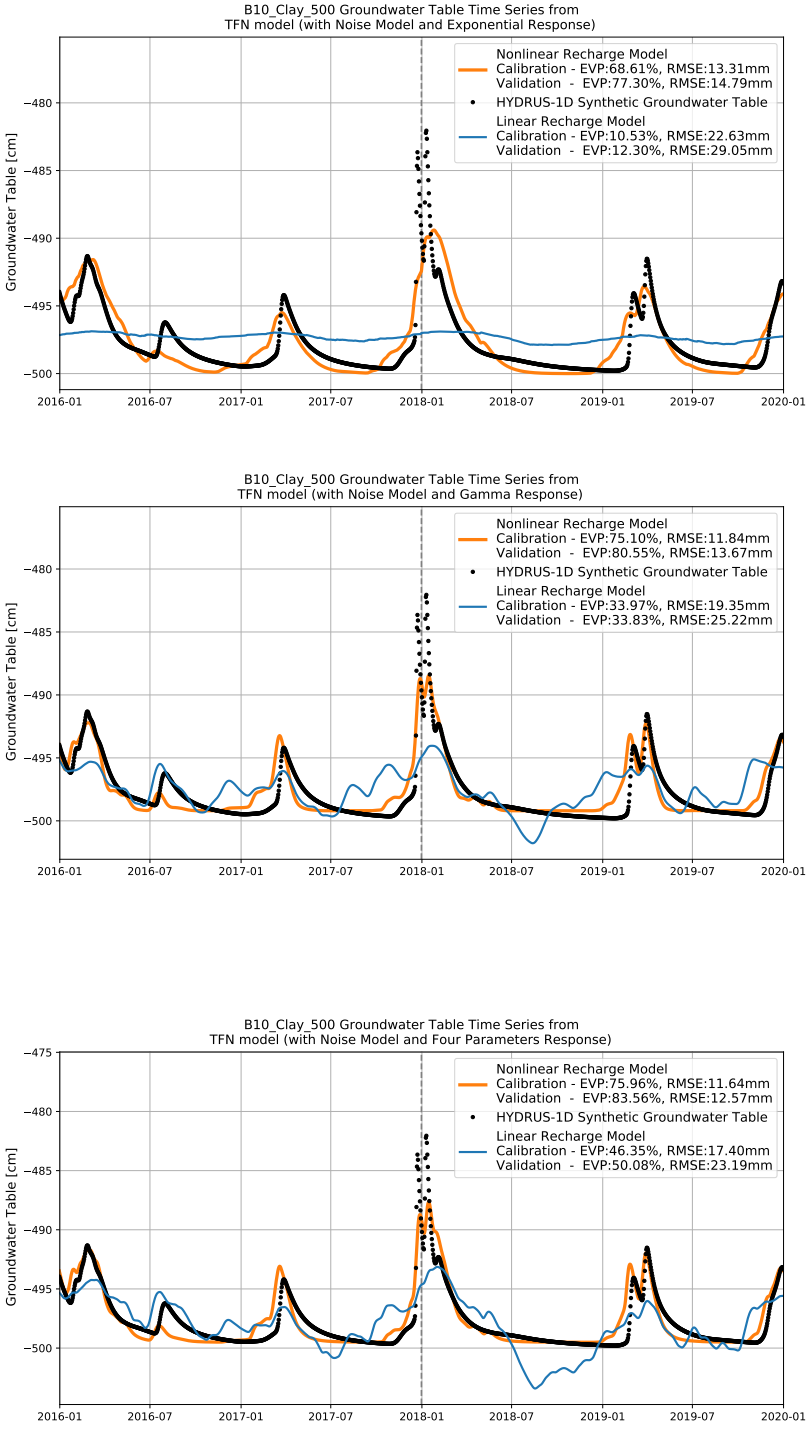

Figure G.7: Clay -500cm

H | TFN Models Silty Loam

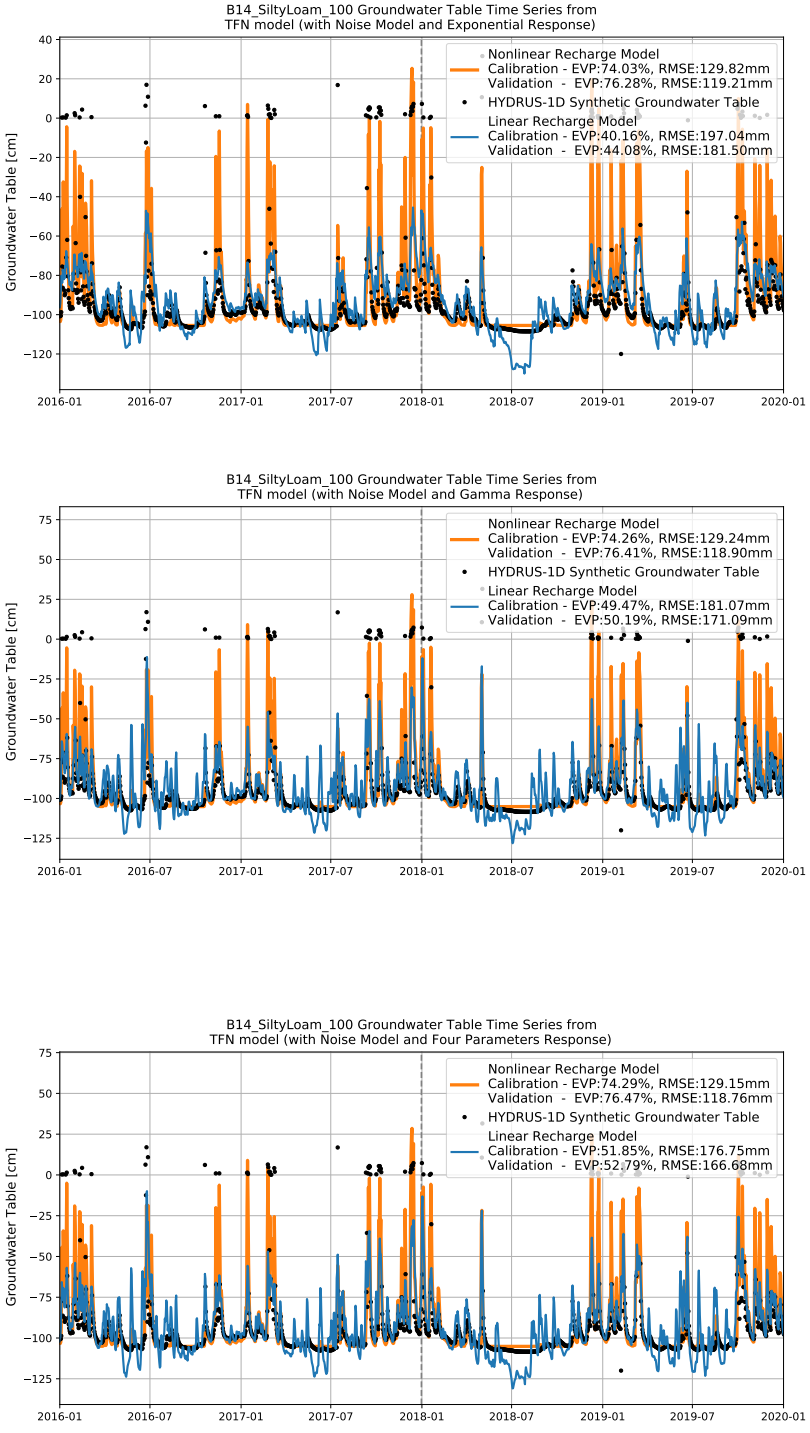

Figure H.1: Silty Loam -100cm

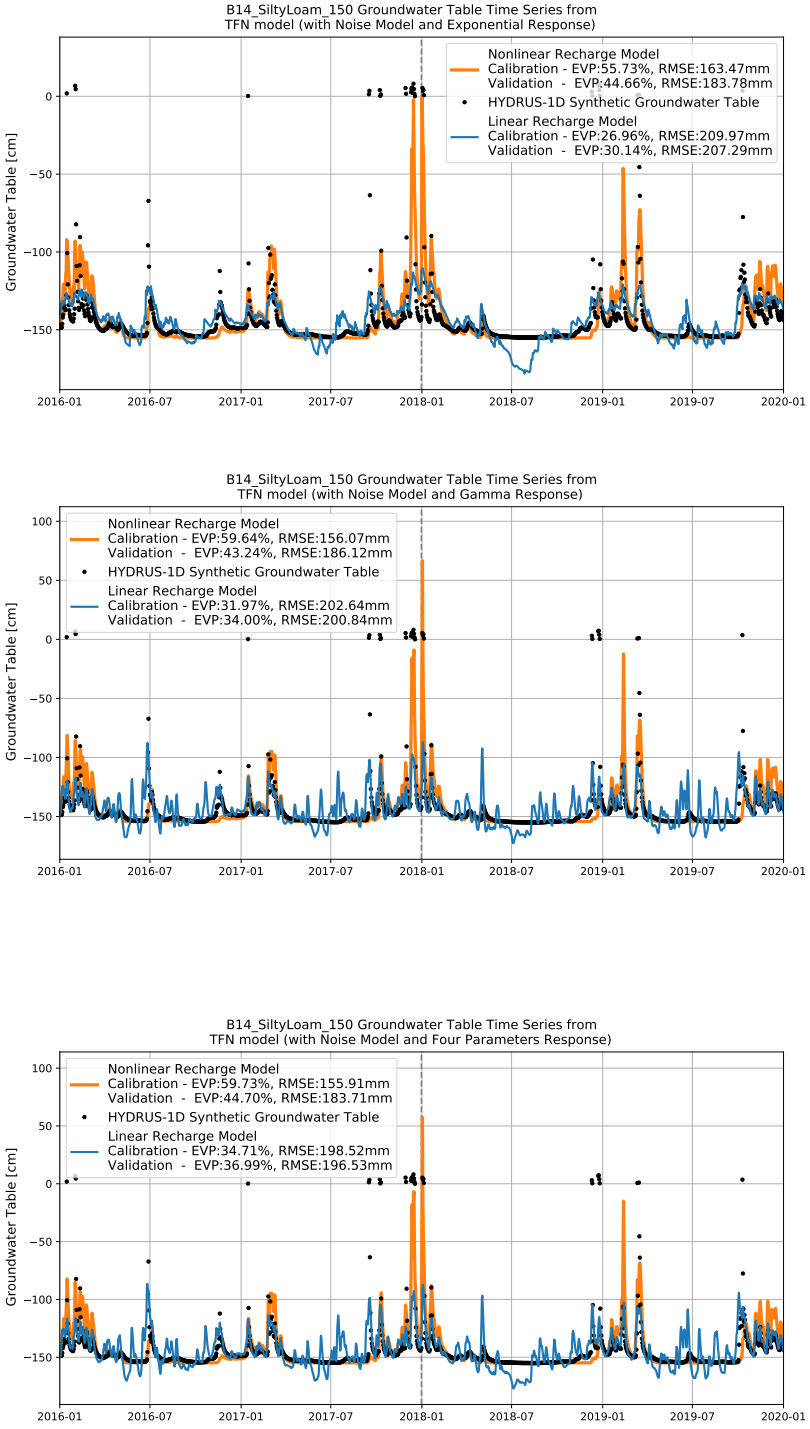

Figure H.2: Silty Loam -150cm

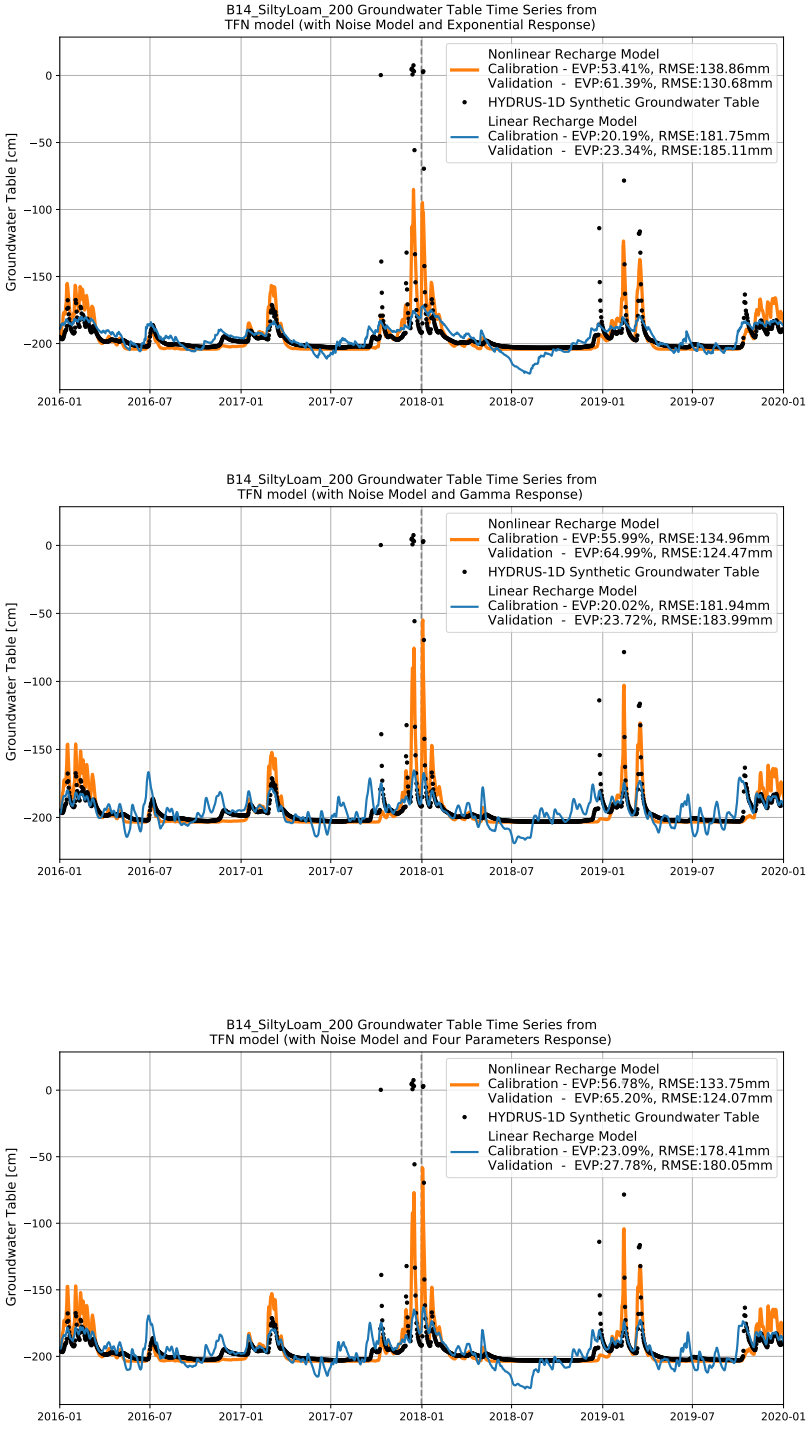

Figure H.3: Silty Loam -200cm

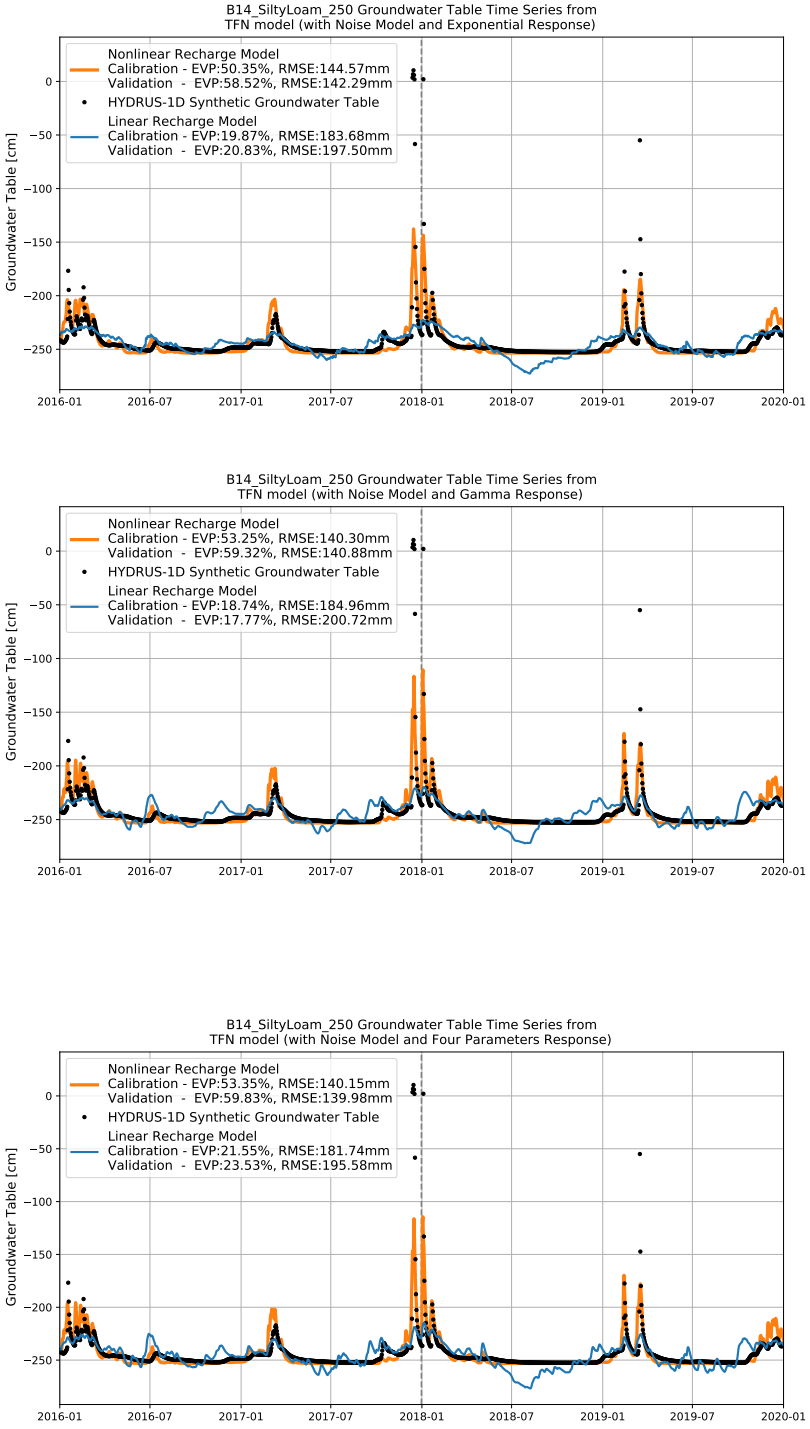

Figure H.4: Silty Loam -250cm

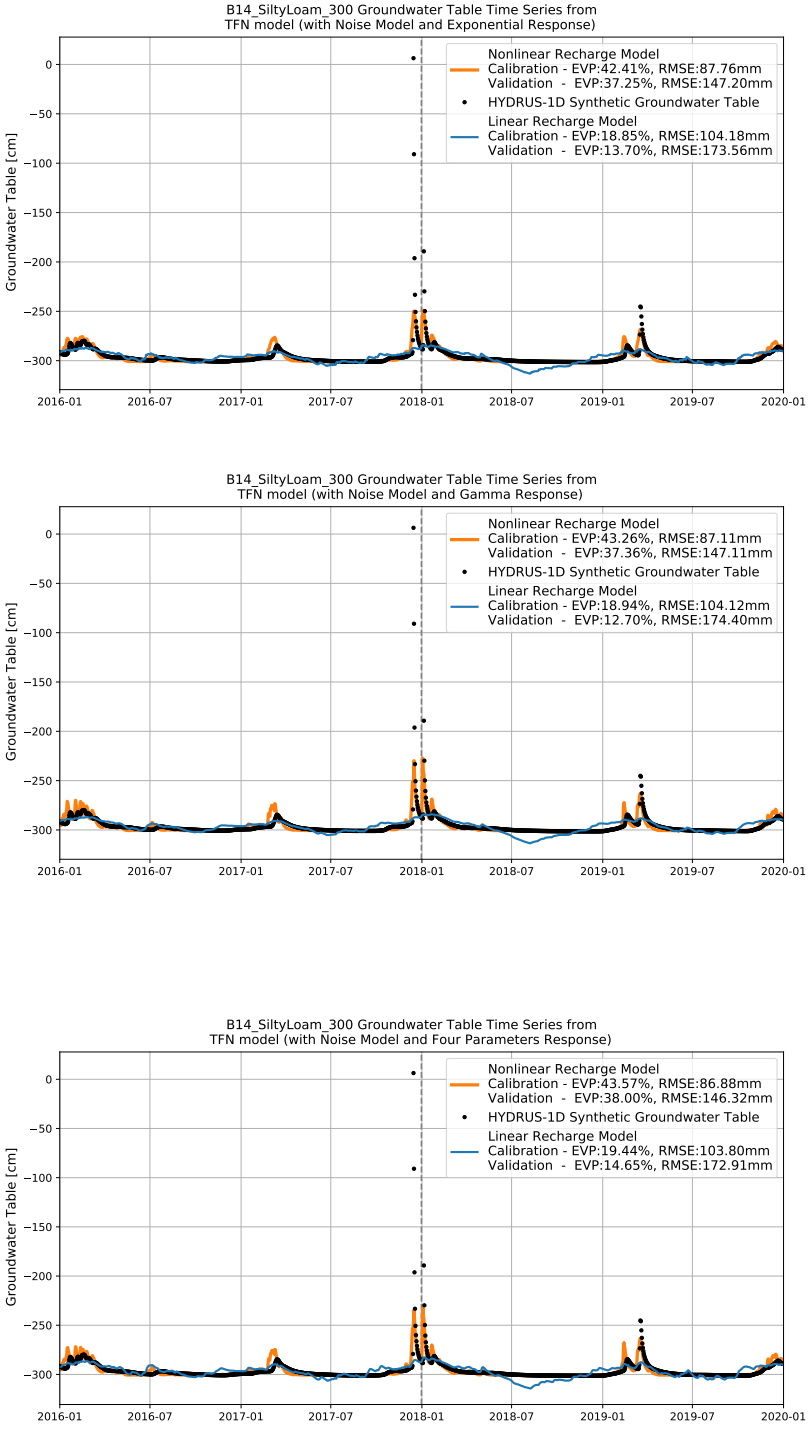

Figure H.5: Silty Loam -300cm

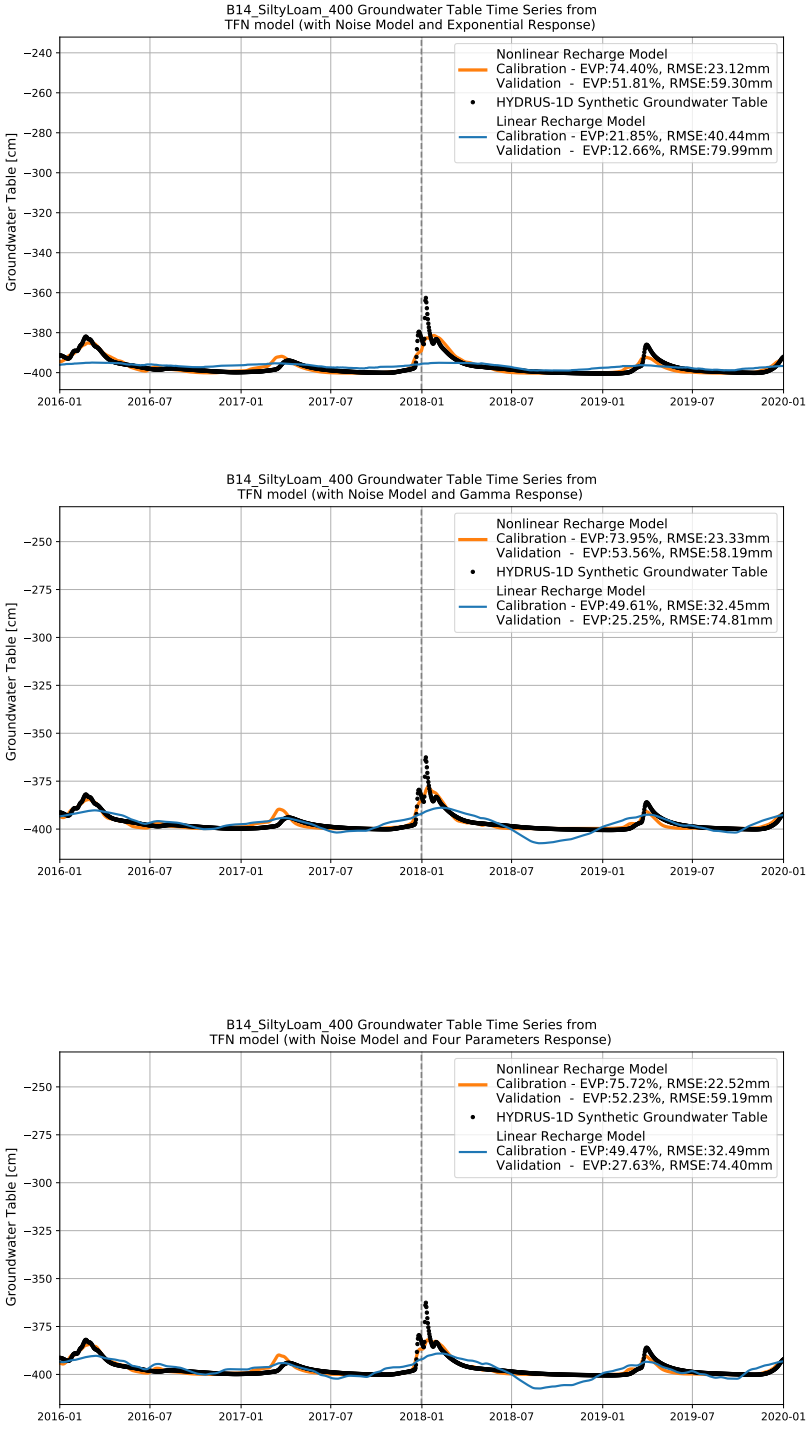

Figure H.6: Silty Loam -400cm

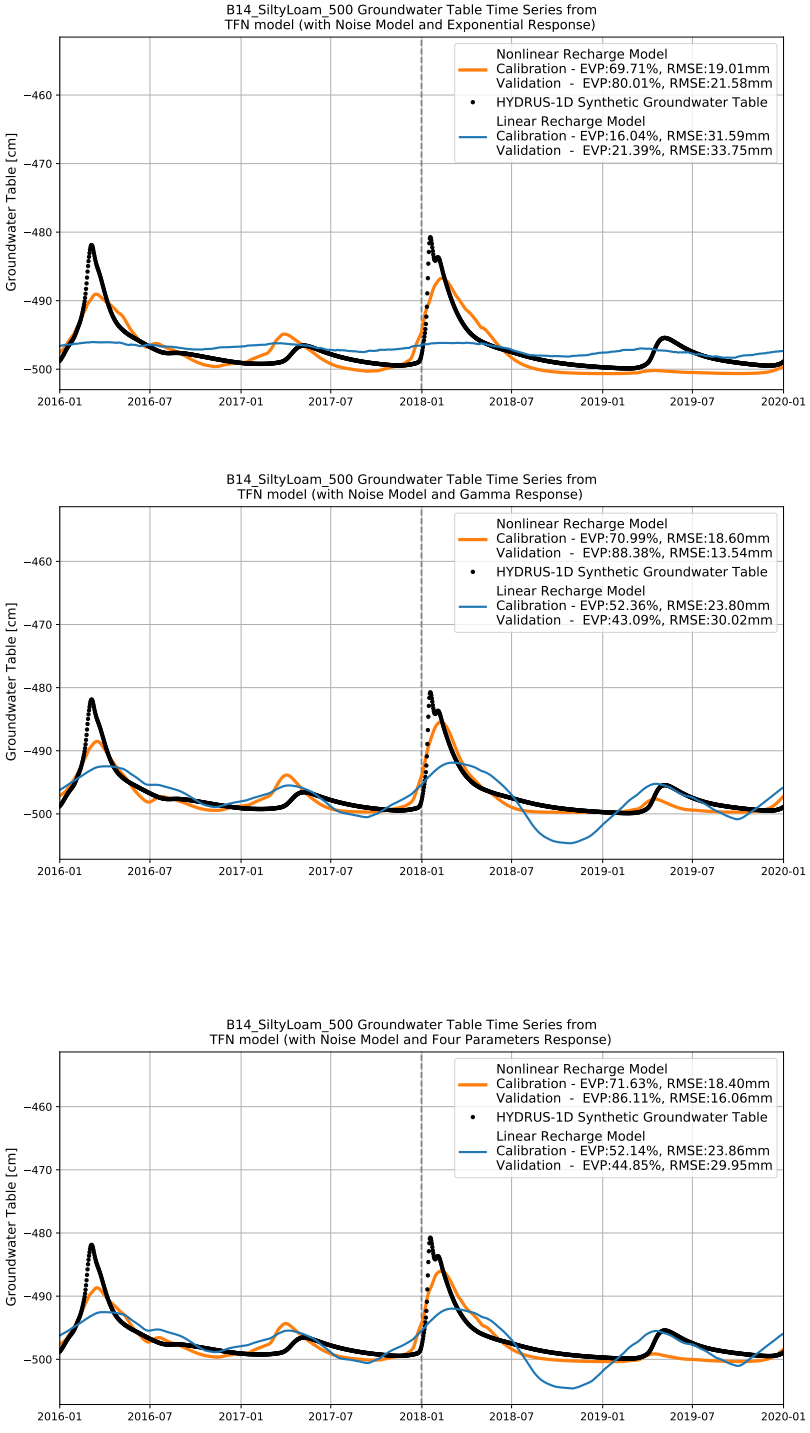

Figure H.7: Silty Loam -500cm